UNIVERSITÁ DEGLI STUDI DI MILANO
FACOLTÁ DI MEDICINA E CHIRURGIA

DOTTORATO DI RICERCA IN FISIOLOGIA

SETTORE SCIENTIFICO DISCIPLINARE BIO-09

CICLO XXV°

Tesi di Dottorato di Ricerca

A novel method for functional analysis of synapses: assay validation and design of expression systems for in vivo experiments on brain circuits.

Dottorando: Dott. Mattia Ferro

Matricola: R08861

Tutor: Prof. Antonio Malgaroli
Università Vita-Salute San Raffaele
Coordinatore: Prof. Paolo Cavallari

Anno Accademico 2011-2012

Index

ABSTRACT

An important avenue in neuroscience is represented by a more in depth analysis of cortical activity, the expectation being to find novel correlations between specific animal behaviours or cognitive functions and unique patterns of activity in neurons and synaptic networks. This goal can be reached thanks to the development of novel methodologies that ideally should be sensitive enough to provide quantitative information about single elements but also providing a view of the activity in the entire cortical network. In my laboratory in the last few years we have developed a series of biosensors for the investigation of synaptic activity both in vitro and in the animal in vivo. In order to develop a genetically encoded indicator of synaptic network activity, we have generated a series of reporters of synaptic vesicle re-use. These sensors have been named as the GreenZip family. These indicators report synaptic activation through the uptake of small fluorescent peptidic markers during cycles of exo-endocytosis, whose frequency is greatly enhanced by synaptic transmission and neuro-transmitter release. These new tools have been engineered by modifying the scaffold of the vesicular protein VAMP2 (Synaptobrevin2) through the insertion, at the intraluminal ending, of a "bait" domain with binding activity for a 4 kD peptide dubbed Synbond. The latter is conjugated with a fluorophore or with other detectable molecules. This pair of binders was selected for their high binding affinity (in the nM range) and the reporter gene was named GreenZip (the prefix Green indicates the presence of a GFP molecule at the N-terminal, cytosolic domain). These constructs have been shown to work in cultured neuronal networks (dissociated cultures of hippocampal neurons). The activity-dependent uptake of Synbond was characterized in detail and found to correlate well with synaptic efficacy and with the frequency of stimulation of presynaptic cells. The sensitivity is indeed very high, allowing individual active synapses to be easily visualized after just a few action potentials. To test the feasibility of this method for in vivo analysis, this family of molecules was expressed by electroporation of cDNA in brain slices (cortical, cerebellar and hippocampal cultured slices) and in vivo in the LGN thalamic nuclei (by cDNA electroporation in retinal ganglion cells). In these experiments, we demonstrated that Synbond, diffuses quickly across brain tissue and reaches synapses and an activity-dependent labeling of GreenZip-expressing that synapses can be achieved. This activity-dependent labeling of presynaptic boutons correlates with stimulus duration and light intensity and is already detectable after just a few light pulses. Therefore, this technique permits unprecedented in vivo recordings from large synaptic networks with very high spatial and temporal resolution. These experiments were run in living animals and the detection of GreenZip-expressing synapses (by GFP) and of Synbond uptake was obtained retrospectively after sacrificing the animal, because the thalamus is located too deeply inside the brain to be reached by available optical technologies. To overcome this limitation and express greenzip molecules also at the brain surface, and potentially in any brain area of our interest, and to run out the validation process I completed the

development of a transgenic animal model capable of overexpressing GreenZip in all tissues and at any time point in the development, exploiting the technology of recombinant DNA and using the genomic locus Rosa26 in association with the Cre recombinase system. In addition, I also achieved the generation of a family of lentivirus constructs, based on a modified HIV virus that aims to be able to express GreenZip in many areas, and in many synaptic networks, selectively using stereotaxic injections of the viral vectors inside specific subgroups of cortical cells and cortical regions including the visual areas.

INTRODUCTION

1.1 FROM SINGLE NEURON TO BEHAVIOUR

The idea that the Nervous system was built from single, basic, functionally and anatomically independent units, was introduced by Ramon Y Cajal at the end of XIX century, and is considered the conceptual milestone that led to the birth of modern neuroscience (Santiago Ramón y Cajal **,** 1894) These units, or nerve cells, are the basic elements with which we are able to process and deliver the information throughout the Nervous System, and are present in a diversity of shapes and sizes, each specialized to carry out many specific functions and tasks. Usually, the general architecture of neurons is composed of the following elements: i) a cell body containing the nucleus and the majority of the organelles that are necessary for cellular life processes.; ii) the dendrites (from the greek *dendron*, "tree"), which enable reception of information (although the functions of these parts appear to be much more complex compared to this definition) as their surfaces are covered by mushroom shaped branches known as the dendritic spines; iii) the axon, a long and very thin cylindrical structure that carries the information away from the soma v) the synaptic boutons, small bulges which are placed throughout the axon branches that, together with the dendritic spines, form the *Synapsis*. *(*term that has been coined by Sir Charles Sherrington during the first half of the 20th century, from the greek sunaptein, meaning "to act together"). Synapses are a sort of "contact point" that are located between the trasmitter cell's synaptic boutons (the presynaptic cell) and a portion of the receiving cell's somatic or dendritic membrane (the postsynaptic cell). However, between these two elements there is no anatomical continuity, as they are two distinct units, support for Ramon Y Cajal's idea of neural cell contiguity and independence. The two membranes, the presynaptic one and the postsynaptic one, face one another from the two parts of the synaptic space, a space containing extracellular fluid, with a variable size (usually around 20 nm). Inside many terminal boutons there are little egg-shape structures, the synaptic vesicles, which contain neurotrasmitters released by these structures in response to action potentials (the "universal language" that the nerve cells use to communicate with one another) at the presynaptic level.

The synaptic phenotype is more complex than it seems at first glance. In fact, there are some synapses that form themselves through the contact between the axon and another cell body, the assosomatic synapses, or between an axon and a dendrite, called assodendritic synapses (they can be located on the dendritic's smooth surface or on the dendritic spines), and more rare, between two different dendrites or two different axons, respectively called dendrodendritic and axonaxonic synapses. These synapses are integrated functional units, each of which carries out one or more specific function. The level of

complexity that neuroscientists have to handle is very large, considering that the mammalian brain contains billions of neurons (approximately 10^{10}-10^{12} neuronal cells,) linked within circuits with every cell getting, on average, 10^{3}-10^{5} synaptic contacts, totalling approximately a thousand trillion synapses inside the human brain. At the end, the goal of neuroscience is to understand the organizational principles of these synaptic circuits inside our nervous system and consequently, to be able to decode how they can process the information, changing it into what we rename as behaviour).

Ideally, neuroscience should set up a casual link between the activity of specific groups of neurons, the neuronal circuits operation, and the behaviour. Now we know that inside the nervous system, any behavioural response, even a more complex one, is based on the alteration of activity of a small group of neurons, often localized at a great distance from each other, which together act as a basic functional unit. Their pattern of activity and their connections, beyond the strength and the propriety of the mutual synaptic interactions, establishes how the neural circuits process the information and subsequently check the behavioural response. Following this, a neuroscientist that would want to understand the physiological mechanisms behind a particular animal's behaviour should know: a) all neurons that are involved and their spatial location; b) all the affected synaptic connections; c) the activity pattern of these neurons during the behavioural response, and d) the activation patterns from all the affected synapses. Having all of this information would enable an understanding of the causal link between a specific behaviour and a particular neuronal circuit. Would it ever be possible to reach this level of knowledge? What are the insuperable limits, at the present moment, to reach these goals? What are the currently insurmountable limits to achieve these goals? There are, of course, limitations related to the size of anatomical structures involved (synapses measure an average of 0.5-1 microns, 0.5-1 x 10-6 mm) but also to the multiplicity of synapses involved and their locations deep within the brain. While these limitations will be discussed further, it is important to emphasize that there is another important limitation relating to the modifiability of neuronal circuits, namely that they are not static, but anatomically and functionally malleable, an essential characteristic called synaptic plasticity.

In the matter of understanding the causal link between a specific behaviour and a particular neuronal circuit , Using an example based on psychological behaviourism, people often wonder what happens in terms of neural mechanisms during a simple case of classical conditioning, a form of learning in which a neutral stimulus acquires the properties of a relevant stimulus, forming an association between the two stimuli. In these situations, a stimulus that previously had little significance on behaviour (eg, a tone at a given frequency) becomes capable of evoking a species-typical reflex type behaviour. For example, a defensive response of blinking can be conditioned by a tone, if coupled with a short puff of air directed towards the eye of an animal. The resulting automatic blinking of the eye will produce an unconditional response, with the stimulus that produced it called an unconditioned stimulus. Therefore, following the presentation of a series of tones at a given frequency, each followed by an equal time interval preceding a brief puff of air, after several repetitions, the animal's eye will begin to close, even prior to administration

of the air blow. The only conditioned stimulus (tone) now causes the response became conditioned by the same tone. (Pavlov I.P 1927, Fig 1,).

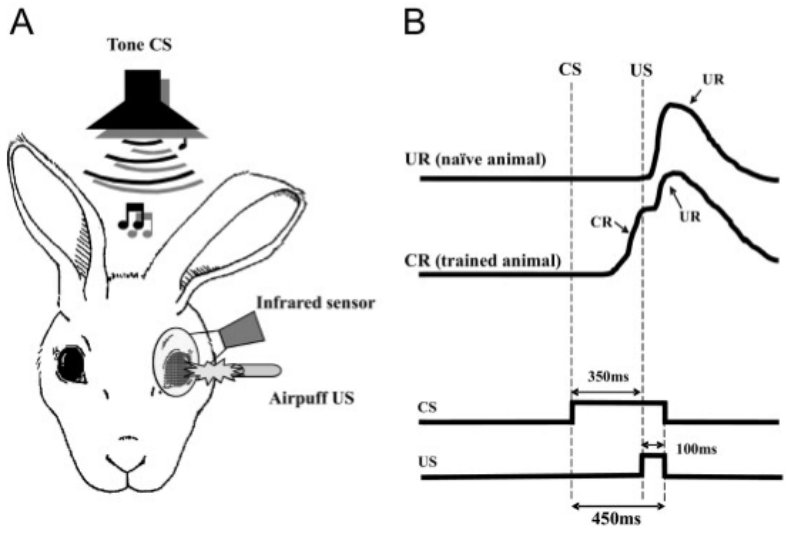

Fig. 1: Schematic of the eye-blink conditioning paradigm. **(A)** Rabbits are presented with a paired tone CS and air-puff US. Evoked eye blinks are recorded with an infrared sensor. **(B)** Idealized eye-blink records in naive and trained animals and the pulse diagram denoting the timing of stimuli. In the delay classical conditioning paradigm, the onset of the CS precedes the onset of the US and the stimuli co-terminate. Naive animals do not respond to the CS, but the US evokes reliably the hard-wired trigeminal unconditioned blink (UR, top; eye-blink trace). Over time, rabbits associate the CS with the US, and they learn to blink in anticipation of the upcoming aversive US. These associatively learned responses are called CRs (the second trace from the top.) (From Bracha V et al,. 2009).

To explain the behavioural phenomenon we could assume that the unconditioned stimulus (the puff of air) is detected by a single neuron in the somatosensory system, while the conditioned stimulus (tone at the given frequency) is detected by a single neuron in the auditory system and the answer (wink) is controlled by a single neuron of the motor system. Examining how this hypothetical circuit works: if we present a tone to an animal, at a given frequency, we observe no reaction because the synapses connecting the neurons sensitive to the tone with the neuron in the motor system is weak. Conversely, if we present a puff of air at the eye, the eye closes. because there is a strong synaptic connection between the somatosensory neurons and motor neurons that cause blinking. To establish classical conditioning we would first have to present the tone at a relative frequency, and then, immediately, the puff of air: only then will the tone produce the response, without the need to administer a puff of air. More than fifty years ago, in 1949, Donald Hebb, a Canadian psychologist, proposed a principle (Hebb, D. 1949) to explain how these experiences can change the neurons and their synaptic connections, thus causing changes in behaviour. This principle, known as Hebb's law, sustains that if a synapse is activated repeatedly, almost at the same moment in which a postsynaptic neuron fires, the structure and chemistry of the synapse will be subjected to changes, strengthening itself. If, therefore, our tone is presented first, the synapses

between neurons in the auditory system and the motor system (synapses T) will become active. If the puff is presented immediately after, the synapse between the motor and the somatosensory neurons (synapses S) will be activated causing the burst (activation) of the motor neuron. These bursts strengthen every synapse connected to the motor neuron, which has just been activated. Of course, this reinforcement also acts on synapse T, which after several presentations of the two paired stimuli, and after a series of increases in the strength, the synapse T becomes sufficiently strong to cause the motor neuron's response. Therefore Learning has occurred. Obviously both the auditory and motor systems contain billions of interconnected neurons, but of all the thousands of motor synapses activated by the tone, only those located on responding neurons will be reinforced. If the unconditioned stimulus was presented as soon as the animal had winked, many of the recently activated cells will be those that control the eye's closure, and will be strengthened only the synapses of these cells. The substance of the idea of Hebb is efficaciously represented in the slogan: "cells that discharge simultaneously connect each other." (Hebb,D. 1949). Although originally Hebb had proposed his theory to explain the nature of learning and memory, this theory was then used to understand other aspects of synaptic functioning, in particular synaptic formation during development.

Behaviour can then easily be seen as an activity of groups of neurons and synapses and quoting J. LeDoux (LeDoux J. 2002), that "most of what the brain does is done by synaptic transmission between neurons and recovering the encoded information from a previous transmission across synapses" and pushing further "the peculiar pattern of synaptic connections in the brain of an individual, and the information encoded by these connections, are the keys to what that person does, what a person is. "

These synaptic plasticity occurrences are very attractive but they represent a major obstacle for those who want to study the organization of the circuits and their link with behaviour. The circuits change both anatomically and functionally, and thus are different from person to person based on experiences that are unique to each of us.

Additionally, another major limitation is represented by the methods of brain activity analysis which are more and more innovative, but still lack the resolution necessary to correlate to the best physiological and cognitive function with specific configurations of neuronal activity and brain cells synaptic subgroups. Ideally these should be sufficiently sensitive to give us quantitative informations on the activity not only from individual neuronal cells but possibly, from all the neuronal cells involved in the physiological process, or better, from all synapses interested in that. (If a method of that was developed, you could have a general vision of the global network activity, in prospect from many, if not all, brain areas involved in the process. As you can imagine, this line of research has many implications that go far beyond the clarification of the circuit and functional connectivity of the brain. For example, it may facilitate the diagnosis but also therapy of many brain diseases, especially in their early stages, when the brain morphology is still intact but somewhere in the brain is already present a state of abnormal activity.

It is from these above considerations that this work in this field has been built, trying to develop some tools created specifically for looking at synaptic activity coming from individual neurons as well as neural networks. But before going to see the technique developed in our laboratory to study the activity that occurs at the level of individual synapses, let's see what are the techniques that are used today to detect brain activity, whether it be at global and at the level of individual cells

1.2 IN VIVO TECHNIQUES FOR THE STUDY OF NEURAL ACTIVITY UNDERLYING BEHAVIOUR

Many of the techniques that are now used for the study of the relationship between brain activity and behaviour are usually summarized under the term of functional brain imaging. The most used functional brain imaging technique is the functional magnetic resonance imaging (fMRI). As is known, these measurements are made through magnetic resonance imaging, using the electromagnetic waves of radio frequency, which act on dipoles that are present in a magnetic field. In the specific case of the measurements performed on the brain, the MRI signal (magnetic resonance) results in large part from the hydrogen nuclei that are located within water, which are the only dipoles present at a significant density to support high-resolution space measurements. The MR signal measures the transition of these dipoles in different energy states. The current images obtained with MR techniques provide representations of how these different transitions depend on the brain's physiological states. When the subject is located within the magnetic field of the MR scanner (called B0) the hydrogen nuclei are in a low energy state, relatively organized. The strength of this magnetic field is specified using a unit called Tesla, and the common range of force of the magnetic field should be 1.5 to 4.7T. In the presence of a strong magnetic field, there is a tendency for the magnetic moments of these nuclei to align parallel or anti-parallel to the main magnetic field (such as when the dipole of a small magnet bar aligns itself with a local magnetic field that is applied). The MR measurements begin when the experimenter produces some radio frequency (rf) pulses that penetrate inside the brain tissue of the subject. These pulses excite the nuclei taking them from one baseline energy state to a higher energy excited state. For each particular dipole, as well as for each hydrogen nucleus, the resonance frequency that generates this behaviour is known as the Larmor Frequency; this frequency is proportional to the strength of the magnetic field and to the gyromagnetic constant (Constant ratio between the frequency of precession of a charged particle and the intensity of the static magnetic field) of hydrogen nuclei. At this frequency the radio pulses give exactly the amount of energy that is required for the nuclei to transition to a higher energy level. Rf pulses and magnetic field gradients superimposed on the magnetic field B0 can be applied in accordance with a wide variety of time

and amplitude parameters. Variations of these parameters allow the investigator to obtain images that reveal some important brain properties: these include structure images (anatomical images), flow images (pictures of vascular perfusion), and most importantly, images on neural functioning (functional imaging or fMRI). (Thulborn, KR et al, 1982).) The information concerning the tissues is derived from the speed at which the hydrogen nuclei are returned to the state of low energy after being excited. The initial orientation of the mean of a population of dipoles can be imagined as a small vector that points within a three-dimensional space; this vector is aligned with the field B0. Excitatory pulses of radio frequency moving average of our population, changing it. The relaxation which returns it to the original state can be described as the changes that occur within two dimensions, known as longitudinal re-growth and transverse relaxation. The temporal constants (T1 and T2) describe the relaxation state of low energy. The T1 constant measures the relaxation in the direction of the magnetic field B0 (re-longitudinal growth). The T2 constant instead measures the transverse relaxation of the dipoles in the xy plane that is perpendicular to the field B0. These changes in the magnetic field are measured by special equipment inside the scanner.

The transverse relaxation, also called spin dephasing is very important for fMRI. The energy transition of some nuclei changes the local field of their neighbors nuclei. These types of exchanges are called spin-spin interactions. Inside of an ideal homogeneous magnetic field, the transverse relaxation follows an exponential decay of the signal (free-induction decay, FID), the time constant of this decay is called T2. However, within the physiological tissues the transverse relaxation is much more rapid and causes the magnetic field to become non homogeneous . When there are non homogeneous, the decay constant is called T2 *. Field variations randomly alter the frequency of proton precession, disturbing the coherence phase and speeding the transverse relaxation.

In the brain the measure of these non homogeneous condition depends on the physiological state and in particular on the local blood flow. This physiological state depends, in turn, on the neural activity which consumes oxygen and which therefore draw a quantity of blood in some way proportional to the activity itself. (Logothetis L,K. 2002)

MR signals are important for neuroscience because it is possible to measure T2 *, with a fairly high spatial resolution at the level of the entire brain. These measurements are obtained by superimposing small gradients above the main magnetic field B0.

The mechanisms that connect the neural activity for the measurement of T2 * values are generally called BOLD contrast mechanisms; these measures are those which are primarily used in studies of cerebral fMRI . As the name suggests the BOLD contrast mechanism alters the parameter T2 * especially through changes in neural activity-dependent on the relative concentration of oxygenated and deoxygenated blood. Deoxyhemoglobin (DHB) is paramagnetic (Pauling, L et al., 1936) and influences the MR signal (Brooks, RA 1975) in a different way from oxygenated haemoglobin. In the presence of DHB, the value T2 decreases quadratically with the magnetic field strength (Thulborn, KR et al, 1982). The effects of

DHB on T2 * are even stronger, as it was noticed for the first time by Ogawa et al. (Ogawa, S et al, 1990) in their pioneering studies on rat brain. Ogawa and Lee had observed that the contrast of the blood vessels varied with the oxygenated blood request or flow. They attributed the increased contrast to an effect of magnetic susceptibility associated with the red blood cells paramagnetic deoxyhemoglobin (Ogawa, S; Lee, TM. 1990). They recognized the importance of their discovery and concluded: "The BOLD contrast adds a peculiar feature to the imaging technique that uses magnetic resonance imaging and by offering an important opportunity for the techniques that attempt to compensate for the positron emission tomography as a measure of the regional neural activity." Consequently, the effects of this methodology were demonstrated in experiments performed on cat brain during periods of anoxia (Turner, L et al, 1991).

Immediately after the neural activation, we would expect that an increase of DHB increases the inhomogeneity of the magnetic field and which reduces, rather than increases, the contrast BOLD. The observed increase is due to an increase in cerebral blood flow (CBF) which compensates for the decrease in oxygen, producing a superabundant oxygenated blood flow (Fox, PT et al; 1986). Currently, however, the reason for the mismatch between supply and consumption of oxygen is not clear. Within a perfectly adjusted system, the levels of oxygenated blood would follow the request as soon as it has a growth of neural activity. An hypothesis is that the extraction of oxygen from blood vessels, compensates for the metabolic need, and the excess oxygen present in the blood would be due to an inefficient delivery process. Specifically, it has been proposed that such an overabundance compensates for the inefficiency of the passive diffusion of oxygen that occurs at high flow velocities (Hyder, F et al.; 1998). According to this hypothesis, the supply of oxygen is closely coupled with neural activity, and the anaerobic processes of astrocytes would represent only a negligible amount of energy that is supplied from existing reserves (Attwell, D et al.; 2001). Nevertheless, there is a noisy contradictory on these theories, which remains an uncertain argument (Mintum, MA et al.; 2001).

A physiological explanation of the BOLD signal can be tested by comparing the amplitude and the time course of the BOLD signal. The time course of the BOLD response in humans towards short stimuli is also called hemodynamic response function (HRF). It was observed that there is heterogeneity in the HRF response within the cortex of the same experimental subject (or animals), just as there is between the various test subjects, and also, of course, in different cognitive tasks (Glover, GH., et al.; 2004). For example, the neural response to sensory or motor stimuli ended fairly quickly, within a few hundred milliseconds, while the BOLD response began roughly 2 s after (Kwong, KK et al., 1992), reached a plateau 6-9 s after the presentation of stimulus and then returned to baseline.

In this regard, attention has been directed to the question of whether the linear systems could be accurate models for the BOLD signal? A number of studies have use the response to short stimuli (2 s) to be able to predict the response to visual or motor acts of longer duration (> 8 s). The simple prediction of a linear time-invariant (LTI) system, in which the responses to long duration events are predicted from those to

stimuli of short duration, is doomed to fail significantly (Robson, MD et al., 1998) (Logothtetis, NK et al.; 2002). It is however possible to make accurate predictions about responses to stimuli presentations on the basis of long-term responses to 6s stimuli as well as for stimuli of longer duration and also to predict responses to brief stimuli from responses to even shorter stimuli.

Many recent works have examined the relationship between the BOLD signal and neural activity (Logothetis, N and Wandell, B. 2004): although there is an incomplete understanding of the process, a relationship between BOLD response and a local increase in the neural activity is now well established (Logothetis, N. et al., 2001). But what kind of neural activity, or rather, what kind of electrical activity, does this technique measure? If we insert a microelectrode in the extracellular space of an experimental animal's brain the real potential that we will measure will reflect different types of electrical activity of different sizes: a certain type of activity will have a high amplitude while another type will be hardly discriminated from the ground noise. This is because the neural spikes appear to be superimposed on other types of waves at lower frequency. Traditionally spikes are separated from subliminal variations across a high- or low-pass filter, respectively, and such separation in frequency bands reflects different types of neural electrical activity. Filtering in the range of 300-400 Hz is used in most of the recordings in order to obtain the so called multi-activity units (MUA, above 400 Hz), and the local field potentials (LFPs, obtained with a filtering below 400 Hz). Summarily it seems that the MUA activity (which turns out to be characterized by high speed) can record the summation of spikes of small neural populations near the electrode (in a sphere of approximately 1-3 millimeters of radius with the microelectrode in the center) that most likely includes dendritic spikes and activity from interneurons. The LFPs activities, on the other hand, reflect predominantly postsynaptic dendro-somatic signals that depend on the activity of inputs (local or afferent); this activity would reflect not only the population postsynaptic potential, but also some soma -dendritic integration processes including fluctuations in voltage-dependent membranes as well as forms of afterpotentials following the somato-dendritic spikes, which, taken as a whole they would represent the local activity of a given region (Logothetis, N. 2008). It was seen by experiments on primates, through a combination of electrophysiological recording techniques from the cerebral cortex with analysis by fMRI BOLD signal, that the changes observed in LFPs correlated to a greater extent with the evolution of the BOLD signal compared to the activity of spiking recordings MUA (Logothetis, N. et al., 2001; Logothetis, N and Wandell, B. 2004). These experiments carried out through a combination of different techniques, suggesting that the BOLD signal reflects the combination of input within a given area and the processing of these inputs through local cortical circuits. Of course, in many cases, this activity will be closely related to the output of the given area. However, in cases in which the incoming signals are modulators, or in cases where projection neurons are inhibited by local interneurons, the activity of spiking measured by the microelectrodes would not be able to adequately predict the BOLD signal.

Therefore, through this nonlinear relationship between neural activity and the BOLD signal, it active neurons and synapses in the brain may be revealed. This approach has, however, some important limitations: First, if we take as example the thalamus (the main relay station for sensory pathways from all over the nervous system,), the input arrives to innervate both inhibitory neurons and excitatory cells, and besides the fact that each connection within it is convergent, as is divergent. In this way, the final response of each neuron is determined by all the synapses that operate in a feedback, feedforward or in a modulatory manner within a given microcircuit which contains a very complex network of excitatory and inhibitory cells working together. The activation of one of these excitatory or inhibitory microcircuit networks will in turn put in motion a sequence of excitation and inhibition that will propagate to the entire network (Douglas & Martin RJ KA, 2004). Computational models suggest that the excitation-inhibition networks of these microcircuits contain a precise balance between excitation and inhibition (Douglas RJ et al., 1995; Shadlen MN et al., 1994; Chance FS et al., 2002.). The principle of that balance would mean that the microcircuits are capable of large changes of activity and at the same time maintain their proportion of excitatory and inhibitory conductances. Now, all these excitation-inhibition changes will influence the hemodynamic response: a high response in the BOLD signal will only be given in response to an excitatory increase? Figure 2 helps us to better understand this problem of what is actually measured in this signal (Logothetis NK, 2008)

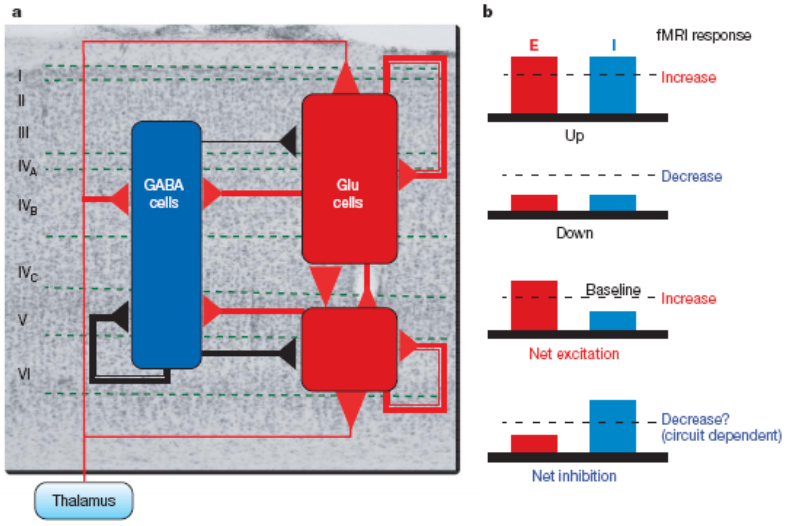

Fig 2: **(A)** prototypic model of a brain microcircuit (Douglas RJ et al., 1989). Three different neuronal populations interact with each other: inhibitory GABAergic cells and glutamatergic excitatory cells. Excitatory synapses are shown in red, and inhibitory in black. All groups receive excitatory input from the thalamus. **(B)** shows changes in proportion to the potential and to the opposite direction between cortical excitation (E) and inhibition (I). May be changes in response to input while maintaining a right balance between excitation and inhibition. A net inhibition or excitation may occur when afferents can drive the overall balance of excitation-inhibition in opposite directions. The proportional changes in the excitation-inhibition activity, which occurs as a result of neuromodulators input, probably have a fundamental role in guiding the hemodynamic response. (From Logothetis NK et al., 2008).

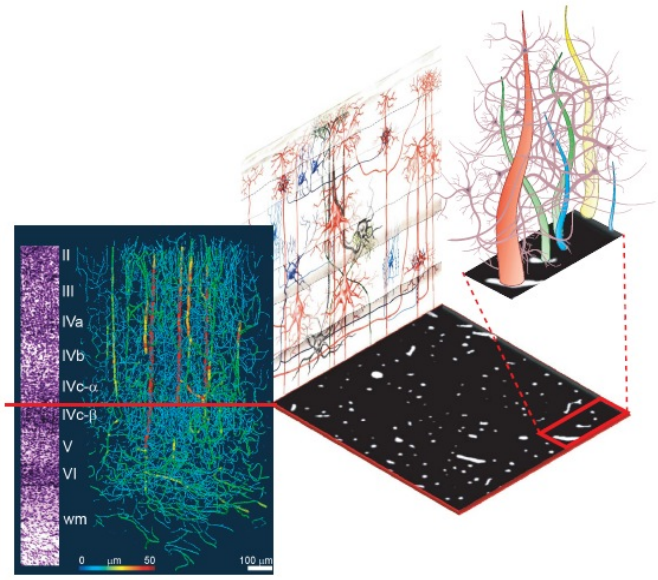

Figure 3: The left panel shows the relative density of blood vessels in the visual cortex of monkeys. The dense vascular intertwining is shown perfunding the tissue with barium sulfate and the image is formed through the x-ray microtomography synchrotron-based. The diameter of the vessel was coded by color. The cortical surface without pial vessels is shown above; white matter is shown at the bottom. On the left panel is represented a slice from Nissl, which shows the layer II density through the neural white matter. Although the vessel density appears to be high in this three-dimensional image, it is less than 3% (in the right section of the white spots are cross-sections of the vessels). The average distance between the small vessels (capillaries) is around 50 pm. this is approximately the distance that the oxygen molecules run through by diffusion within the blood's limited transit time. The dense neurons population, synapses and glia occupies the intervascular space as shown in the drawing at the top right, which represents a hypothetical distribution of vascular and neural elements in a small section (red rectangle). The design background shows some typical neurons (red: large pyramidal cells, dark blue basketball inhibitory cells, blue: chandelier neurons inhibitors, gray: stellate cells) and their processes. (From Logothetis NK et al., 2008).

In addition to reading a signal indirectly, changes in neuronal activity, which are known to last for only a few milliseconds, are by far shorter than the compensating vascular and metabolic phenomena. In addition, this time difference is exacerbated by the process of data acquisition that can not take place in real time due to the weak signal to noise ratio of the method. This is in relation to the large vascular and metabolic brain background activity and forces one to perform some overall averages of the signals on time windows of many seconds-minutes. Because of this high background activity, one is forced to apply the subtractive procedures through a comparison with the brain activity images of the same subject at rest condition. The underlying assumption is that, whatever activity takes place in the brain at rest, is added linearly with the increase in activity induced by a cognitive task or behaviour. This hypothesis is difficult to sustain not only because of the non-linearity that is hidden in the acquisition method but also in the

brain's hemodynamics and in the processes of neural activity. The most striking limit however, concerns the limited spatial resolution. The voxels (ie, the minimum unit of detection) is at most in the order of 1 mm3, well beyond the size of a neuron (1000 μ m3: 6 order of magnitude less) or a synapse (1 μ m3: 9 orders of magnitude less)! (Fig 3). this means that in such a large volume (in the case of magnetic resonance imaging)of signal detection units, the many phenomena that will occur at the level of individual cells and of the individual synapses not be able to be grasped by the machine, but this will be processed only the phenomena that are resulting indirectly by neural and synaptic activity (for example the BOLD signal described before).

For all these reasons, the recording of neuronal and synaptic activity by fMRI and the BOLD response can not ever give the direct resolution of single neuronal cells which is essential to correlate small local responses with cognitive and behavioural functions. It should be noted however that part of these problems can be overcome by increasing the power of the scanners used, through the use of more sophisticated machines (which may produce more powerful magnetic fields), and through the creation of experimental designs that consider the resources and limitations offered by these machines. Today we know that many of our complex behaviours result from the activation of small groups or even individual neuronal cells (Cohen & Newsome 2004; Cohen & Newsome 2009). This of course assumes that the techniques used have adequate sensitivity.

1.3 ELECTROPHYSIOLOGICAL TECHNIQUES FOR THE BRAIN ELECTRICAL ACTIVITY STUDY

A more direct option which allows us to investigate neural activity consists of applying electrophysiological recording methods to individual neurons or cell groups through intra-or extra-cellular measures made with microelectrodes. The preparations on which such methods are conducted include: I) living organisms II) cut tissues III) dissociated cells from cut tissues IV) cells or tissues artificially grown V) genetically modified cells marked with indicator lights. In this section we will take into consideration the most commonly used techniques, trying to detect their application potential as well as their limitations.

Single cell microelectrodes recording

These techniques include cell membranes voltage and / or current measurements. To perform a recording the end tip of a microelectrode (generally a glass micropipette with a diameter of <1 micrometer) must

have electrical access inside the cell. To obtain such continuity the micropipette is filled with a solution having similar ionic composition to the intracellular fluid of the cell. The pipette is in turn in electrical continuity (through an electrode conductor and an appropriate RC circuit) with a particular amplifier of electrical signals that allows recording and signal processing. The voltage measured through the electrode is compared to the voltage of a reference electrode, generally a silver wire coated with silver chloride in contact with the extracellular fluid around the cell. Generally the smaller the electrode tip, the higher the electrical resistance, in this way an electrode will be built on the basis of a compromise between the size (small enough to penetrate a single cell trying to cause the least damage) and the resistance (low enough to discriminate small neural signals from the noise produced by the electrode tip).

A different approach for the recordings of single cells is exploited by the patch clamp technique: a patch-clamp microelectrode consists of a micropipette with a relatively wide tip diameter. The microelectrode is placed on the surface of the cell and then a weak negative pressure suction is applied so as to attract a small piece of the cell membrane (the "patch") inside the electrode tip; the glass tip forms a high resistance seal (GΩ) with the cell membrane. This configuration is referred to as "cell-attached" mode and can be used to study the activity of ion channels that are present in the membrane patch. When a further suction is applied, the small patch of membrane can be opened within the electrode tip, leaving the electrode sealed to the rest of the cell. This method called "whole-cell" allows for very stable intracellular recording. The disadvantage compared to the thin standard tip (used for the potential recordings inside the membrane, with minimal effects on the intracellular fluid ionic constitution) consists in the fact that the cell's intracellular fluid is mixed with the solution inside the recording electrode, and then some important components of the intracellular fluid may be diluted. A variant of this technique, the technique of "perforator patch", can minimize these problems. Instead of applying the suction to open the patch of membrane, it is possible to make small holes at the patch level with certain antibiotics that form some pores of such dimensions that the large molecules, such as proteins, are not able to cross them.

The measures described above are found to have an excellent time resolution, unfortunately these recordings can only provide information from a cell, unable to catch the interaction within neural networks.

Measures with microelectrodes arrays

The extracellular fluid constitutes a vehicle of conduction around the neuron. We know that when the neuron is in a rest state, its membrane is uniformly polarized and the net flow of charges is equal to 0. When a neuron is active, however, it is not uniformly polarized: the dendrites are at a different potential with respect to the soma which is located at a different potential than the axon and at the moment in which the action potential propagates along the axon, different axon regions may be at different potentials. This spatial inhomogeneity of the potential produces a flow of ions, and then current, from one to another part of a neuron exploiting the extracellular space as a conductor. So the extracellular fluid, as we say, can be regarded as a conductor, inside which the current flow generates electric fields that can exert a force on the conductor's electric charges. This force is the one that we measure as a form of potential difference.

The Microelectrode arrays (MEAs) are multiple electrode recording plates, essentially acting as an interface that allows to connect the neural cells to an electronic circuit. There are two main classes of MEAs: implantable MEAs (used in vivo) and non-implantable MEAs (used in vitro). Very briefly, during the recording the electrodes located on MEAs translate the voltage change generated by ion fluxes in electronic currents. When stimulated, the electrodes transduce the electronic currents into ionic currents which trigger the voltage-sensitive ion channels on the membranes of excitable cells, causing cell depolarization and potentially the genesis of an action potential. This technique is generally used to perform electrophysiological experiments on tissue slices or cell cultures. The main advantages of this method are: 1) allow you to record from multiple electrodes rather than individual, 2) you can select different recording sites within an array that can contain hundreds of cells, 3) can simultaneously receive data from multiple sites. So with extracellular matrices of electrodes it is now possible to extracellulary monitor neuronal activity by recording the action potentials that are produced by a population of nerve cells in the brain. These electrodes may be implanted chronically in freely moving animals, and in this way it is possible to have an overview of the properties of the neural network from which we are recording. The disadvantage is that each of the electrodes composing the matrix records the activity of spikes (action potential) from a certain number of neurons, those closest to the tip of the single electrode. This turns out to be useful, however, when the behavioural task has a significant effect inside the population of neurons, but this method of recording the spatial information that can be obtained on the different brain areas involved is very limited because more than few matrix cannot be positioned.

The problems and limits of the classical electrophysiology may be overcome when employing a mix of such methods with optical techniques, in combination with indicators or probes developed through modern genetic engineering.

-Electroencephalogram (EEG)

To decipher the brain activity with a level of accuracy useful to correlate it with behaviour, it is necessary a higher number of parallel and independent measures from individual neurons, carried out by relatively large brain areas. There are some methods capable of measuring the electrical activity of the brain in parallel by many points. This method is called electroencephalography (EEG): it is made by extracellular electrodes placed on the scalp, which detect the action potentials of neurons more close to each other. These extracellular recordings make it possible to detect even the synchronized activity of large cell aggregates; called field potentials. These field potentials have the shape of individual transient events, called "peaks", with slow temporal resolutions (from hundreds of milliseconds to seconds). The EEG is constituted by a set of field potentials recorded from many electrodes placed on the surface of the scalp. The set of sites where the electrodes are placed is called montage. The montages can be constituted by monopolar dispositions in which each electrode records the electrical activity at a unique site on the scalp (active electrode) with respect to a site farthest (indifferent electrode). On the contrary, the electrical activity can be recorded with reference to pairs of electrodes placed on the scalp, in this case both electrodes are active. The EEG electrical activity is an attenuated measure of the extracellular current flow generated by the summation of the activity of many neurons, however, not all the cells contribute equally in the EEG signal. The EEG depends predominantly on the cortical neurons present near the electrode, while the structures located deep in the brain, such as hippocampus, thalamus, and brainstem, do not contribute directly to EEG. The EEG signal is inevitably distorted by filtering and attenuation produced by the bone and nerve tissue layers interposed between the electrode and the active nerve cells. Therefore the amplitude of the EEG potential (in the order of microvolts) is much smaller than the voltage variations that occur at the level of individual neurons (in the order of millivolts). EEG is applied commonly to the study of different cognitive processes, and in this case, such techniques are called evoked potentials, in which are recorded the electric potentials of the nervous system that follow the presentation of a stimulus, in this case they are known as sensory evoked potentials and, depending on the organ that is stimulated, they can be called visual, auditory, somatosensory potential, etc. ..

Although it provides a simultaneous reading of the electrical activity from many brain areas, unfortunately the limit of this technique, as already mentioned, resides in the fact that we can acquire, from the surface of the cranial theca, only the signals of neuronal populations heavily filtered by the volume conductor. In addition, the cortical areas from which the integrated activity originates are never well defined (electrodes close to each another record approximately the same EEG activity) and since individual responses vary widely in size, you usually have to perform a time average on many subsequent recordings to underline the signals of interest.

None of the methods previously described are therefore particularly efficient in directly measuring the brain activity due to lack of both temporal and spatial resolution.

1.4 OPTICAL INNOVATIVE TECHNIQUES FOR VUSUALIZATION OF BRAIN STRUCTURES

A major challenge in neurophysiology is the ability to record the activity from multiple, or ideally from all, the neurons over time. The optical microscopes, together with specific fluorescence indicators of neuronal activity, will be of great importance for this purpose. As we shall see in the next section, thanks to such techniques, voltage sensitive direct images of membrane depolarization have been achieved,

Over the last few years many new medical-biological applications have been developed (Helmchen, F & Denk, W., 2002, Merz, J., 2004, Svoboda, K & Yasuda, R., 2006) that are based on the use of the interaction between light and biological materials which often utilize fluorescent chemical compounds in order to visualize both nervous tissue morphology under vital conditions and the acquisition of functional information. The technology of confocal microscope imaging has allowed unprecedented three-dimensional high resolution imaging of neuronal preparations both in vitro and in brain tissue. The photon confocal microscope was developed, thanks to the work of Watt Webb in the early 80s, in order to collect light from the focal plane, eliminating the acquisition of light from other regions located above and below the focal plane. This result was achieved with a puntiform laser source and collecting the fluorescence emitted through the spatial filter (pinhole). The pinhole restricts the photons collected at the focal point on the analyzed sample. Through a scan of this point that is illuminated on the axes XYZ of the image, can be rebuilt an optical section of the brain tissue. The resolution of these optic imaging methods is much higher than that coming from the standard brain (for example that obtained by magnetic resonance imaging) and allows to display boutons or synaptic spines with a diameter less than one micrometer.

Meanwhile, confocal laser scanning microscopy (CLSM) is distinguished from classical optical microscopy by the higher image resolution. At the base of this improvement is the use of a laser source as a source of illumination; the laser light is coherent, monochromatic and concentrated in a collimated rectilinear ray.

The main CLSM characteristic resides in the fact that, different from classical optical microscopy, it allows the acquisition of the fire point only, a characteristic called confocality. The cone of light produced by a laser ray, at a given wavelength, will affect both the focus point and what is around (producing a "Surrounding" noise represented by the light coming from the regions around and below the confocal plane) and any excited matter will emit a light of higher wavelength. If the emitted light was to pass solely through a spectral filter, only an image of the focal point would be obtained,; in a one photon

CLSM (1PCLSM) emitted light must pass through a adjustable spatial filter (pinhole) that eliminates the"surrounding" emitted light The pinhole is nothing more than an opening that works in a similar way to our pupil, the more closed the pinhole less light will be able to cross it, or rather, the only light emitted from the point of fire will be able to pass through it, while the light emitted from the surrounding areas will be excluded (Fig. 4). It follows that the more the pinhole will be closed the greater the confocality will be and, consequently, the image clearness. The light emitted by the sample is captured by a photomultiplier and processed through special software that generates an high resolution digital image, which can be later analyzed.

The possibility of using a source of monochromatic light enables us to excite the material to a single wavelength and the signal output displayed comes only from the photo excitable groups activated at that particular wavelength. Consider for example the well-known GFP (green fluorescent protein) and its many variants excitable at different wavelengths as the RFP (red fluorescent protein), the YFP (yellow fluorescent protein), CFP (cyan fluorescent protein) etc. … and we consider the two variants of GFP and YFP: these two molecules possess partially overlapping of excitation and emission spectra (fig 4), with the classical fluorescence microscopy would be virtually impossible to separate the signals coming from single molecules simultaneously present in the same sample, while with the CLSM this is possible. By using a series of emissions that excitation spectral filters CLSM is able to separate bands of wavelengths in the range as low as a few tens of nanometers, in this way it is possible to distinguish spectra partially overlapped with absolute precision.

Another fundamental characteristic of the CLSM is the depth of field: the physical characteristics of the laser light to allow photons to penetrate deeper than the light sources used in a conventional type optical microscopy. This feature allows to scan optical slices at different depths (Z-stack scanning), then their acquisition and subsequent 3D reconstruction.

More recently we are present at the development of optical imaging techniques based on the use of nonlinear interactions between light and matter (Helmchen, F & Denk, W., 2002, Merz, J., 2004). These optical phenomena can be induced through the use of coherent light sources with high intensity such as pulsed lasers. The main feature that makes this technology so useful for the modern study of the nervous system is the reduced susceptibility to the scattering phenomena that makes feasible a visualization of fluorescent molecules located deep inside the brain tissue, and with high resolution and great contrast. In particular, the confocal 2 photons laser microscopy (Denk, W et al., 1990), combined with the most modern techniques of fluorescent labelling, has opened a largely evolving field, attempting to image the brain under living conditions (for a review see Svoboda, K & Yasuda, R., 2006).

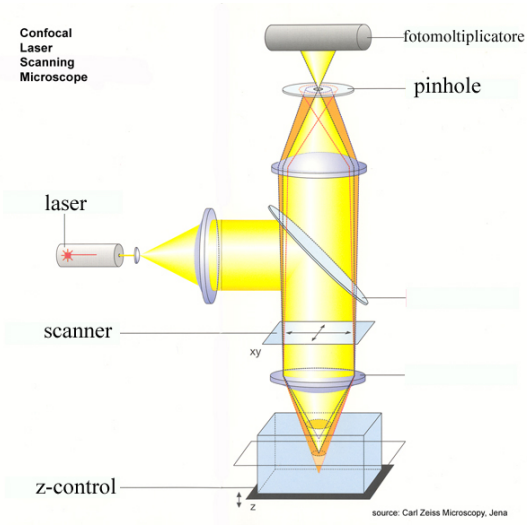

Fig 4: organizational scheme of a 1 photon confocal microscope: Note the cone of light produced by a laser ray that will affect both the focal point both his around. The light emitted from matter excited will cross an adjustable spatial filter (pinhole), the more it will be closed, the greater the light emitted from the areas surrounding the point of focus will be excluded. The light will come later captured by a photomultiplier, and through special software will generate a digital image with high resolution (Adapted from Oheim M, et al., 2006).

Today, we can see into the cerebral cortex, up to about an inch in depth, and identify its vessels, neurons, dendrites, dendritic spines, synapses and glial cells, This can be done without any damage to the nervous tissue which can be kept in living conditions for long periods and then retested several weeks to months later (Svoboda, K & Yasuda, R., 2006). However, can you distinguish between an optical microscopy technique that uses a linear technique of excitation and one which is uses non-linear excitation? What are the advantages? The traditional techniques, including confocal microscopy, generate a contrast that results from the interacting light-matter, in which the elementary process involves a single photon of light. In this case the result is linearly dependent on the intensity of the incident light. The non-linear techniques are fundamentally different and exploit light-matter "higher order" interactions where more photons are used to generate contrast. The non-linear processes which may be generated are various. Among them, multi-photon fluorescence microscopy is surely the most used technique. If two photons hit simultaneously, in less than a femtosecond their energies sum, and they emit a fluorescent photon, which excites the molecule that has just been hit (Fig. 5). In a similar way, three or more photons can be combined to generate these electronic transitions, and then excite the molecules (Fig 5). Typically the multi-photon absorption occurs at more near-infrared wavelengths (700-1000nm), while the emission occurs in the spectrum of visible light. The near-infrared wavelengths, lower energy, are able to penetrate more deeply into the tissue, but are also less phototoxic, thanks to the near absence of endogenous

molecules in the tissue, which can absorb this spectral range. This is a significant advantage for deep tissues imaging in living conditions.

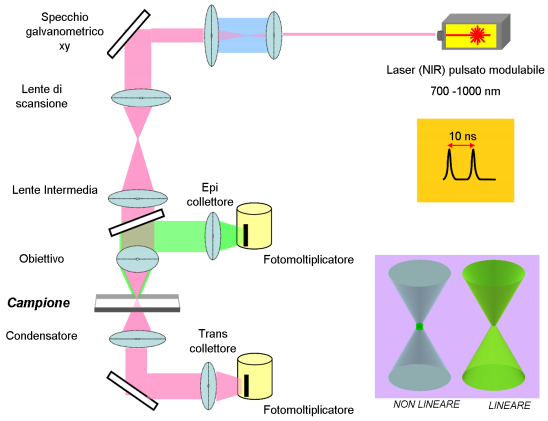

Figure 5 - Schematic organization of a 2-photon confocal microscope. A laser source provides the pulses close (at a distance of 10 ns) in the infrared. The insert in the lower right is shown the spatial confinement of the signal generated due to a non-linear excitation compared to that produced with an excitation linear: in the first case, the phenomenon occurs only in the point of fire, in the second case it involves the entire cone structure (Adapted from Oheim M, et al., 2006).

.

The multi-photon absorption efficiency depends on the physical characteristics of the molecule and is affected by the spatial and temporal distributions of the arriving excitation photons. The probability of these multi-photon transitions are extremely low at low excitation intensities . When the excitation light is focused, thanks to an objective glass, the spatial density will rise at the point of focus and becomes sufficient to generate transition events. Furthermore, thanks to the use of pulsed source lasers with varying wavelengths, the frequencies of excitation necessary to excite the molecules of interest can easily be reached on the other hand, thanks to their characteristic "ultrashort" pulsations (fraction of a picosecond) , which concentrate the energy, the electronic transitions are further facilitated, enhancing the excitation process. It is interesting to observe that in all the nonlinear contrast processes, the signal produced depends on the photons density in a supra-linear manner (Merz, J., 2004). Consequently, when a laser ray is focused through an optical lens, the multi photon absorption is further confined to the perifocal or observation region. The absence of absorption at regions outside the focal plane is in contrast to classical confocal microscopy, where the absorption of a single photon occurs within the whole cone of excitation (Figure 5).

This lack of absorption from the planes outside the focal point significantly reduces the damage caused by photo-toxicity and improves tissue viability, crucial for prolonged imaging. Furthermore, the spatial localization of excitation allows a fine three-dimensional resolution, which avoids the use of a spatial filter or pinhole that is used both to limit the emission to capture only photons coming from the point of fire but also reduces the number of photons captured and subsequently the emission intensity: the absence of a pinhole and a high numerical aperture objective can allow even photons emitted by the surrounding tissue to be caught. These photons are in a scattering state and travel with a different space – angular range. These optical imaging techniques are revolutionary but if you intend to apply them to the functional study of the brain, they need to be combined with "ad hoc molecules" that produce optical signals capable of detecting changes in brain functioning. Below we will list some of the molecules and technologies that are combined with 2-photon microscopy to allow the capture of functional information.

1.5 OPTICAL IMAGING CHANGES IN THE MEBRANE POTENTIAL OF INDIVIDUAL CELLS

In recent decades thanks to an increasing advancement of genetic engineering, it has beenmade possible to develop specific genetically encoded indicators for neural activity aimed at providing one of the more elegant solutions for the detection of images from defined neural populations. These activity indicators are special dyes, or engineered proteins, with most recent attention on a wide variety of protein-probes as alternatives to synthetic indicators (A. Miyawaki, 2005). These indicators consist of genetically encoded fusion proteins, fluorescent components of voltage-gated ion channels (Ataka K & Pieribone VA.; 2002) and voltage dependent phosphatases (Dimitrov D et al., 2007). Conformational changes in the transmembrane sensors for voltage are coupled with changes in the luminescence of individual XFPS, (proteins used in genetic techniques known as a repressor trap, strategies that are based on random insertions within the target gene's genome that are under the control of promoters, where the transgene is expressed randomly, according to the specific pattern conferred by the proximity to the site of integration). The voltage indicators are then brought to the plasma membrane of the specific cell populations. The advantage of this consists of the fact that only cells that possess the transgene will express the modified protein, greatly reducing the background due to nonspecific incorporation, which is more likely to occur when using certain types of fluorescent voltage.

Although the responses of these voltage indicators are generally too small to be useful for routine measurements at the individual neurons level, recent developments have led to cautious optimism. For example, a hybrid sensor has been developed which combines a genetically encoded fluorescent probe (a

GFP, green fluorescent protein, anchored to the membrane) with the dipicrillammina, a synthetic molecule sensitive to the voltage that is divided within the plasma membrane, providing a broad fluorescence signal and a rapid response (Chanda et al., 2005).

The following are the dyes and proteins most commonly used in these optical imaging techniques:

-Dyes

With voltage-sensitive optical probes it is possible to measure membrane potentials at the organelle or cell level that are too small for microelectrodes. Furthermore, by using them in conjunction with the optical imaging techniques, these probes can be used to map variations in membrane potential at the level of excitable cells (Witkowski FX et al., 1998) with a spatial resolution that is very difficult to achieve with the use of microelectrodes.

How do these probes work? The plasma membrane of a cell, as was previously discussed, has a transmembrane potential that is around the value of -70 mV (interior negative) as a result of gradients of K +, Na + and Cl-which are retained through the processes of active transport . The probes sensitive to the voltage offer an indirect method for detecting transfer of these ions, since the ionic fluorescent indicators may be used to directly measure the changes in specific ion concentrations.

Increases and decreases in membrane potential, respectively understood as membrane hyperpolarizations and depolarizations, play a fundamental role in various physiological processes such as the propagation of the nerve impulse, cellular signaling or ion channel opening. These probes are very important tools for the study of these processes, as well as for the study of many other known mechanisms in cellular and molecular biology (see in this respect Nicholls DG & Ward MV., 2000).

What are the best probes? What are the purposes for which these best apply? Select the best probe sensitive to the voltage that may be complicated for the different variations in their optical response, for their different phototoxicity and for their interaction with other molecules. The voltage sensitive probes can be divided into two different categories based on their mechanism of response:

I) Fast-response probes: Operate through changes in their electronic structure, and consequently in their fluorescence properties, as a function of changes in the surrounding electric field (Fig 6). Their optical response is sufficiently fast to be able to detect transient changes in potential (speaking of milliseconds) of excitable cells, including individual neurons. However, the changes in their fluorescence (depending on the potential) appear to be small, with fast-response probes typically showing a change in fluorescence of 2-10% per 100 mV!

II) Slow-response probes: show changes in fluorescence depending on their cellular potential according to their transmembrane distribution (Fig 6). The size of their optical responses is much higher than that of fast-responding probes (a 1% change in their fluorescence for every mV). The slow response probes are

suitable for detecting changes in the average of the membrane potentials at the level of not excitable cells which may be caused by the activity or respiratory changes in the permeability of ion channels.

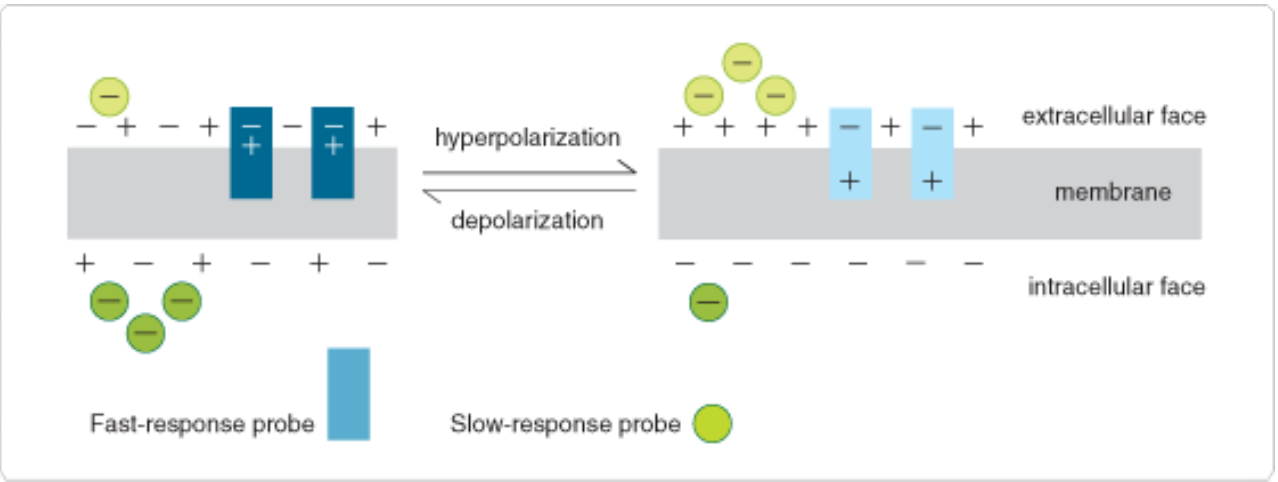

Fig 6: response mechanism of probes sensitive to membrane potential. The electric field driving changes of probes in response to rapid intramolecular distribution of charges, which in turn produce changes in the intensity of their fluorescence (represented by the color change of the illustration). The slow response probes are lipophilic anions (as in the drawing) or cations that are translocated across the membrane with the use of electroporation. The changes in fluorescence associated with redistribution in the membrane (represented by the color changes in the illustration) result from the sensibility of the probes to the intra-and extracellular environment. In this way, the speed of sensitive response to the voltage directly reflects the time constants of the underlying processes - rapid intramolecular redistribution of the electrons versus slow movement of the entire transmembrane molecules (From http://www.invitrogen.com).

Some fast and slow response probes, which will serve as an example for what has been said above, include:

i) The ANEP DYES represent a family of dyes (AminoNaphtylEthenylPyridinium) that have been developed by Leslie Loew et al. (1985) (Flühler E, Loew LM, 1985) and are considered among the most sensitive probes for rapid response. For example, the 4-ANEPPS and- the 8-ANEPPS show uniform changes in fluorescence intensity of 10% for 100 mV. These probes were tested in a variety of tissues andcells (neural, cardiac, etc.)and into a variety of membrane models (Loew LM et al., 1992). The range of response time (milliseconds) of these dyes compensates for their small amplitude response (Fig 7).

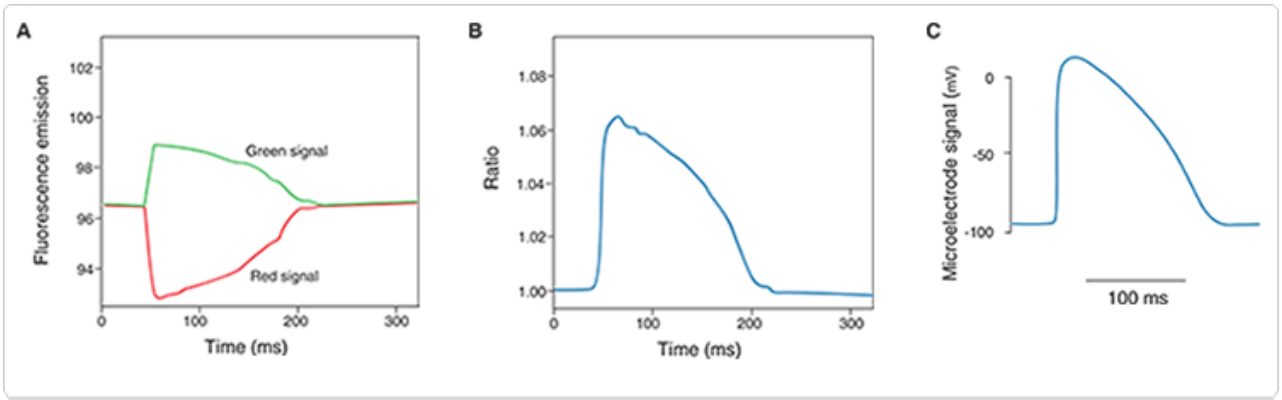

Figure 7: Detection of action potentials in intact rabbit hearts obtained through the use of 4-ANNEPS. Cut rabbit hearts were loaded with 4-ANNEPS in a medium containing the dye. The fluorescence was excited at 488 nm with an argon ion laser. The emission components at 540 ± nm (green) and> 610 nm (red) were identified simultaneously through two photomultipliers **(A).** The signals ratio from green to red show an increased fractional change during the cycles of action potentials with respect to each of the signal components; this also follows the transmembrane voltage curves recorded simultaneously by an intracellular microelectrode **(C).** Furthermore, the fluorescence measures levels of reduced motion artifacts which typically distorts the optical signals detected by the cardiac contractions (From Loew LM et al., 1992).

Both 4-ANEPPS and 8-ANEPPS respond to hyperpolarization with a decrease in their excited fluorescence at 440 nm and with an increase in the excited at 530 nm (Montana, V et al. 1989). Such a shift of the spectrum allows the use of methods to calibrate ratiometric changes in the membrane potential on the relationship of the changes in the fluorescent signal (Zhang, J et al., 1998). Using 8-ANEPPS, Loew et al. were able to follow the changes in membrane potential along the surface of a single cell of a mouse neuroblastoma (Bedlack, RS. Loew LM 1992) and were thus able to define some differences between the transmembrane potential of the soma and neurite.

The CARBOCYANINE: In the wide range of slow response dyes (Carbocyanine, Rhodamine-probes, Merocyanina Oxonols) we can take for example the first that have been developed as fluorescent probes, namely the Indo-, thia-and oxa-carbocyanine (DiI, DiS and DiO) (Sims, PJ et al., 1974). These cationic dyes accumulate on hyperpolarized membranes and are transported along the phospholipid bilayer (Guillet, EG et al., 1981). They aggregate at the level of the inner membrane border and generally cause a decrease in fluorescence, although the magnitude and direction of the fluorescence response seems to depend in a massive way on the concentration of the dye and its structural characteristics (Sims, PJ et al., 1974) .

The carbocyanine most commonly used as a colorant for measurements of membrane potential was DIO6 (3) (Rottenberg, H. Wu, S.; 1998). In measurements of cytometry flow, the intensity of carbocyanine fluorescence not only depends on membrane potential, but also on the size of the cell. There have also been developed in bacteria some methods of measuring the fluorescence that exploit the shift to red (for the measures of dependent potential shift) within the emission spectrum of DIO2 (3) (Shapiro, HM.

2000). Furthermore, among the many cellular phenomena that can be studied by applying such probes, DiIC1 (5), a indocarbocyanine excitable to a wavelength of 633 nm (Pham, NA et al., 2000) was used to measure the mitochondrial potential of apoptotic cells. (Hakem, R et al., 1998).

One of the most interesting areas, with greater potential for future development, is represented by genetically modified proteins. In order to understand how voltage-gated ion channels are able to "feel" the membrane potential and to act in a fully synchronous way with it, you need to thoroughly study the electric field of proteins. We know that the classical methods deriving from electrophysiology (as has already been discussed above) have the significant limitations of spatial resolution. They provide us with information about the average changes of the entire cell voltage using intracellular recordings, even if the electric field potential in biological systems tends to be rather nonhomogeneous. For this purpose there have been engineered many families of fluorescent probes to study the strength of the electric field of the ion channels and to detect changes in the membrane potential of genetically specified neuron groups that are located on brain slices. Using optical methods (such as the use of fluorescent probes), it is possible today to thoroughly measure the electric field and to follow changes in the potential with high spatial and temporal resolution. Unfortunately, these probes are equipped with high hydrophobicity, causing their retention on the superficial layers of the tissues and preventing them from further penetration and from marking cells found in the deeper layers. Additionally, this inconvenience carries a high fluorescence background.

Building on this, we briefly describe some applications of these modified proteins that give us the opportunity to study the changes in potential at the individual cell level:
The voltage sensitive ion channels consist of tetramers (channels K +) or monomers having four domains (channels Na + and Ca2 +) each with six transmembrane helices. In each monomer or domain the fourth transmembrane helix (S4) contains a number of positive charges on lysine or arginine which are separated by hydrophobic residues (Noda et al, 1984). Changes in membrane potential drive changes in the conformation of the S4 helix, which cause the opening of the channel's pore with the subsequent ion flux (Aggarwal & MacKinnon, 1996). With the introduction of a fluorophore, through a linker, at the SH group level of a cysteine, it was possible to study the changes of the local conformation of these channels to their opening. The dipoles of certain dyes, such as-4-and-8 ANEPPS (see above) interact with the electric field (Zhang et al., 1998) and, as a result, the emission spectra are shifted in proportion to the electric field. The shift of the wavelength in the spectrum of excitation and emission is also given back as an electrochronic shift. The choice of a particular combination of excitation and emission through the interference filters allows to translate this shift in intensity changes. Loew and colleagues (2003) created a chromophore (of ANEPMI-1-and-1-ANEPIA) (Asamoah et al., 1997) with which, it is possible to merge these dyes in predetermined places, in order to detect local changes in the strength of the electric field, as

shown by the studies that have applied these techniques to the study of K + channels “shaker” mutated in Xenopus oocytes under conditions of voltage clamp (Cha & Bezanilla ,1998) When you try to view a specific tissue function or neural network using optical instruments, there are some important questions regarding the characteristics of the probes used by us. One of these involves the ability of the probes to penetrate deep within the tissue. Even more important is the fact that the probes are specific and target only some electrically active neurons and not, for example, surrounding glial cells surrounding, as this would add only background to the true fluorescent signal (Konnert et al., 1987). Also, it could record the signal from a selected subset of neurons in order to assign the recorded signal to the cells from which it is derived and, therefore, identify the nature of the various circuit elements within the neural processes. There are some fluorophores, such as GFP, which have been successfully employed in the measurements of the concentrations of Ca2 +, Cl-and pH (Miesenbok et al., 1998; Kuner et al., 2000; Ng et al., 2002; Wang et al., 2003; Rogers et al. 2005.). For the purpose of detecting the membrane potential, a construct was designed based on a GFP fused with K + and Na+ channels (Fig 8). Given that conformational changes in ion channels sensitive to the voltage are the result of membrane voltage changes, coupling these with a chromophore such as GFP may detect the intra-protein movements that follow changes in membrane potential. The first reporter protein of this type, called flash, was generated by the insertion of GFP within the C-terminal of the 6 propellers (Warrior & Isacoff, 2001; Siegel & Isacoff, 1997). The fluorescence of this construct was governed by the kinetics of the C-type inactivation so that the response time was found to be relatively slow. The construct SPARC, where the GFP was inserted within a sodium channel, between domains II and III, has much faster kinetics with a response time constant below 0.7 ms (Ataka & Pieribone, 2002).

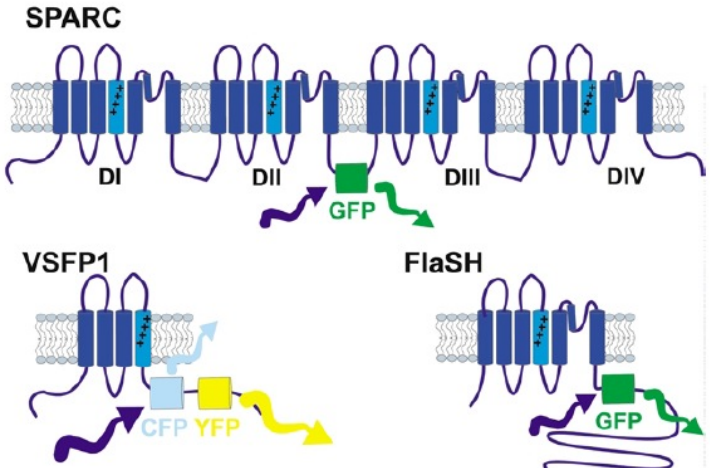

Fig 8: Schematic of genetically encoded fluorescent voltage sensors. Specifically, the figures represent voltage sensors based on ion channels sensitive to the voltage. SPARC consists of a channel rSKMN1 with a GFP introduced between the II and III domains. VSFP1

includes the voltage sensor of the channel Kv2.1 fused with a tandem of CFP and YFP at the C-terminus. In FLaSH GFP is fused to the Shaker K + channel C-terminal segment S6. (From Ataka & Pieribone, 2002).

Although all of these tools successfully record the changes in the potential of the model systems, the fluorescence response of in vitro systems appears to be very small and therefore, even less, the signal cannot be identified in more complex systems such as fabric portions.

1.6 OPTICAL IMAGING VARIATIONS OF Ca2 + INTRACELLULAR CONCENTRATIONS IN THE INDIVIDUAL CELLS

The activity of neuronal spiking can alternatively be measured with sensors capable of detecting the changes in the concentration of intracellular ions produced by the electrical activity. As we have already discussed above, when a neuron produces an action potential, the change of the membrane voltage that follows determines the opening of membrane channels that in turn produce a flow of several ion families in and out of cells. In particular the opening of voltage-sensitive Ca2 + channels causes significant increases in the concentration of intracellular Ca2 + thanks to the very favourable ionic gradient (2 mM [Ca2 +] out; 50 nM [Ca2 +] in a gradient of 40,000 times). Although the cellular expression of Ca2 + channels is extremely variable among the different types of neuronal cells, this method is able to detect signals produced by individual cells (see Helmchen, F & Waters, J., 2002). The dyes for Ca2 + have high spatial and temporal resolution And the fluorescent probes that show a response to the calcium binding are extremely useful to investigate the changes in the intracellular concentration of Ca2 + using fluorescence microscopy (as well as the flow cytometric and spectroscopy fluorescent) (Burchiel SW et al., 2000). These indicators of fluorescence, many of which were derived from chelating agents of Ca2 + (RY Tsien, 1980), have been developed from the work of Roger Tsien and colleagues. These molecular probes work in a concentration range between <50 nM and> 50 uM. When you want to select a fluorescent indicator of Ca2 + there must be taken into account some important factors:

I) The shape of the indicator (generally a salt, ester or dextran conjugate), will influence the method for loading, retention and intracellular distribution of the same (for example the salt and form dextran conjugate are generally loaded in cellular level via microinjection, electroporation or reagents that act through flows of pinocytosis).

II) Measurement mode, depending on the type of data required, qualitative or quantitative, of the ionic concentration. Only certain types of dyes have ratiometric properties and allow to accurately calibrate the

molar amounts of calcium, others will only allow a qualitative estimate on the increase of fluorescence compared to a control condition.
III) The dissociation constant (Kd), which must be compatible with the range of calcium concentration of interest.

1.7 OPTOGENETIC

With the identifcation of the gene for a light-responsive membrane protein in microorganisms called bacteriorhodopsin (BR), Stoeckenius and Oesterhelt (1971) set the foundation for a technology, which is today described by the term "optogenetics" (Oesterhelt and Stoeckenius 1973; Deisseroth et al. 2006). Three decades had passed before scientists were able to take advantage of the potential of this seven-transmembrane domain containing light-transducing proton pumps, which in nature serves as a regulator of homeostasis and phototrophy in microbes (Beja et al. 2000). Encoded by a single open reading frame, it works as an optical controller of transmembrane ion flow combining fast action and coupling of sensor and effector in a monocomponent system (Oesterhelt and Stoeckenius 1971). Later, rhodopsin mediated responses were also studied in the alga Chlamydomonas (Harz and Hegemann 1991) and since the photocurrents were ultra-fast the authors claimed that the rhodopsin and the channels were intimately linked (Holland et al. 1996). This concept was proven true by Nagel and colleagues when they showed that the Rhodopsins are directly light-gated ion channels. They used amphibian and mammalian cells as hosts to express channelrhodopsin-1 (ChR1), a light-gated proton channel from the green algae Chlamydomonas rein- hardtii. In a modified patch clamp set-up they proved that rhodopsins react functionally upon laser illumination also in mammalian cells (Nagel et al. 2002). What was initially used as an experimental model system to study channelrhodopsin function turned into the precursor of a novel scientific tool. With the functional characterization of ChR2, a directly light-gated cation-selective membrane channel, Nagel et al. (2003) showed that mammalian cells expressing ChR2 could be depolarized simply by illumination. The full conversion of this approach into an optical control device of cell activity happened in 2005 when it found its way into neuroscience. The Deisseroth lab (Stanford University) applied lentiviral gene delivery to express ChR2 in rat hippocampal neurons. In combination with high-speed optical switching, neuronal spiking was elicited by photostimulation in milliseconds (Boyden et al. 2005). In parallel, the labs of Yawo, Herlitze and Gottschalk independently demonstrated the feasibility of ChR2-based optical neuronal manipulation (Li et al. 2005; Nagel et al. 2005) They used pulsed light delivery to take full advantage of the fast kinetics and high conductance of ChR2. This strategy was made possible with fast optical switches, but other increasingly common equipment, such as

pulsed lasers, would also suffice. Unlike electrical stimulation, glutamate uncaging (Katz, L.C. et al., 1994) and high-powered laser excitation methods (Hirase, H, 2002) ChR2 can be genetically targeted to allow probing of specific neuron subclasses within a heterogeneous neural circuit, avoiding fibers of passage and the simultaneous stimulation of multiple cell types.

The interplay of optics, genetics, and bioengineering in this novel approach was the inspiration to coin the term "optogenetics", which can be defined as optical control of cells achieved by the genetic introduction of light-sensitive proteins (Deisseroth et al. 2006). Another milestone in the evolution of optical control was the discovery of an inhibitory opponent of ChR2. Although relative reduction of neuronal activity had previously been shown for the Gi/o protein-coupled vertebrate rat opsin (Ro4, a type II opsin) by activating G protein-gated rectifying potassium channels and voltage-gated calcium channels (Li et al. 2005), complete and fast silencing was achieved by using a microbial (type I opsin) chloride pump. Halorhodopsin (HR) (had been discovered decades before its conversion into a research tool (Matsuno-Yagi and Mukohata 1977). Halorhodopsin Is a light-driven ion pump, specific for chloride ions, and found in phylogenetically ancient Archaea, known as halobacteria. Expression of Natromonas pharaonis HR (NpHR) in neuronal tissue enables optically induced cellular hyperpolarization by pumping chloride into the cells. Consecutive inhibition of spontaneous neuronal wiring can be achieved on a millisecond time scale (Zhang et al. 2007, b; Han and Boyden 2007). A major advantage compared to Ro4 is the manipulation via Cl-, an ion that is not involved in intracellular signaling such as calcium and the use of all-trans retinal instead of 11-cis which is functioning as a chromophore in Ro4. Due to the spectrally separated activation maxima of ChR2 and NpHR, bidirectional optical modulation is possible, offering excitation and silencing of the same target cell. Even more efficient optical silencers, the proton pumps Arch and ArchT, with similar activation spectra were found in archaebacteria after screening various species (prokaryotes, algae and fungi) for microbial type I opsins (Chow et al. 2010; Han et al. 2011). In an attempt to establish a simultaneous multi-excitatory optical control system by using spectrally separated opsins, red-shifted ChR1 from Volvox carteri (VChR1) was identified. VChR1 works like ChR2 as a cation channel and extended the optical spectrum of cellular excitation toward green light (Zhang et al. 2008). Yet VChR1 applicability in mammalian cells was strongly limited by small photocurrents due to insufficient mem-brane expression; a limitation that has been circumvented by the generation of a chimeric channelrhodopsin (C1V1) composed of channelrhodopsin-1 parts from Chlamydo- monas reinhardtii and Volvox carteri (Yizhar et al. 2011). In a very recent publication, a new channelrhodopsin from Mesostigma viride (MChR1) with a similarly red-shifted action spectrum has been identified and mutated (Govorunova e tal. 2011). Heterologous expression of native MChR1 in HEK293 cells indicated peak currents comparable to VChR1 with faster current kinetics making MChR1 a potential candidate for red-shifted optogenetic control, although toxicity and expression levels in neuronal tissue remain to be analyzed. Channelrhodopsins show structural homology to other type I

opsins, however, in their working principle they fundamentally differ from NpHR and BRs like Arch and ArchT (Fig. 9). ChRs are non-selective cation channels that open when illuminated by green light with passive infux of predominantly Na+ and, to a lesser extent, Ca2+ ions along a membrane gradient resulting in the depolarization of cells expressing these molecules (Nagel et al. 2003). In contrast, HR and BR are ion pumps that work against an electrochemical gradient across the membrane (Racker and Stoeckenius 1974, Schobert and Lanyi 1982). With an excitation maximum at 589 nm, NpHR pump chloride ions into the cell when activated by yellow light, causing a hyperpolarization with consecutive silencing of the target cell. Arch and ArchT also hyperpolarize cells, but by pumping H+ outwards and in a more rapidly recovering manner. Excitation maxima are at approximately 566 nm for Arch and ArchT (Chow et al. 2010; Han et al. 2011).

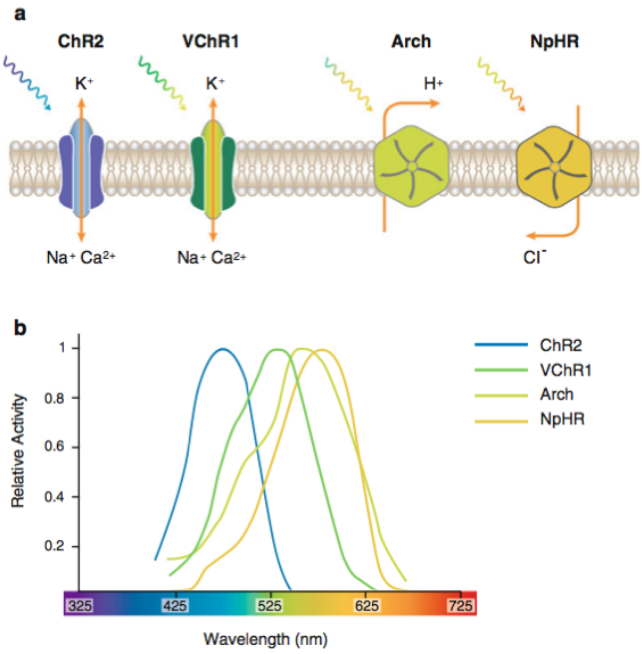

Fig. 9: The optogenetic princi-ple: changing the membrane voltage potential of excitable cells. **(A)** Activating tools—chan-nelrhodopsins: channelrhodop-sin-2 from Chlamydomoas reinhardtii (ChR2) and channel- rhodopsin-1 Volvox carteri (VChR1) from nonselective cation channels leading to depolarization of target cells. Silencing tools—ion pumps: archaerhodopsin-3 (Arch) from Halorubrum sodomense works as a proton pump and leads to hyperpolarization of the target cell such as the chloride pump NpHR (NpHR) from Natrono- monas pharaonis. **(B)** Spectral working properties of light- sensitive membrane proteins (From Rein ML, 2011)

The most common method of delivering optogenetic transgenes into the nervous system is to infect cells with a replication deficient virus, typically a lentivirus or adeno-associated virus (AAV), that contains the transgene of interest driven by a short promoter or enhancer element (Luo L, et al. 2010). Cell-type specific promoters that have been used to drive optogenetic transgenes include Ef1 α (strong, ubiquitous expression) (Tsai HC, et al. 2009) SynapsinI (expression limited to neurons) (Zhang F, et al. 2007), CamKII (expression limited to excitatory neurons) (Boyden ES, et al. 2005), and GFAP (expression limited to astrocytes) (Gradinaru V, et al. 2009). There are a small number of short (<3kb) promoters that

ensure targeting to specific cell-types in the brain, such as the ppHcrt promoter that targets hypocretin (Hcrt)-expressing neurons in the lateral hypothalamus (Adamantidis AR, et al. 2009), or the synthetic PRSx8 promoter that targets noradrenergic and adrenergic neurons that express dopamine beta hydroxylase (Abbott SB, et al. 2009). Unfortunately, the short promoters that fit into viral vectors (<3 kb) often do not retain cell-type specificity (Luo L, et al. 2009).Optogenetic constructs with much longer promoter sequences can be utilized in mice generated with transgenic technologies. For example, the Thy-1 promoter is used to drive high expression levels of a transgene in a random subset of neurons (Luo L, et al. 2009). Founders of these Thy-1 lines are selected for expression patterns based on the needs of the investigator. Several transgenic mouse lines (Arenkiel BR, et al 2007) and one transgenic rat line (Tomita H, et al 2009) carry ChR2 under the Thy-1 promoter. Other transgenic mouse lines use Thy-1 to drive expression of NpHR (Zhang F, et al. 2010). In utero electroporation can be used to introduce optogenetic transgenes at specific developmental time-points. For example, transgenes can be delivered to specific cortical layers of the brain by electroporating mice at embryonic day E12.5 (layers V and VI), E13.5 (layer IV), or E15.5 (layers II and III) (Zhang F, et al. 2010). Several studies have used this approach to deliver ChR2 to specific cortical layers for subsequent photo-stimulation when the mice reach adulthood (Hull C, et al 2009, Adesnik H, Scanziani M. 2010). In utero electroporation can also be used to deliver optogenetic transgenes to inhibitory neurons of the striatum or hippocampus (Luo L, et al. 2010). Viral, transgenic, and in utero electroporation strategies can be used in combination to overcome the weak transcriptional activity of most endogenous promoters (Zhang F, et al. 2010). For example, conditional AAV vectors that carry Cre-dependent transgene cassettes under the control of strong, ubiquitous promoters such as Ef1 α have been developed that exploit numerous transgenic mouse lines from individual labs, GENSAT (Gong S, et al. 2007) and the Allen Brain Institute (Madisen L, et al. 2010) that express Cre recombinase in specific cell types. The tissue specificity of optogenetic transgene expression is prescribed by the promoter elements driving Cre, whereas the efficiency of transgene expression is prescribed by the Ef1 α promoter (Atasoy D, et al. 2008) Multiple optogenetic studies have capitalized on this excellent system (Cardin JA, et al. 2009).

Finally, it is possible to specify expression of optogenetic transgenes using anatomical-based cell targeting (Gradinaru V, et al. 2010). Proteins such as wheat germ agglutinin or tetanus toxin fragment C exhibit anterograde- and retrograde-transport properties and can be fused to Cre recombinase to be trans-neuronally delivered to up- or down-stream neurons in other brain regions (Gradinaru V, et al. 2010). Thus, it is possible to restrict expression of optogenetic transgenes to specific cell types even if those cells do not express unique genetic regulatory elements. The combination of viral, transgenic, physical, and anatomical gene targeting technologies provides scientists with multiple strategies for expressing optogenetic probes in specific neural populations. These technologies also allow for the expression of probes in non-traditional genetic model organisms, such as rats and primates. Often, the first step in

optogenetic studies is to validate the correct expression of an optogenetic probe (tagged with a reporter protein) using histological techniques. The next step is to target the brain for in vivo light delivery, which we describe below.

In addition to targeting specific cell populations with optogenetic transgenes, it is necessary to deliver light. In vitro light delivery to cultured neurons or brain slices can be achieved using conventional light sources such as halogen/xenon arc lamps, light-emitting diodes (LEDs), and lasers, all of which can be directly coupled to a microscope's light path (Zhang F, et al. 2010). In vivo light delivery is more challenging because surgical implants must be stereotaxically placed adjacent to target regions and therefore must penetrate the skull. Light must be delivered very close to target regions because mammalian brain tissue scatters light exponentially, with only ~10% of light intensity remaining at a distance ~500 μm from the light source. At present, the most common method for delivering light in vivo is to implant a guide cannula for placement of a lightweight fiber optic cable (Figure 10) (Aravanis AM, et al. 2007). This strategy allows targeting of relatively deep brain structures. Mice can tolerate up to 300 μm diameter fibers and rats can tolerate up to 400 μm fibers. Optical fibers are typically connected to a laser diode, although it is also possible to connect to a LED. The challenge of using optical fibers within guide cannulas is that fiber breakage can result from repeated insertion through the cannula guide, resulting in a clogged cannula and loss of an animal subject. Therefore, many investigators now permanently implant a short fiber segment in the target region (Zhang F, et al. 2010). During experiments, this short fiber can be coupled to a longer fiber connected to a laser by a custom fiber-to-fiber connector. This strategy avoids fiber breakage and reduces the likelihood of infection due to environmental exposure through the cannula.

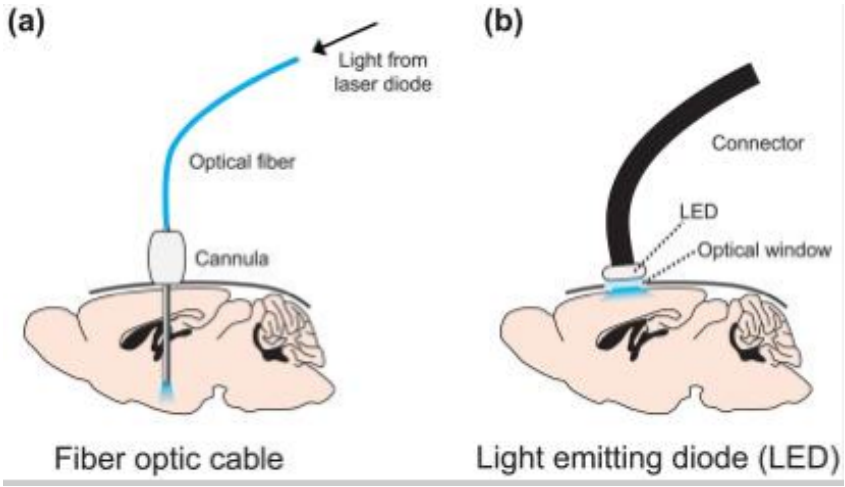

Fig 10 Strategies to deliver light to transduced neurons in vivo. **(a)** A guide cannula is stereotaxically implanted above a target region for subsequent placement of an optic fiber. The fiber is attached to a laser diode, which might be attached to a computer or pulse generator for automatic stimulation protocols. **(b)** An optical window is stereotaxically implanted above a target region. A light-emitting diode (LED) is placed above the window to illuminate surface neurons and is connected to a computer for automatic

For optical modulation of superficial cortical neurons, small LEDs can be mounted above the brain over a cranial glass window (Figure 10b) (Carter M E., 2011). These LEDs are powerful enough to deliver light to all cortical layers and thin enough not to add significant weight to a mouse.

The simplest form of optogenetic experiments (although simple does not imply easy) involves transducing a population of neurons with an optogenetic transgene and investigating the effect of directly stimulating/inhibiting these cells on animal behaviour or neural activity in a downstream brain region (figure 11). For example, photo-stimulation of Hypocretin-expressing neurons is sufficient to cause sleep-to-wake transitions (Adamantidis AR, et al. 2007), and micro-stimulation in the mouse barrel cortex can drive a sensory-induced learning task (Huber D, et al 2008).

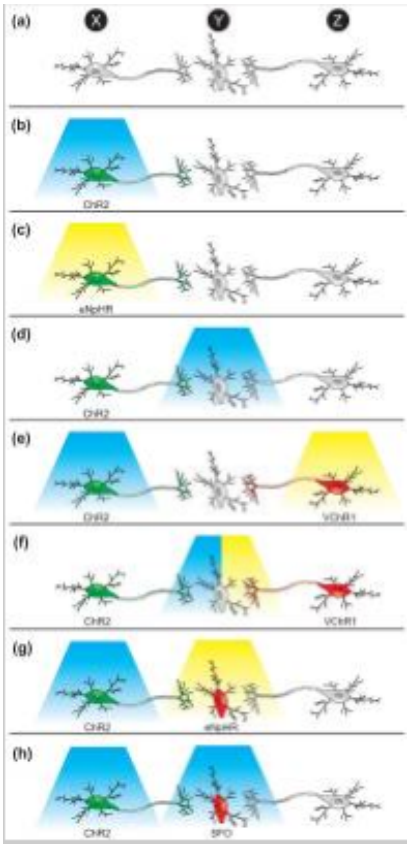

Fig 11 Optogenetic strategies to investigate neural circuits in vivo. **(a)** A schematic of a neural circuit in which a population of neurons, Population X, projects mono-synaptically to Population Y, which also receives projections from Population Z. **(b)** To determine the effect of stimulating X on behaviour, Population X neurons could be transduced with ChR2 (or a variant) and stimulated with blue light. The effect of stimulating X on neural activity in Y could be determined by simultaneously placing an electrode in Y. **(c)** To determine the effect of inhibiting X on behaviour, Population X could be transduced with eNpHR (or another inhibitory probe) and stimulated with yellow light. The effect of inhibiting X on neural activity in Y could be determined by simultaneously placing an electrode in Y. **(d)** To determine the effect of stimulating the projections of X onto Y on behaviour or neural activity in Y, Population X could be transduced with ChR2 and light

could be delivered to Y. The blue light will only activate ChR2 on the distal projections and thus the role of the specific synaptic connections can be probed. **(e)** To determine the relative contributions of activity in X or Z on behaviour or activity in Y, Population X could be transduced with ChR2, Population Z could be transduced with VChR1, and X could be stimulated with blue light and Z with yellow light **(f)** To more specifically determine the relative contributions of activity in X or Z on activity in Y, Population X could be transduced with ChR2, Population Z could be transduced with VChR1, and the projections onto Y could be stimulated with either blue or yellow light while recording with an optrode. **(g)** To determine the necessity of Y on the ability of X to influence behaviour, Population X could be transduced with ChR2, Population Y could be transduced with eNpHR, and X could be stimulated with blue light while Y is inhibited with yellow light. **(h)** To determine the effect of turning up the gain of activity in Y while stimulating X on behaviour, Population X could be transduced with ChR2, and Population Y could be transduced with anSFO that converts a single light pulse into a graded increase in membrane potential. Then X could be stimulated while Y is stimulated to subthreshold potential with a single pulse of blue light. (From Carter M E., 2011)

Instead of stimulating the soma of cells transduced with optogenetic transgenes, it is often also possible to stimulate their distal projections (Figure 11d) to measure functional post-synaptic activity in downstream neurons. For example, the relative contributions of thalamo-cortical versus cortico-thalamic projections in feedforward excitation/inhibition circuits were studied by transducing thalamic neurons with ChR2 and stimulating their projections in the cortex, or transducing cortical neurons with ChR2 and stimulating their projections in the thalamus (Cruikshank SJ, et al. 2010). Stimulating fiber projections rather than somas can also be helpful in determining whether behavioural effects of stimulating a specific cell population are mediated by specific synaptic connections in a downstream population. For example, a recent study demonstrated that stimulation of either layer V motor neurons in the motor cortex or their afferent projections to the subthalamic nucleus is sufficient to relieve the symptoms of Parkinson's disease (Gradinaru V, et al. 2009). If two neural populations project to the same area, it is theoretically possible to dissect their functional role in behaviour and anatomy by using combinatorial optogenetics and transducing each with ChR2 or VChR1, as both optogenetic probes are activated by different wavelengths of light (Figure 11). Finally, it is also possible to investigate whether the gain of activity in one neural population affects the role of another population in mediating behaviour or neural activity in downstream regions. For example, if a population of neurons causes a behaviour and projects to a downstream region, it might be possible to transduce the neurons with ChR2 and the downstream region with eNpHR. Thus, optogenetics could be used to stimulate one region while simultaneously inhibiting the other. Alternatively, the downstream region could be targeted with a step-function opsin (SFO) to increase the membrane potential to determine whether the gain of activity in this region affects ChR2-mediated effects of the upstream population. Many of these strategies have been used to study functional neuroanatomy, behaviour, and neurological ailments.

Although optogenetic technology has only existed for 5 years, dozens of studies (Rols, A. et all., 2011, Covington H, E. et al., 2011. Madisen, L. et al., 2012) have utilized these tools to answer important

questions about anatomy, behaviour, and disease. These methods permit direct investigation and dissection of complicated neural circuits that would otherwise be intractable for in vivo study. However, there is still substantial room for growth. For example, to allow for “combinatorial optogenetics” and the ability to stimulate multiple cell types in the same tissue preparation, it will be necessary to engineer a panel of channels that each respond to different wavelengths of light. This will be similar to the mutations made to green fluorescent protein (GFP) that allow variants of this protein to exhibit excitation and emission wavelengths across the visible spectrum of light (Shaner NC, et al. 2004). To limit the potential side effects of heat, it will also be desirable to increase the conductance of various channels so that less light stimulation is necessary. To better mimic endogenous neural activity, it will be interesting to record natural patterns of neural firing and then use these recordings to “play-back” neural stimulation in patterns of light pulses. Finally, to use optogenetics therapeutically, it will be necessary to develop gene delivery strategies and light delivery implants that are amenable to human patients.

Even though there is room for growth, the contemporary optogenetic toolkit can be applied to many previously intractable questions ranging from what motivates us to eat and drink to the neural basis of complex decision making. The use of light to study the brain has proved to be a remarkably useful strategy, and indeed the future of optogenetics seems very bright.

1.8 NEW TOOLS FOR THE STUDY OF SYNAPTIC TRANSMISSION IN VITRO AND IN VIVO

In eukaryotic cells, intracellular membrane fusion involves many families of proteins such as SNAREs, Rab proteins, and proteins Sec/Munc-18 (SM proteins). The SNAREs belong to a superfamily of small proteins mostly anchored to the membrane that show a common motif of 60 amino acids ("SNARE motif"). The SNAREs are assembled in a reversible manner through closely packed propeller bundles, called core complexes. It is this complex that likely performs the function of pulling the membranes towards each other so inducing their union. The SM proteins comprise a family of soluble proteins that bind certain members of the SNAREs and prevent the formation of CORE complexes, while Rab proteins are GTPases that are subjected to GTP-GDP regulation. However, the key to vesicle fusion is undoubtedly represented by the SNAREs protein family which mediate membrane fusion at all steps during the pathway of secretion and in most processes of endocytosis. These proteins are generally located on opposite sides of the membrane and induce fusion through the formation of helical bundle complexes that guide the membranes to merge, thereby creating narrow connections. After fusion, the recycling of SNAREs is obtained through the dissociation of the helical bundles mediated by the N-ethylmalemide-sensitive factor (NSF) (). Originally, the SNAREs were classified as vesicular-SNAREs

(vSNAREs) and target-SNAREs (tSNAREs), on the assumption that there was a strict separation between the SNAREs residing in the "donor" compartment, (generally a vesicular compartment) and the "acceptor " compartment (the plasma membrane, in the case of exocytosis). The formation of the so-called SNARE complex is mediated by the spontaneous association of motifs present in all SNAREs ("SNARE motif"), which form the helix core complex with extraordinary stability, using the free energy released by changes in conformation of the four Helices. The bundles contain 16 layers to the site of interaction of the chains. With the exception of the layer "0" which contains three highly conserved residues of glutamine (Q) and an arginine (R), the other layers are generally hydrophobic. In accordance with this model the additional SNARE motifs are classified as extra-Qa, Qb, - Qc and R-. In short, the SNAREs of the three main families involved in the process of exocytosis are: VAMP (Vesicle Associated Membrane Protein) and Syntaxin respectively contribute to the formation of R-SNARE motifs and Qa-SNARE, whereas SNAP (Synaptosome Associated Protein) contributes to the Qb- qc motifs and their N-and C-terminals. The assemblage of the three functional SNARE complexes is required to end the formation of the fusion pores; an assumption supported by some evidence, including the fact that many target neurotoxic and proteolytic cleave specific neural SNAREs inhibiting exocytosis (Schiavo, G et al. 1993; Blasi, J et al. 1993; Blasi, J et al. 1993). Moreover the neural SNAREs are alone capable of inducing membrane fusion if reconstituted artificially within artificial liposomes (Pobbati, AV et al. 2006; Weber, T et al.1998). In mice, Synaptobrevin - / - and SNAP 25 - / - was measured residual vesicular release, looking at spontaneous synaptic vesicle fusion and the fusion induced by hypertonic sucrose, but this was attributed to some sort of compensation by other vesicular proteins (Synaptotagmin 1) (Schoch, S et al 2001; Sorensen, J et al. 2003). During assembly the complex is initially formed in a "trans" configuration in which the SNAREs reside on separate membranes. Then, the complex undergoes a conformational change, forming a "cis" configuration, which coincides with membrane fusion. At this level the SNAREs (or SNARE proteins) are all located on the same membrane. The subsequent disassembly requires the action of some adapter proteins such as ASNAP and AAA-ATPase NSF, which liberate the SNAREs for a new cycle (Jahn, R & Scheller, RH 2006). The biological signal for vesicle fusion is an increase in intracellular Ca2 + with synaptic vesicle fusion occurring within 1 ms following the flow of calcium ions. Immediately after synaptic depolarization there is a first vesicular exocytosis burst called synchronous or evoked release. This step is followed by a second isolated exocytosis burst, called asynchronous release. Both phases are Ca2 + dependent but are only partially dependent on different molecular machinery (Geppert, M et al. 1994). The SNAREs complex is sufficient to direct the synaptic vesicle fusion, but cannot act alone. There have been identified some molecules that are required for Ca2 + dependent exocytosis in the synaptic terminal, the most important of which are Synaptotagmin-1 (calcium sensor), Munc18 and Munc13. Synaptotagmin-1 is a "special partner" for the SNARE complex, being that it is the only molecule over the SNARE complex which has a direct effect on the exocytosis kinetics (Nagy, G et al. 2006).

Also, previously, methods were developed to monitor vesicular dynamics, with a resolution that allows to resolve single synaptic variation, utilizing the knowledge acquired from synaptic proteins. For example, the organic dye FM1-43, is an amphiphilic molecule with a lipophilic tail and a positively charged head. This protein possesses a fluorogenic whch is composed of two aromatic rings linked through a double bond. The lipophilic tail allows FM1-43 to enter the bilayer of the synaptic membrane, while its polar head denies complete crossing of the membrane and therefore access to the interior of the cell. Once embedded in the membrane, the FM1-43 interacts with the lipid molecules causing a significant increase in its fluorescence (in the order of 30 times). Consequently, any membranes that have incorporated FM1-43 become very fluorescent And during exocytotic release of neurotransmitters, the synaptic vesicles exhibit, for a short interval of time, their luminal portion to the outside world. The inner membrane of the vesicles can, in this manner, mark itself, provided that the FM1-43 is present at the extracellular fluid level bathing the synapses. Once the vesicles are recycled back into the synapse, the FM1-43 will remain trapped within them and then the synaptic terminal will become fluorescent. The FM1-43 has been tested successfully in many types of synaptic terminals, including the neuromuscular junction and different types of neurons. Most of the FM1-43 molecules which are embedded in the membrane of the vesicle will be lost during the subsequent use of the vesicles: the speed of loss of the dye will allow to estimate the vesicle fusion rate at the level of each individual synaptic cleft. The decolourization fraction provides direct information about the number of vesicles released per stimulus and consequently the probability of release of a given synapse. The FM1-43 works very well in single layered cultured neurons, but unfortunately, due to its lipophilicity can lead to a non-specific signal at the membrane level. this high non-specific staining of the membrane cannot be easily used for experiments on brain slices or in vivo. During exocytosis, the intraluminal components of synaptic vesicles are briefly exposed on the surface of the synaptic terminal. There is an interesting experimental approach that allows the visualization of the exo-endocytosis process by exploiting the cyclical exposure of synaptic antigens. The vesicle fusion and the following recycling are displayed through the uptake of specific antibodies able to recognize intraluminal epitopes of specific vesicular membranes proteins, such as for Synaptotagmin-1 (Malgaroli, A et al. 1995). By the addition of specific antibodies against Synaptotagmin-1 in the medium of neuronal cell cultures will allow binding of synaptic vesicles luminal epitopes that are exposed during exocytosis. Consequently endocytosis and vesicle recycling of the same vesicles will allow it to be possible to permanently mark the synapses that were active during the time of exposure and follow them at different times. These results demonstrated that it was possible to mark the synaptic terminals with a tool based on a highly specific antigen-antibody interaction. An important advantage resulting from this method is that the antibodies are retained inside the synaptic vesicles even after numerous cycles of the same vesicle exo-endocytosis and this greatly simplifies the staining

procedures. In this field, ratiometric approaches that use sequential uptake of two different fluorescent anti-Synaptotagmin-1 antibodies can be exploited to monitor changes of synaptic weights (Malgaroli, A et al. 1995). In these experiments, the relative amount of internalized antibody can be estimated using two antibodies labeled with two different fluorophores. This simple ratiometric method provides a measure of the changes that follow an experimental manipulation and allow each synapse to have a reference value obtained in control conditions. Despite the remarkable sensitivity and very remarkable spatial resolution of this method, the antibody probes are too "bulky" (150kDa) in order to be used in vivo: their deep diffusion into neuronal tissue is not easy viewing the considerable mass of these antibodies. For this reason it is not surprising that these tools work well in vitro but do not give acceptable results in vivo.

To attempt to overcome these limitations genetically engineered probes have been developed, including Synapto-pHluorin, a pH sensitive protein, that is able to measure vesicle fusion and correlate with the alkalinization of the vesicle interior (Miesenböck, G et al., 1998) (Fig 12a). This molecule can actually be used for the study of synaptic vesicles release not only in vitro (Sankaranarayanan, S & Ryan, TA 2000) but also in vivo: in particular Synapto-pHluorin was used for mapping neuron activity in the olfactory antenna lobe of the fly (Ng, N et al., 2002) and in mouse olfactory bulbs (Fig 12b,c) (Draft, T et al., 2004). These methodologies, although interesting, still do not reach the necessary signal-to-noise ratio for individual functional mapping of synaptic activation in vivo, when activated by one or a few trains of action potentials. Therefore, an important goal is to develop more efficient indicators through the use of genetic engineering. The development of these molecules and their use with more advanced optical methods may allow the application of the activity imaging on defined sets of neurons and synaptic terminals inside the brain.

A

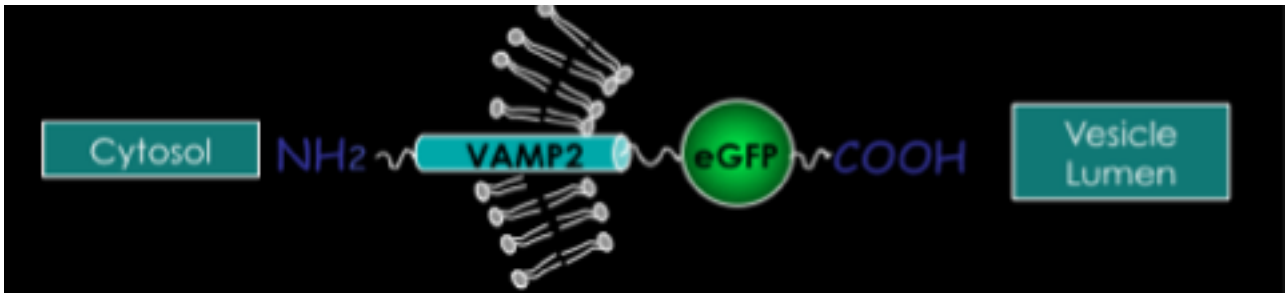

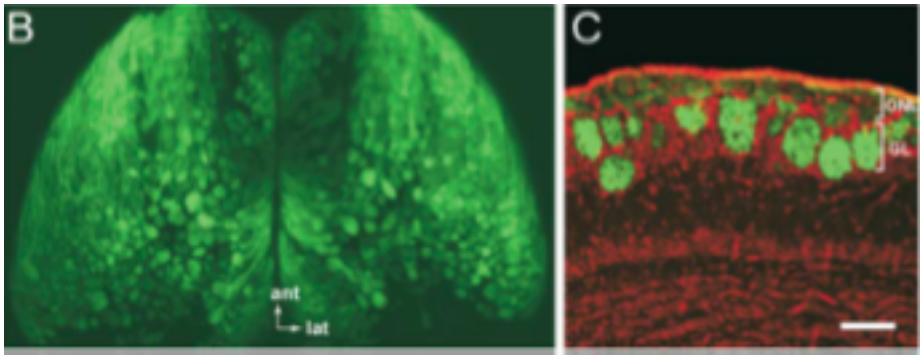

Fig 12 **(A)** Vesicular engineering protein VAMP-2 Framework. (Adapted from Miesenböck, G., 1998) **.(B)** Whole-mount view of the left and right dorsal olfactory bulbs from a homozygous OMP-spH mouse using confocal fluorescence microscopy. SpH labels glomeruli (round structures) and axon bundles which cover the surface of the bulbs. Anterior (ant) and lateral (lat) are indicated. **(C)** Section through the olfactory bulb from a homozygous OMP-spH mouse showing preferential labeling in the glomerular layer (GL) and less intense labeling of the overlying olfactory nerve layer (ONL). The section is counterstained with the nuclear dye TOTO-3 (red). Scale bar, 400 □m in (B); 100 □m in (C) (From Bozza T., 2002).

1.9 THE ZIP-BOND PAIRS: AN INNOVATIVE TOOL FOR THE STUDY OF SYNAPTIC TRANSMISSION IN VITRO AND IN VIVO

In line with this general idea, our laboratory is currently developing some novel and advanced genetically encoded indicators of brain synaptic network activity through the design of a series of innovative indicators of synaptic vesicles re-use, which occurs following synaptic transmission. The novelty is that these indicators report synaptic activation by uptake of small fluorescent peptidic markers during cycles of exo-endocytosis, whose frequency is greatly enhanced during synaptic transmission. These new tools have been designed starting from the scaffold of the vesicular protein VAMP2 or Synaptobrevin2 with the insertion at the intralumenal end of an aminoacidic acidic sequence cassette which is recognized by a bait, a small basic peptide of ~ 4 KDa (Synbond) conjugated with a fluorophore (available in various wavelengths) or with other detectable molecules. This pair of binders was previously selected for its high binding affinity which is in the nanomolar range (Fig 13).

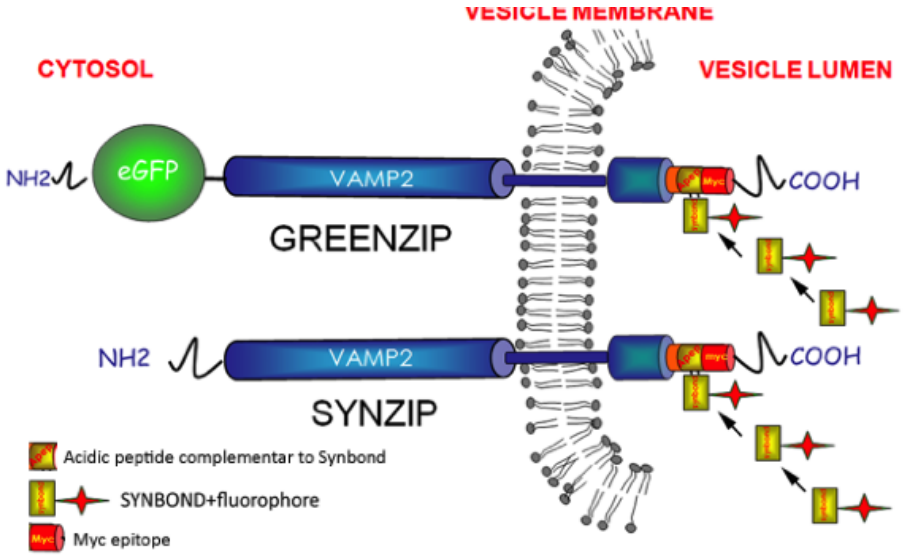

Fig 13 Schematic representation of SynZip and GreenZip and the location of the "Zip module" inside the intraluminal side of the vesicle, and the eGFP on the cytosolic side. If the fusion of a vesicle appens at the membrane level, the peptide acid will be exposed and will bind Synbond previously applied, making it fluorescent.

This family of molecules was named Synzip or GreenZip (The prefix Green indicates those constructs which contain GFP molecule at the N-terminal cytosolic domain). The idea at the basis of these constructs is that whenever the synaptic vesicle expressing SynZip or GreenZip fuses with the presynaptic membrane, the intraluminal part of the molecule (the bait), is exposed to the outside world. If the fluorescent reporter Synbond is present in the extracellular medium, the prediction is that it will be caught by the bait thus making the vesicle membrane fluorescent. At the moment in which the vesicle will perform endocytosis, it would become fluorescent in color in the interior of the synapse. This colour should be specific since Synbond is a charged molecule which cannot freely cross the cell membrane. In other words the synapse, which is surrounded by a plasma membrane, will be colored only if Synbond endocytosis will occur from the extracellular environment. The coloration of the vesicles should also be durable due to the high affinity of Synbond for its acidic counterpart (in the nanomolar range) with a link which is therefore almost irreversible. The characteristics of the two peptidic partners should thus allow an enduring label of the vesicular compartment through the simple application to the extracellular medium of the fluorescent reporter Synbond. However the greatest innovation of this probe is represented by the small size of the fluorescent sensor, Synbond, which, with a weight of only 3.9kDa is 30 times smaller than the IgG antibodies used previously to mark synaptic vesicles (150 kDa)!

During the construction phase of the probes, we have also generated a fluorescent version of the molecule SynZip by the addition of an eGFP sequence fused to the N-terminal, in the region of the cytosolic protein VAMP2. This variant was named GreenZip (Fig 13). The correct expression and localization of our constructs were tested in different eukaryotic cell lines and in neural cells. Through standard western

blotting techniques and fluorescence imaging it has been shown that SynZip and GreenZip are i) properly expressed in their entirety, and ii) localized in the correct orientation into functional vesicular compartments and iii) with regard to neuronal cells, they are properly transported and localized at the level of synaptic vesicles boutons. As our construct is a transmembrane protein, which sinks into the bilayer enclosing the vesicles, it will follow the fate of the portion of the membrane in which it is inserted. For this, it has become necessary to do in situ characterization of the binding between the two partners. For characterization of the expression-uptake relationship eukaryotic HeLa cells (which do not possess the endogenous VAMP2) were transiently transfected with SynZip cDNA (our modified VAMP-2 without GFP variant). After transfection, these were incubated for 30 minutes with Synbond (5 nM) in standard conditions (37 ° C, 5% CO2), before the cells were chemically fixed. The estimation of uptake level and expression was evaluated retrospectively by immunostaining with specific antibodies against VAMP2. As can be seen in the graph represented in fig 15, the internalisation of Synbond depends linearly on the expression level of the protein when working at non-saturating concentrations, as in this case. The linear relationship and direct proportionality is a key feature for a sensor that intends to measure the levels of activity, since this feature makes it a direct method and easy to use for the cumulative measures for both the internalisation and the activity of vesicular trafficking. (Fig 14).

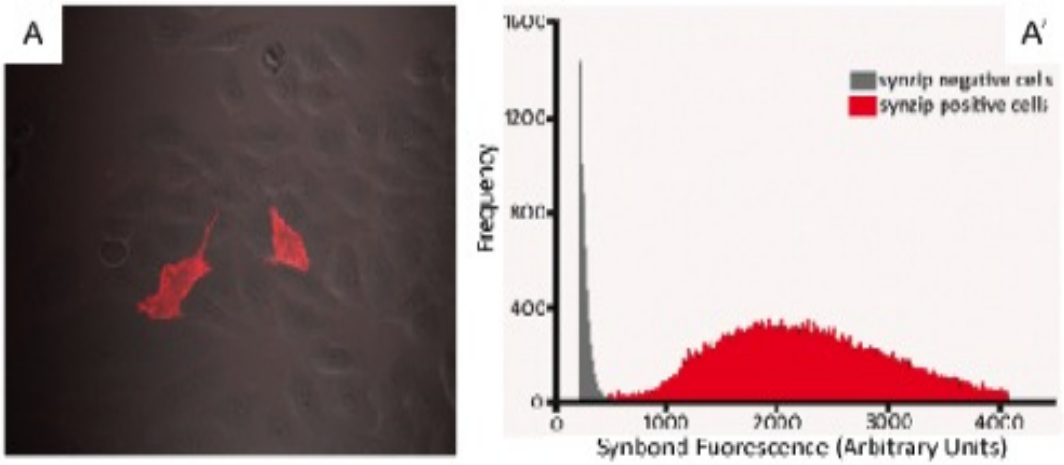

Fig.14: Specificity of Synbond in HeLa cells. A: image of the fluorescence of Synbond internalized in HeLa cells. B histogram that represents the quantification of the fluorescence of Synbond internalized in HeLa cells derived from three different experimental types : the red bars represent the internalization of Synbond in cells that express SynZip, the gray bars represent the background signal originating from cells that do not express SynZip Note the separation between histograms of expression and non-expression, which indicates the high specificity of our peptide.

We also conducted a series of additional experiments to determine the stability of binding and the ease of Synbond release after internalization into synaptic vesicles. In the first experiments, HeLa cells were transiently transfected with SynZip and subsequently incubated for 1h with Synbond (5 nM) in standard conditions (37 °C, 5% CO2). These fluorescent cells were then observed in vivo for a period of 6h 30' minutes. As can be seen from Figure 15 there is no significant loss of fluorescence throughout the period of observation, indicating that the recycling of the vesicular compartment to the membrane does not cause the loss of Synbond and therefore the loss of fluorescence (as happens with other colorants such as vesicular FM1-43). In these cells, in basal conditions, the same vesicles recycle every 15 minutes.

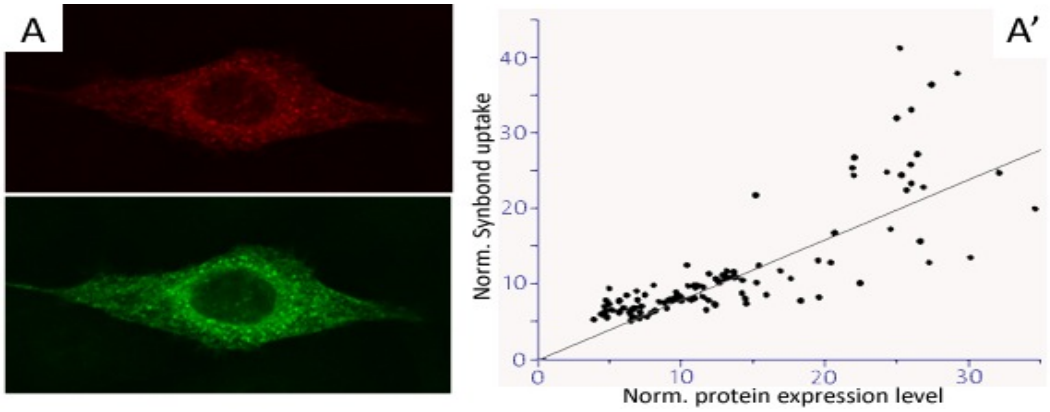

Fig. 15: **A** HeLa cells expressing SynZip: red: in vivo endocytosed Synond. Green: post-fix staining with anti-VAMP2 antibody. **A'** represent the linearity between SynZip expression level and Synbond uptake. Living HeLa expressing SynZip were incubated for 30 minutes with Synbond 5nM fixed and stained with anti-VAMP2 antibody. A sample of 70 cells was analyzed. Fluorescence in Synbond emission wavelength and secondary antibody used to tag VAMP2 was taken from SynZip expressing and plotted as in **A'**.

To understand if these molecules could be discharged after uptake inside vesicles we run a few experiments to determine the stability and the unbinding of the peptides from the baits. To test the stability of the binding HeLa cells were transfected with SynZip and incubated 1h with Synbond 5nM. Fluorescent cells were then observed time lapse in living conditions for a time window of 6h30minthen we assessed the possible displacement of the link between these two molecules: in this case, HeLa cells transiently transfected with SynZip were "pre-loaded" in saturating conditions with Synbond647 (1 hour; 100nM) under standard conditions. The fluorescent cells that had incorporated Synbond647, during the first incubation period were then maintained in vital conditions for the entire duration of the experiment. The fluorescent signal from Synbond647 endocytosed by cells (λ emission 633nm) was followed in time. After the first 15 minutes Synbond488 (λ emission 525nm) was added to the medium perfusion always at saturating concentrations (100nM). The fluorescence emitted from the cells that had incorporated Synbond647 was monitored and analyzed as shown in Fig 16. Even in this case no loss of fluorescence was observed from the signal emitted by Synbond647, indicating that saturating concentrations of the same peptide (the only difference is the type of fluorescent molecule that it brings bound and which

allows to differentiate the various molecules) were not able to break the bond between the couple "Zip-Bond", making it difficult to reverse.

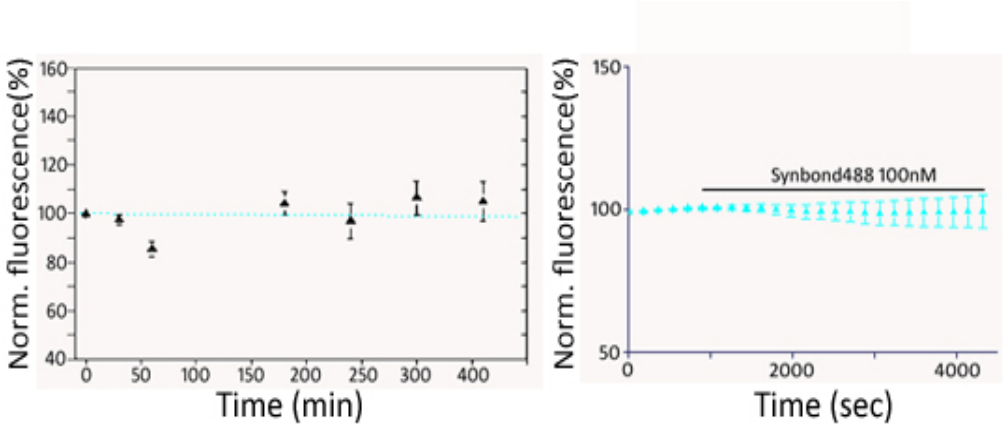

Fig. 16: **Left:** Synbond is not discharged**.** Fluorescence analyisis of a population of 30 HeLa cells transfected with SynZip and bathed with Synbond followed in vivo for more than 6h, no significant loss in mean fluorescence occurs after 6h30min. **Right:** Synbond is not displaced. HeLa cells were transfected with SynZip and bathed with Synbond647 100nM (saturated concentration) then fluorescence of a population of about 20cells was followed in vivo by adding Synbond488 100nM. No significant loss in mean fluorescence occurs up to 1h.

Since the binding of Synbond appeared to be irreversible (within the experimental time used), and since the number of copies of the bait for vesicle could also vary, it was decided to treat HeLa cells with two different Synbond molecules which emit two different wavelengths (Synbond-alexa-647, Synbond-alexa-488). The HeLa cells were exposed to a given quantity of these two molecules, where the concentration of Synbond488 was varied in a range going from 0.1 to 100 nM, while the concentration of Synbond647 was maintained constant. After 1h of incubation the cells were washed at 4 ° C and then fixed. We would have expected, therefore, to observe a decrease of Synbond647 dependent on what was the relationship between the two molecules. The expectation proved correct. By calculating the ratio of fluorescence between Synbond647/Synbond488 for each cell it was then possible to obtain the curve shown in fig 16. From this analysis we estimated the best concentration of Synbond to be in the range of 1-5 nM. As this concentration is far from being in a saturation condition, it has been possible to label sequentially the same compartments, in order to have the possibility of studying the same vesicles at different times. Then, using three different Synbonds, conjugated to three different fluorophores, it was possible to mark the same vesicles, since theseare re-exposed to the extracellular medium at different times during their cycles of exo-endocytosis, Fig 17 and 18.

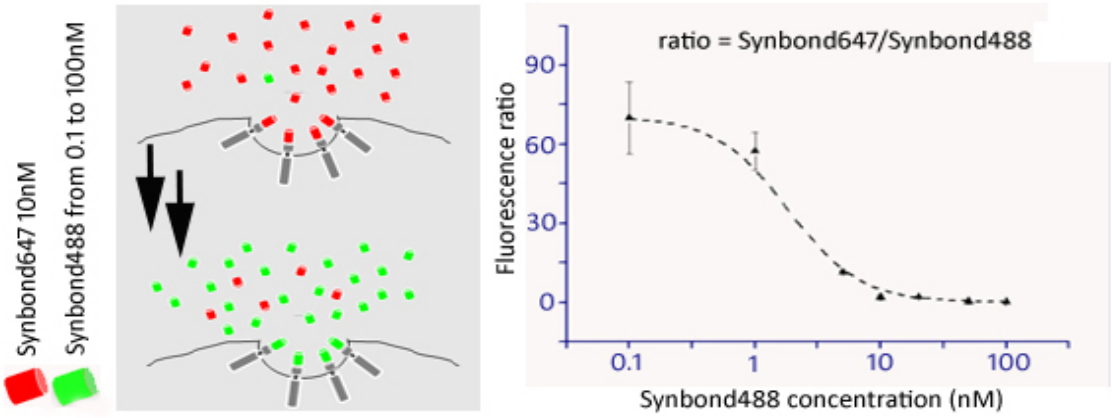

Fig. 17: **Left:** a schematic cartoon explaining experimental conditions applied to obtain the in vivo saturation curve shown in **right panel.** For this experiments HeLa cells transfected with SynZip were used. Synbond647 concentration in extracellular medium was maintained constant, while the concentration of Synbbond488, present at the same time on the same set of cells, was increased from 0.1nM up to 100nM. Cells were then fixed and fluorescence was analyzed. The fluorescence ratio Synbond647/Synbond488 from the same cell was calculated and the mean ratio of 70 cells for each condition was plotted.

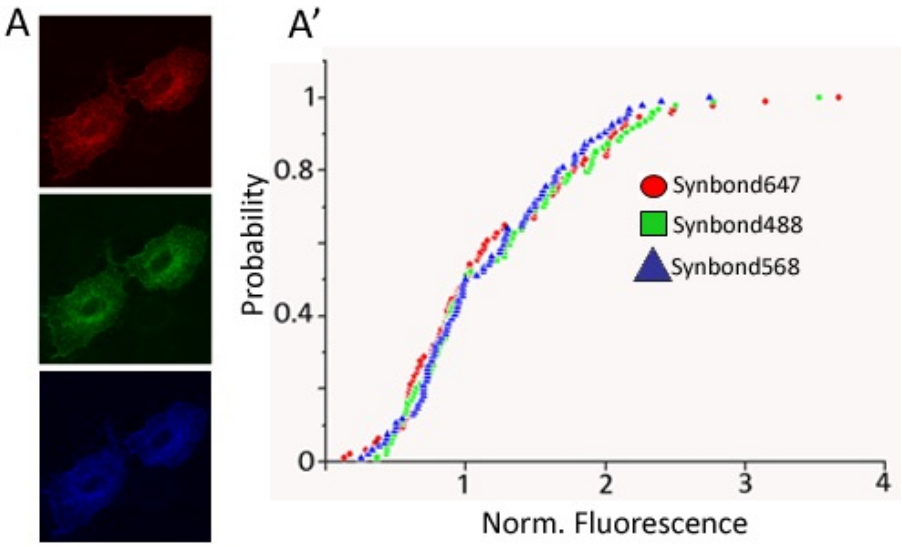

Fig. 18: Sequential labelling of Hela cells with 3 different fluorescent Synbond molecules. **A** the same HeLa cells transfected with SynZip were incubated in three different epochs, 15 min each, with three different Synbonds 5nM (Synbond647-Synbond488-Synbond568). 15minutes pulse are selective pulses that stain recycling endosomes, a particular vesicular compartment that re-expose to plasmamebrane. **A'** fluorescence analysis of the so pulsed cells, the fluorescence signal coming from different Synbonds completely overlaps. Synbond is not discharged and allows sequential labeling of vesicular compartments

Similar results were obtained by the expression of the Zip family in cultured neuronal cells using different transfection methods for neural cultures (Fig 19) and slices. In the first case we used the calcium-phosphate method of transfection, while in the second case electroporation was used. The expressed proteins were inserted into synaptic vesicles (as demonstrated by analysis at the EM level) which were then sorted to synapses (based on the expression of GFP molecules and the retrospective staining for synaptic markers). Greenzip positive synapses were easily visualized in cultured neurons and based on specific uptake of Synbond molecules, were clearly fusion competent.

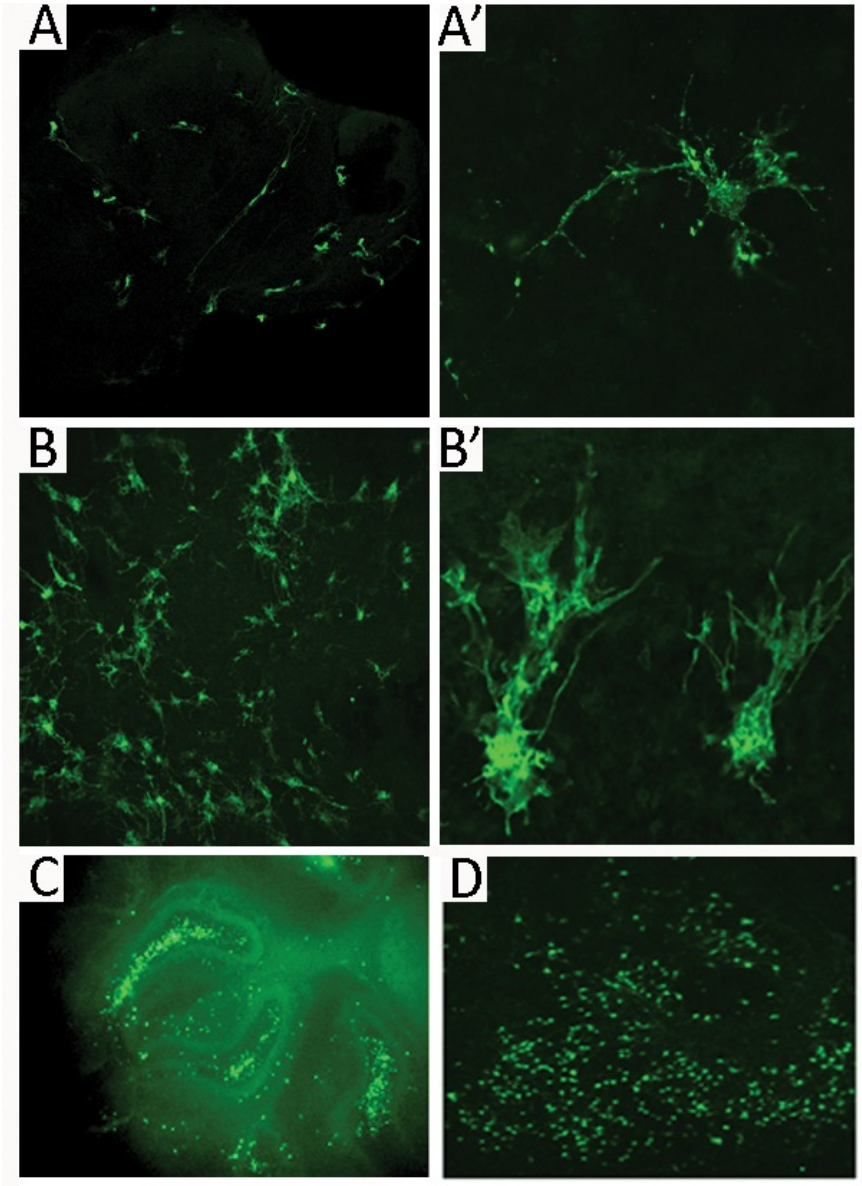

Fig. 19: DNA transfection different protein constructs of brain organotypic slices. **A:** hippocampus expressing β-actin-eGFP **A'** higer magnification of A. **B**: cerebellulm expressing β-actineGFP, **B'** higher magnification of **B** showing 2 Purkinje transfected cells. **C**: cerebellum expressing nuclear construct PCKN at low magnification. **D:** cerebellar slice electroporated with GreenΔZip at low magnification

It was found that the proteins of the family Zip had good expression levels, with the correct localization of the proteins. The cell bodies, as well as the dendrites, were positive but the more impressive signal was found to be the one coming from the synapses, specifically, the one at the level of presynaptic boutons. This observation reflects the localization of synaptic vesicles, by means of traveling along the soma and dendrites, and concentrated at the level of presynaptic boutons. VAMP2 has a peculiar way of localizing along the axon: vesicles that express it are first distributed throughout the neuron, including to the dendrites and membranes, then are selectively removed from all non-axonal and synaptic locations.VAMP2 is always "sent" to the axon by vesicular transport and selectively retained there, by

mechanisms not yet fully understood. For these reasons, if you look at the distribution of the VAMP2 protein in neuronal cells, it will be ubiquitously distributed, but concentrated at synapses. In addition, recent data (reference) indicates that VAMP2, which is considered a typical presynaptic protein, may participate in the dendritic exocytosis phenomenon, a hypothesis that would explain its presence in dendrites. Our constructs do not seem to be an exception to this rule: the addition of the various modules included native VAMP2 do not impede the normal anatomic distribution, not even the physiology. In our studies we observed that the distribution of a certain fraction of the construct is present on the plasma membrane of axons and synapses. A certain level of VAMP2 expression on the membranes is physiological and follows the exocytosis of synaptic vesicles: part of the membrane that was previously part of the vesicles themselves will be left to the presynaptic membrane after fusion and with it will be left all membrane proteins that are inserted in this small patch left by the vesicle.

In slices that were cultured and bathed with Synbond it was possible to show, with an extraordinary signal-to-noise ratio, the activity derived from spontaneous potentials and quantal release of single synaptic buttons active during the incubation period (Fig 20).

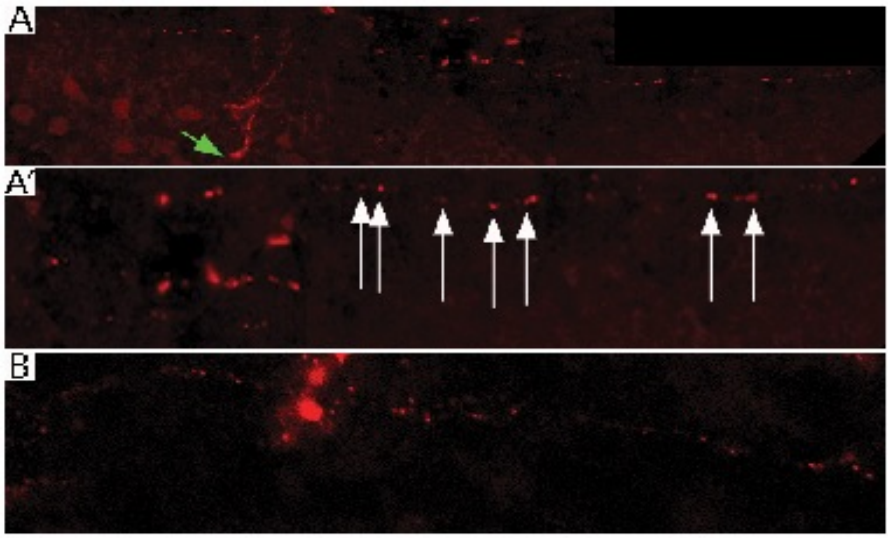

Fig. 20: **A:** a cerebellar slice electroporated with SynZip. In red spontaneous uptake of synbond by the entire axon of basket cell. Giant synapse it makes under the soma of a Purkinje cell (green arrow), and synaptic contacts it takes with the dendritic tree of the same Purkinje cell are also visible. **A':** particular of **A** at higher magnification, single synaptic boutons are clearly visible thank to endocytosed Synbond. **B:** hippocampal slice transfected with SinZip and bathed with 5nM Synbond. Particular extracted from a pyramidal neuron axon single presynaptic are visible without noise interference.

The most relevant data obtained from these experiments pointed out that this exo-endocytosis of synaptic activity produces an evident internalization of our fluorescent peptide with an excellent signal-to-noise ratio, not only at the most superficial level of synapses but also at the level of organotypic slice deep synapses located between 100 and 300μm in depth. Thanks to the Zip-Bond pairs it is therefore possible to detect the activity, both threshold and subthreshold, of in situ synapses localized in three-dimensional portions of the brain tissue at considerable depths and with a spatial resolution that reaches the level of a single button and with a specificity such as to reach a unprecedented signal-to-noise ratio.

In a series of preliminary electrophisyological experiments between pairs of hippocampal neurons, the activity dependent uptake of Synbond molecules was characterized in detail and found to correlate well with the synaptic efficacy and with the frequency of stimulation of the presynaptic cell (Fig 21). The signal-to-noise ratio that could be attained was very high, and active synapses were easily visualized after just a few action potential stimuli.

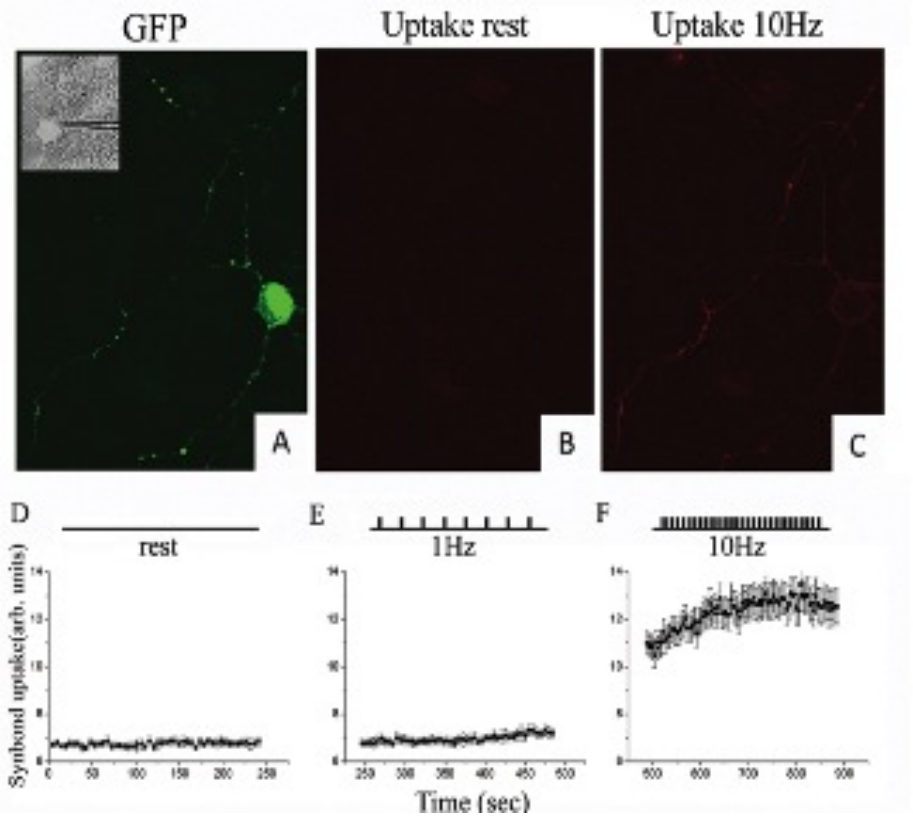

Fig 21: Internalisation dependent on the generation of action potentials in neuronal cells: **(A)** hippocampal cultured neurons transfected with GreenZip. The cell body and the synapses are green due to expression of the fluorescent protein GFP present in the Greenzip sequence. **(B)**: Synbond uptake in the same neuron at rest (rest) before stimulation. **(C)**Synbond internalization in the same neuron after stimulation at 10 Hz. The neuron was stimulated at two different frequencies of firing: 1Hz **(E)** and 10 Hz **(F).** It is clearly visible that the slope of the curve, showing the internalization, becomes steeper at higher frequencies of firing (F). The final quantity of Synbond internalization, after stimulation, is greater than 5 times compared to basal conditions. While in the rest condition, there is not any visible uptake **(D**).

We analyzed, then, through a tri-dimensional reconstruction, the degree of internalization of our fluorescent peptide and its signal to noise ratio with respect to different levels of depth Z-axis, up to a depth of 100 micron from the surface of the brain's slice, which represents the anatomical limit of the thickness. In these experiments some organotypic cerebellar slices expressing GreenZip in vivo were put together with our peptide Synbond, and were added, at the same time, some specific antibodies for the recognition of specific intraluminal epitopes of synaptic vesicles (anti-Synaptotagmin or anti-p65) or myc antibodies (which recognize a tag which is also present in the portion of intraluminal GreenZip). In

these experiments (as shown in Fig 22) it was found that, while the 1h incubation with the antibody provided a visible signal only for those synapses that were at the level of the surface portion of the slice, Synbond, at the same period of time, could spread to points very deep, without an apparent loss of signal (Fig 22).

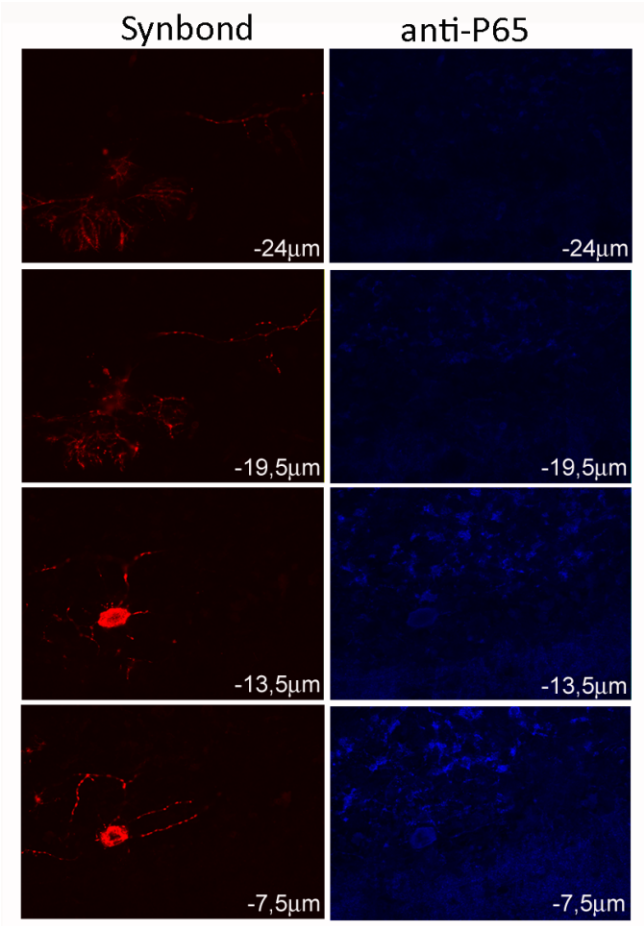

Fig. 22: comparison between diffusion of Synbond and anti-synaptotagmin or P65 antibodies in cerebellar slices. Presynaptic varicosities made by a Purkinje cell expressing GreenZip can be easly visualized by Synbond uptake **(red)** with an excellent signal-to-noise while the fluorescence coming from endocytosed antibody **(blue)** get lost after few microns in the Z-axis.

MATERIALS AND METHODS

Animal Care

All experiments desribed in this report were conducted in agreement with the stipulations of the San Raffaele Scientific Institute Animal Care and Use Committee (I.A.C.U.C).

Recombinant DNA techniques

Microbiological and biochemical procedures related to preparation and analysis of DNA constructs and to the handling of oligonucleotides were essentially performed as described in the cloning manual (Molecular cloning : a laboratory manual; T. Maniatis, E. F. Fritsch, J. Sambrook; 1982, and subsequent editions). E. coli DH5a was the host strain used to replicate the DNA , and recA1 endA1 gyrA96 thi-1 hsdR17(rK- mK+) supE44 relA1 (SCS1 Supercompetent Cells from Agilent Technologis) was used for the ligation protocol . Typical enzymatic reactions included digestion with restriction enzymes (New England Biolabs inc, 4-5 Enzyme Unit per cDNA microgram, 37° 2h); dephosphorylation of terminals with Calf Intestinal Phosphatase (CIP) (New England Biolabs inc.); blunting of ends with DNA polymerase I, large (Klenow) fragment (New England Biolabs inc.) ligation with T4 DNA ligase (New England Biolabs inc.). Large scale plasmid preparation was with a column kit (Qiagen) or by double banding in a cesium chloride gradient, as required. Oligonucleotide synthesis and DNA sequencing with the Sanger method were done by Primm srl (Milan). Electrophoresis on agarose gel has been used both for analytical purposes (degree of completeness of the enzymatic digestion, and estimation of the length in base pairs of nucleic acids) and for purification of DNA fragments. The gel was prepared by dissolving the agarose powder, at 1% and 2% concentrations, in appropriate TE 1X volume buffer. EtBr was added after boiling of the mixture (1 microgram/ml final concentration). Samples were prepared by adding loading buffer at a final concentration of 1X. Once polymerized into the holder, the gel was subjected to a potential difference of 60/100 V for a time ranging from 30’to 240'. At the end of the electrophoretic run the gel was exposed to UV light to

visualize DNA; the size of the DNA bands observed were evaluated according to the molecular weight markers run on the same gel (DNA ladder mix, MassRuler). Purification of DNA fragments: for purification of DNA fragments, low melting agarose temperature was used. At the end of the electrophoretic run, the band of interest was isolated by UV visualization .The commercially available PCR Gel clear-up system kit (Promega), was then used to extract the DNA from the agarose band, following the manufacturers instructions. DNA quantification: The quantification of DNA was obtained using both i) the EtBr fluorescence following electrophoresis, comparing the sample loaded with an amount of known DNA and by ii) measuring the DNA absorption at 260 nm through a NanoDrop spectrophotometer which provides an estimation of solution purity through the the 260/280 absorbance ratio. phenol extraction: for enzyme purification of DNA (is this what you are saying?) equal volume of phenol/chloroform was added to the digestion mixture and this was shaken vigorously and centrifuged for 5' at 1200 g. This allowed the separation of two phases to be obtained, a lower organic (containing proteins) phase and an upper aqueous (containing the DNA) phase. The upper phase was then taken to proceed to alcohol precipitation. Alcohol precipitation: DNA was precipitated by adding 0.1 volumes of Na acetate ($NaCH_3OOH$) 3 M pH 5.2 and 2.5 volumes 100% EtOH to the product of the phenol extraction. After mixing several times, the mixture was left for 1 h at -20 ° Cand then subsequently centrifuged for 2 h at 13.000 g at 4 ° C. The pellet was washed with cold 70% EtOH to remove residual salts, was centrifuged again for 30'at 4 ° C and left to air dry. The DNA was resuspended in TE1X (TE = 10 mM Tris pH 7.4, 0.1 mM EDTA pH8) or in H_2O and stored at -20 ° C.

Immunofluorescence

Immunofluorescence was performed on brain slices from both animals (rats an mice) and cell cultures (HeLA and hippocampal neurons) as described in the previous section.

Primary antibodies:

Anti-VAMP2, mouse monoclonal 1:300 (Synaptic System)

Anti-Myc, mouse monoclonal 1:300 (Upstate)

Anti-GFP, rabbit polyclonal 1:300 (Molecular Probes

Anti-C fos, rabbit polyclonal 1:300 (Santa Cruz biotechnology)

Anti-NeuN mouse monoclonal 1:300 (chemicon)

Anti-Gad67 mouse monoclonal 1:300 (Chemicon)

Secondary antibodies:

Donkey FITC-conjugated anti-mouse IgG 1:200 (Jackson)

Donkey FITC-conjugated anti-rabbit IgG 1:200 (Jackson)

Donkey Texas Red-conjugated anti-mouse IgG 1:200 (Jackson)

Donkey Texas Red-conjugated anti-rabbit IgG 1:200 (Jackson)

Donkey Cy5-conjugated anti-mouse IgG 1:200 (Jackson)

Donkey Cy5-conjugated anti-rabbit IgG 1:200 (Jackson)

2.1 GREENZIP CLONE AND IN VIVO TRANSFECTION

GreenZip clone

The parental clone of VAMP2 was modified by PCR mutagenesis in order to convert the stop-codon (TAA) to a serine codon (TCT) for in-frame insertion of the Zip module at the end of the VAMP2 CDS. The procedure involved, 1) PCR amplification of a Tth111/I-Bsu36/I fragment (position 233 - 437 in the reference cDNA sequence: NM_012663) using the sense primer:
VAMP25merUP 5'-GAGGGTGAATGTGGACAAGGTCCTG (Tth111/I site underlined)
and a mismatched antisense primer:
VAMP34merDOWN-5'-CAGGGCAGACTCCTCAGGGACAGAAGTGCTGAAG, (Bsu36 I site underlined); and 2) removal of the original Tth111/I-Bsu36/I fragment, thereby generating a plasmid derivative designated "VAMP2 stop-minus". The procedure caused the loss of a 231bp Bsu36-I fragment (position 437-668) from the 3' UTR of VAMP2, while most 3' UTR (1.5 Kb) was retained from the VAMP2 parental clone. The new plasmid carries a unique Bsu 36 I site used for in-frame insertion of the "Zip" module.

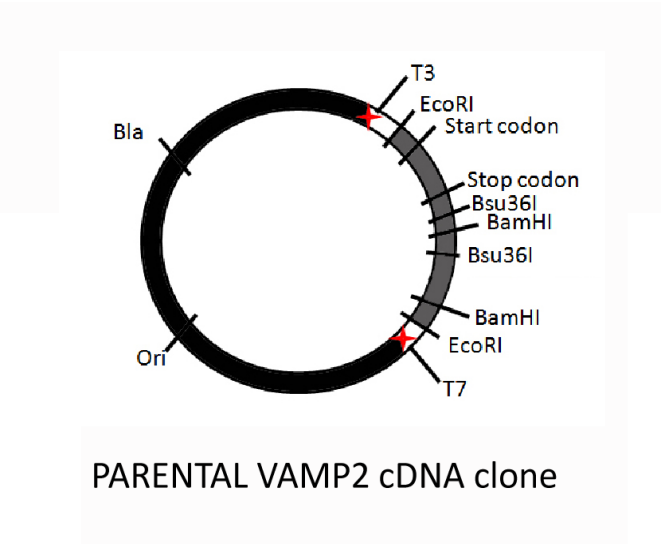

Fig 23 Drawing of the parental VAMP2 cDNA (dark gray) in pBluescript (black). The multiple cloning site (white) and other critical restriction sites are indicated.

The "Zip" module consists of sequences encoding (5'→3'): a short spacer (13 codons) derived from the juxtamembrane TfR domain (Grote, Hao, Bennett MK, Kelly 1995), the "acidic peptide "Zip sequence" (30 codons), myc epitope (10 codons) followed by a stop codon. The nucleotide sequence was obtained by backtranslation using the Entelechon Backtranslation Tool (www.entelechon.com) with Rattus norvegicus codon preferences, and then refined, using code degeneracy, in order to minimize regions of self-complementarity that are disruptive to correct base pairing during the annealing of single strand oligonucleotides. The dsDNA molecule containing the 54 codons plus adaptor sequences (total length ~200 bp) was assembled stepwise and inserted in-frame in the Bsu36/I site of the VAMP2 stop-minus plasmid. Clones carrying the "Zip" insert in the appropriate orientation were identified by analytical PCR from single colonies and restriction analysis and were designated SynZip. Two expression vectors were prepared: first, the SynZip cDNA excised from pBluescript was inserted as Hind III - Sac I fragment in a vector harboring chicken β-actin transcriptional regulatory sequences (kindly provided by Mathus) (Fig 10); second, using a PCR-based procedure, the SynZip CDS was appended in-frame to the end of the CDS of Enhanced Green Fluorescent Protein (EGFP) in the context of pEGFP, a commercial vector carrying the cytomegalovirus promoter/enhancer sequences, giving rise to a new fusion construct encoding EGFP-SynZip and retaining the 3'UTR, designated GreenZip.

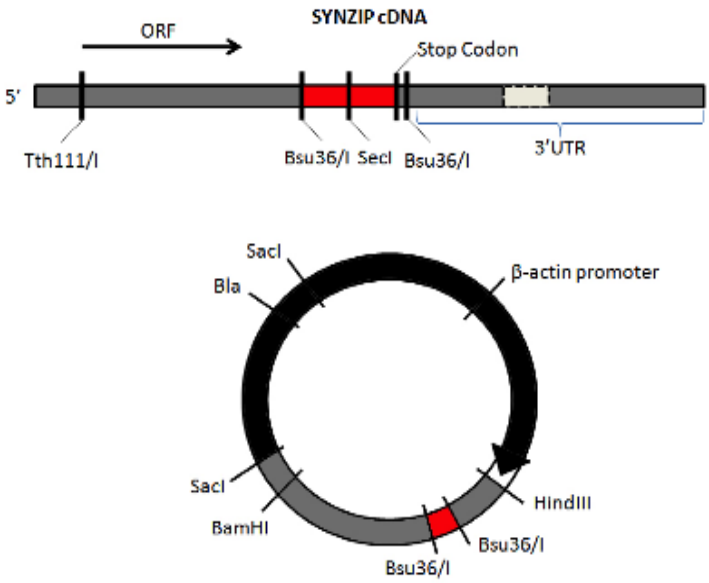

Fig. 24: Drawing of the SynZip cDNA (upper panel) in pBluescript (black, lower panel). The "Zip module" is highlighted in red.

From the topology of the VAMP2 protein, it is predicted that the GreenZip protein exposes the EGFP moiety on the cytoplasmic side and the Zip moiety in the vesicular lumen.

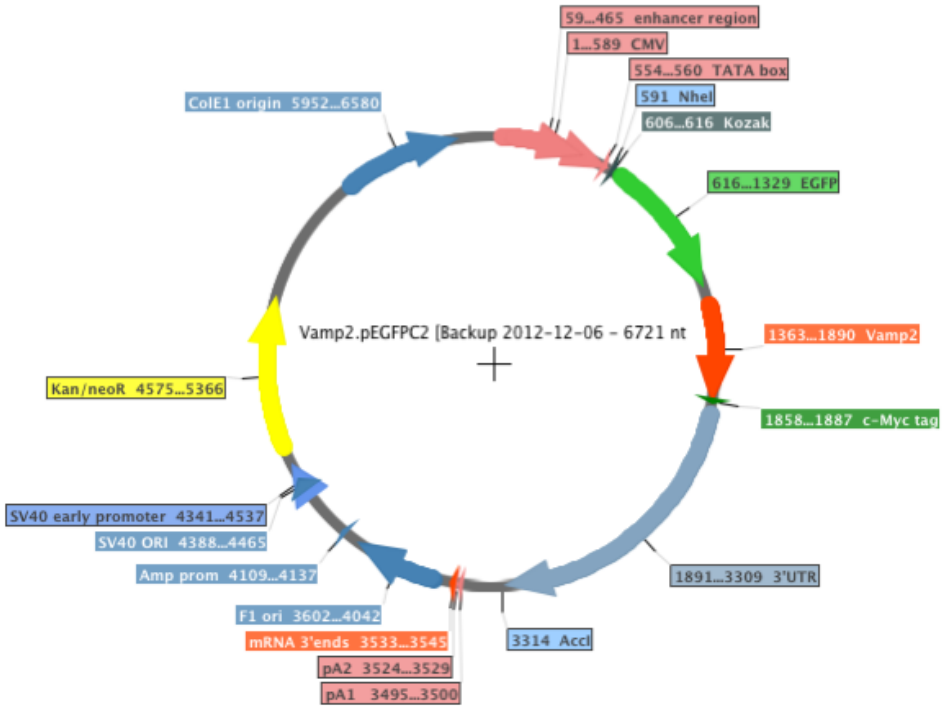

Fig 25 GreenZip construct: we can note the various components of the plasmid: The portion that will be inserted into the plasmid vector Rosa26 comprises the coding regions for: Kozac Sequence (Grey); eGFP (Green) fused in frame with VAMP2 (Orange)

followed by a small myc tag (dark green) and the VAMP2 3'UTR (Blue). Enzymes used for excision are NheI and AccI (as show in figure).

Animals

For in vivo experiments adult male Sprague-Dawley rats (n=4) weighing between 180-230g were used. Each animal was kept in a cage that allowed free access to food and water and was exposed to cycles of light / darkness of 12 hours in an environment with constant temperature of 23 ± 1 ° C. The cage was changed once every two days. Animals are repeated from above but this section is better than the first.

Confocal microscopy and data analysis

Fluorescence was detected by one photon confocal microscopy. Zeiss LSM510 laser scanning microscope, with proper excitation and emission filters. Images were acquired by Zeiss LSM510 acquisition software analyzed with ImageJ software (http://rsb.info.nih.gov/ij/) and mounted with Adobe® Photoshop®. Mathematical and statistical elaboration of the data was run with Microcal™ Origin® 7.5 (Microcal Software, Northampton, MA, USA)

In vivo retinal ganglion cells electroporation

In vivo eyes were electroporated by optimizing a method previously described by Yokoyama and colleagues (Yokoyama et al. 2005). Sprague Dawley rats of 275-300g were used, DNA dissolved in TE buffer was injected into the vitreous by a 31gauge needle. Vitreous volume was calculated as about 50μl. 7μl of DNA mix solution (80μg DNA in TE) were injected, under stereoscopic guide, 1mm behind the limbus. Application of midriatic agent on the eye allowed the visualization of the needle tip through the rat dilated pupil, by this way it has been possible to discharge DNA very close to the region which in humans corresponds to the fovea, the retina region richest in ganglion cells. After 5-10 minutes of incubation, to let DNA diffuse, electroporation was applied. Two custom gold electrode were developed (Fig 26). Eye was grasped between the electrodes, corneal electrode was attached to the cathode scleral one to the anode, square-wave pulses, as follows, were run:ΔV = 15-24 V, Pulse duration = 100-150ms, Interpulse = 1s, Number of pulses = 5-10.

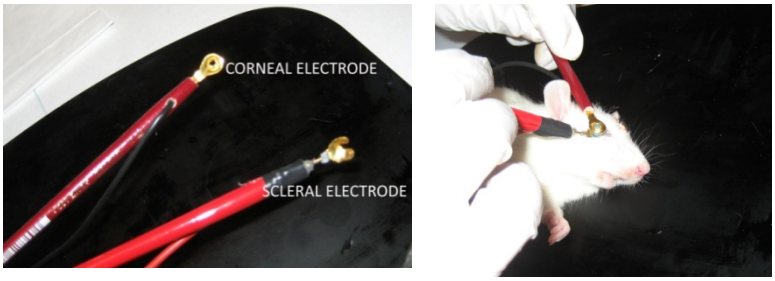

Fig 26: **A** panel shows custom made eye electrodes, scleral electrode shapes a sort of slide track in which optic nerve can be accommodated, while corneal one posses a hole in order to prevent sclera from potential mechanic damage. **B** panel shows application of electrodes by grasping eye ball of anesthetized animal

Light-induced firing of RGCs

Animals were pre-conditioned in total dark 1 daylong, with free access to food and drink. Living animal's RGCs were light-stimulated by a custom made light-box developed for this use, the device is shown in Fig 27. The box is large enough to allow animals to freely move inside it, also a ventilation system is present. 6 led bulbs (3 emitting white and 3 red) provided by Osram , for a total power of 735Cds, were mounted and directed inside the box .The interior side of the device is made of mirror walls and roof (Plexiglas), in order to totally reflect the light emitted from the leds in all directions. On this walls black stripes were applied every cm to generate contrast-zones and prevent lateral inhibition. Light box was connected to an isolation time unit (Winston Instruments), that allowed different frequency protocols for light stimulation. Animals were put inside this box and stimulated for 1-2h and different frequencies protocols were checked, the best for our aim resulted the one that provides 5minutes of light and 20minutes of darkness. Activation of RGCs was detected as above both in LGN slices and in the whole retina by retrospective immunostaining.

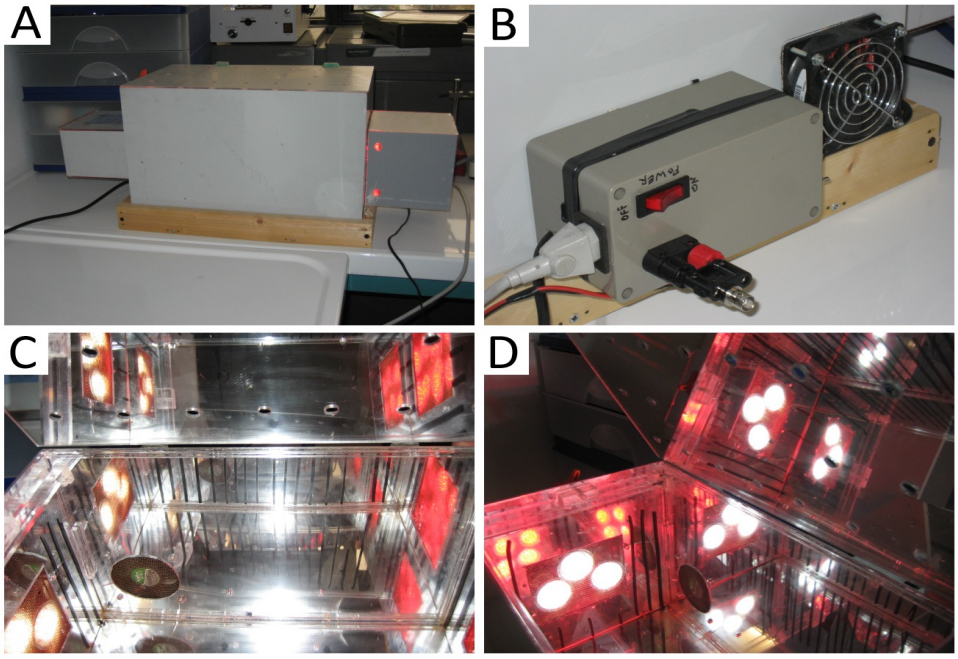

Fig 27: **A:** Light box as appears from exterior. **B:** relay unit with BNC input connector for cabling with timing unit. **C-D** light box as appears from inside when lights are turned on. Bulbs groups and black stripes attached on the mirror walls are visible.

In vivo Synbond aplication

Both lentiviral injection and Synbond peptide were made via stereotactic surgery, by injecting the constructs directly into the involved brain regions (Fig 28).

To ensure good sterility during the positioning of a needle into the brain, all surgical instruments and electrodes were kept immersed in 70% ethanol. The animal, appropriately anesthetized (via continuous inhalation of Sevoflurane), was subjected to subcutaneous injection of dexamethasone (0.2 mg / kg) intraperitoneally, and gentamicin (1.5 mg / kg), while the area of surgical interest was shaved and subjected to three washes of alternating Betadine and 2% Chlorhexidine.

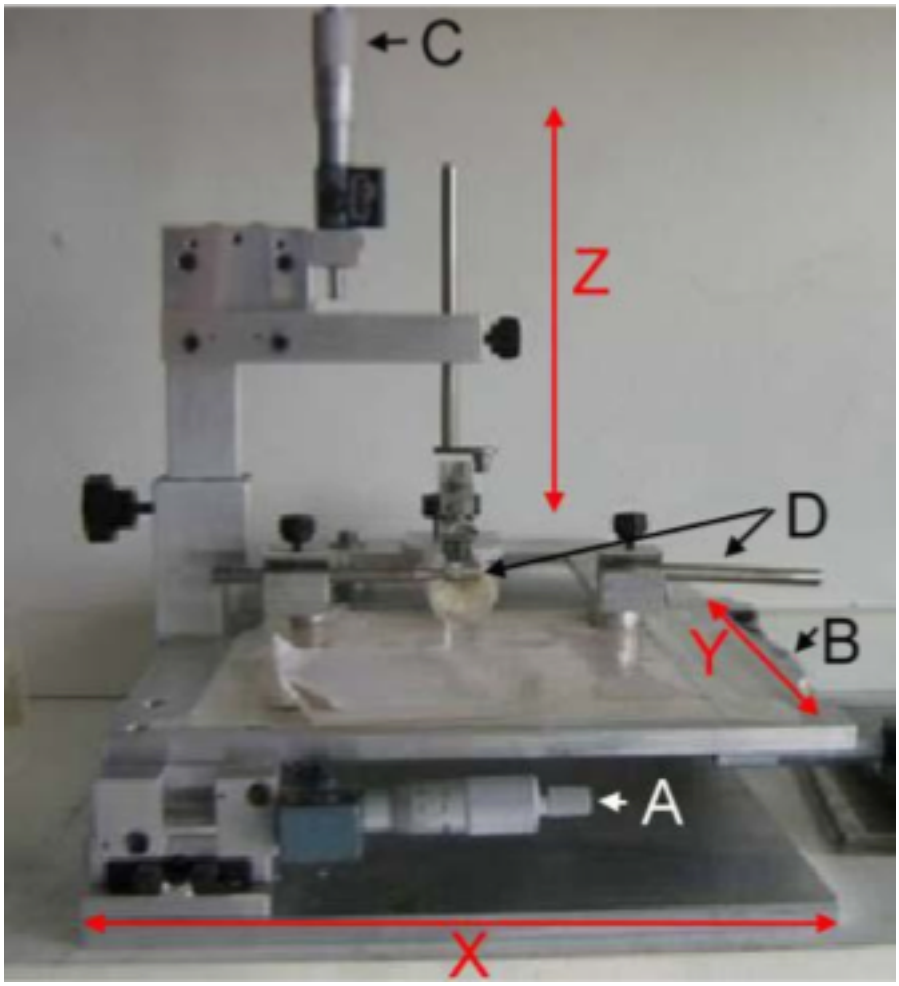

Figure 28: Device used for stereotactic injection: A knob moves the plane of the device horizontally, the B knob moves the plane vertically knob C will advance or retract the arm to which is attached the needle. The bars are used to secure the animal to the plane (D).

The device is equipped with three small knobs designed to guide the needle from which the probe was injected at the site provided. One of them allowed the movement of the plane, in the range of a few mm, horizontally (X axis knob A), the second, allowed to move vertically (Y axis, knob B), while the third (knob C) could advance or retract the arm of the device on which was mounted the needle along a hypothetical axis Z, thus allowing the needle to penetrate deep into the animal's brain.

The exact coordinates to achieve the desired positioning sites were calculated using those from a stereotaxic atlas of the rat brain (Fig.29).

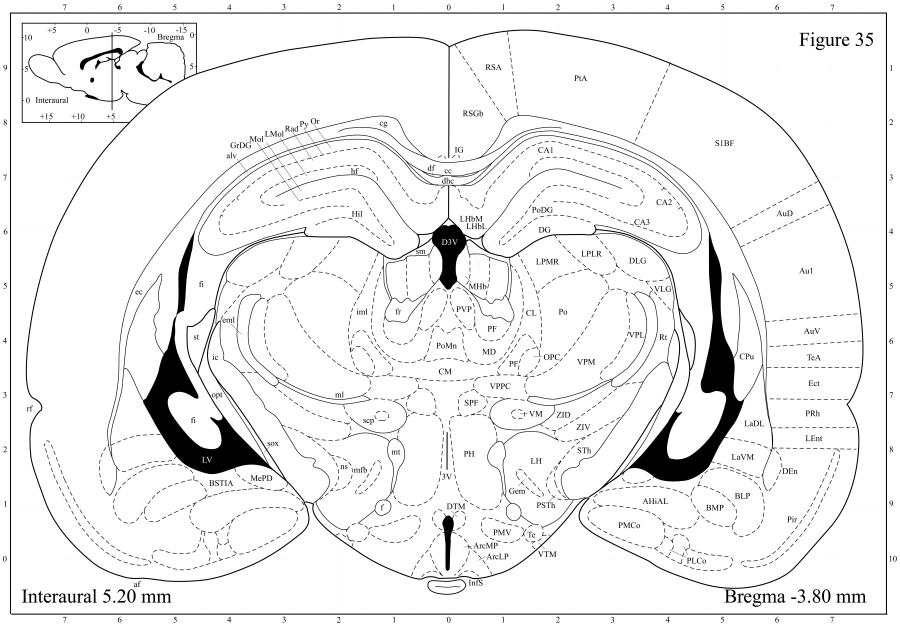

Fig 29: Exact coordinates to reach the left LGN were provided using those from a stereotaxic atlas of the rat brain (G. Paxinos, the rat brain in stereotaxic coordinates) adapted to the weight of our animals (175-200g).

With the purpose of making visible the bregma (reference point where the coordinates of the stereotaxic device are set to zero) and the sites for the injection, part of the scalp was removed and surface of the skull scratched, in order to expose the cranial bone. Following this, the animal was mounted on to the stereotactic apparatus, with the needle positioned just above the bregma, allowing the calculation of the injection site coordinates on the axes x, y, z. Once this point was reached, a small hole was cut (using a little milling machine) so as to be able to insert the needle into the desired region of the brain. For the application of Synbond, and the relative stimulation (see results) this is always executed via stereotaxic apparatus. In this case, to keep the animal still and conscious throughout the duration of the experiment an endotracheal intubation for the continuous infusion of anesthetic (sevoflurane) was performed, in conjunction with administered boluses of curare by IV, to ensure the release of smooth muscle .

2.2 TRANSGENIC ANIMALS

Targeting Vector

Targeting to the ROSA26 locus was conveniently achieved by introducing the desired gene into the first intron of the locus, at a unique XbaI site approximately 248 bp upstream of the original gene trap line (Soriano et al., 1998). A construct using the same splice acceptor as used in the original gene trap allele (from adenovirus), followed by the gene of interest and polyadenylation site, was inserted at the unique XbaI site of pROSA26-1. A floxed neomycin resistance cassette was included in the targeting vector, followed by a STOP cassette. ROSA26-1 already possessed a diphtheria toxin gene for negative selection, allowing high rates of homologous recombination. Targeted clones were then verified using a flanking probe (pROSA26-5' or the 337 bp Not I fragment of pROSA26 promoter) and later genotyped using oligos derived from the locus flanking the insertion. The Knockin vector contains an additional item: a CAGG promoter derived from pCAGGS (Niwa et al., 1991) The resulting vector contains 5' and 3' homology arms, for the homologous recombination in the ROSA26 genomic locus, of 2.3 kb and 5.7 kb, respectively, which targets the construct to the Xba1 site of intron 1 at the ROSA26 locus (see Figure 30).

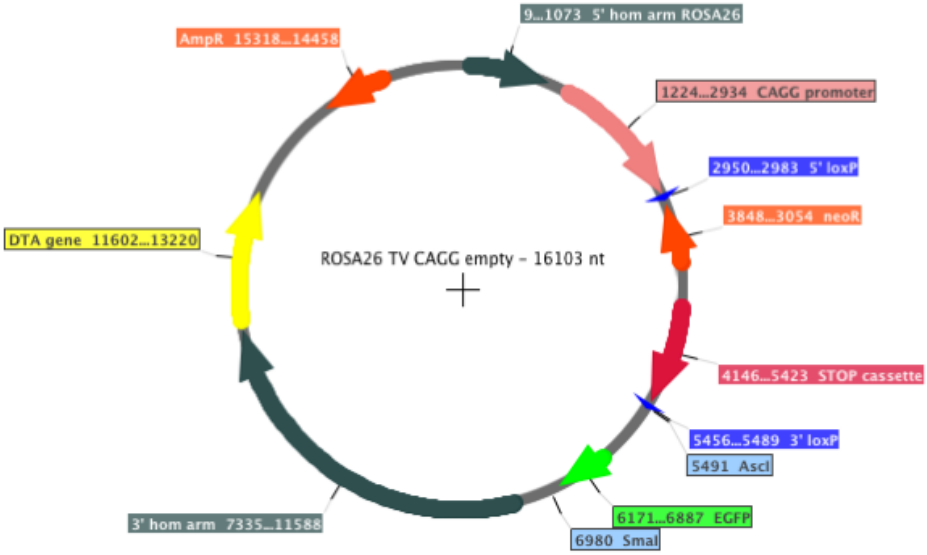

Fig 30: Rosa26 construct: we can note the components of the plasmid: the homology arms for recombination within the genomic locus Rosa 26 (dark green); LoxP sites that are excised by the enzyme Cre (Blue); the stop sequence (Fuxia); the strong promoter pCAGGS (Pink); the gene for diphteria Toxin A (DTA gene) (Yellow); the Ampicillin resistence and that for neomycin (Orange); GFP (Green) that will be excise through appropriate restriction enzymes (SmaI and AscI, as show in figure) in order to include the coding sequence for GreenZip.

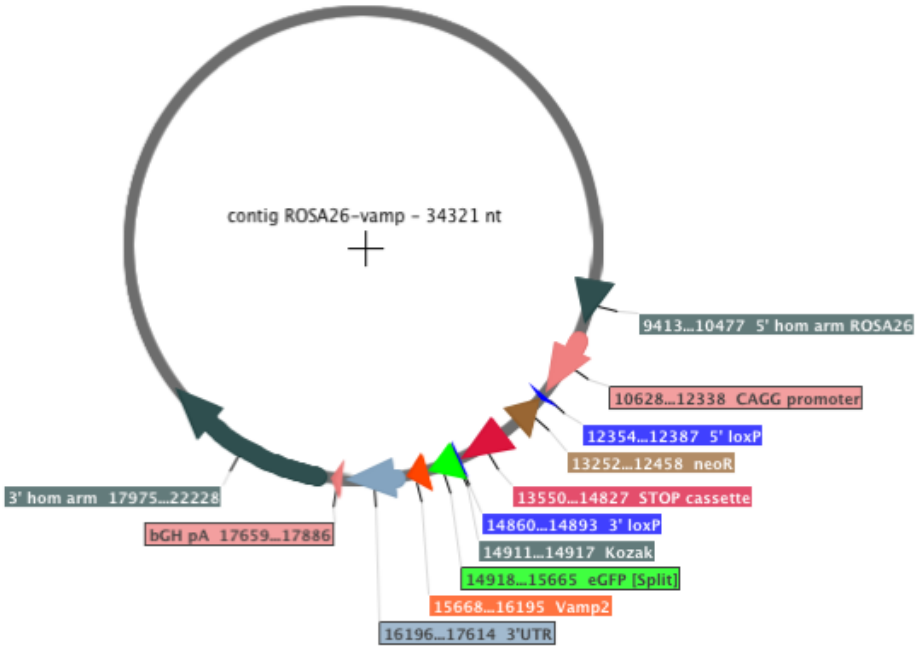

Fig 31 RosaGreenZip construct, portion for the recombination into ES cells: deriving from the fusion of the module GFP.VAMP2-3

'UTR of the construct GreenZip instead the GFP of plasmid vector Rosa26: Note The stop sequence (in Fuxia) which is located just upstream of the module GFP.VAMP2-3 'UTR (in Green, Orange and Grey), removable by the enzyme Cre as it is located between two LoxP sites (in blue).

ROSAGreenZip cloning

To generate the plasmid RosaGreenZip, the region of the cDNA encoding eGFP -VAMP2-3'UTR (see above GreenZip clone) was extracted from the original GreenZip plasmid, using the restriction enzyme sites NheI and AccI (2754 bp amplified), and then gel purifying the digested plasmid . The desired band for cloning was recovered and blunted with Klenow enzyme (both enzymes, NheI and AccI cut a 5' protruding end): 5 micrograms of GreenZip cDNA were used in the blunting reaction. Next, 3.6 microliters of 1M Tris pH 7.5, 6 microliters of 0.1 M MgCl2, 6 microliters of b-mercaptoethanol 0.1 M and 0.5 microliters Klenow were added and the mixture was incubated at 12 ° C for 10 minutes. This was followed by the addition of 2.5 microliters of 2mM dNTPs and incubation for 1 h at 12 ° C, prior to which inactivation of 5 'at 70 ° C. The final step, purification of the solution was performed through a column, using a commercially available kit (Promega). Regarding the rosa26 carrier, from this we removed the GFP that was present in the original construct, to be able to insert our Vamp2-GFP, using the enzymes SmaI and AscI. As AscI also cuts a 5' protruding end, we applied the procedure described above, after plasmid gel purification, also to rosa26. Before performing the ligation between Rosa26 and GreenZip, the construct Rosa26 was dephosphorylated using Calf Intestinal Phosphatase (CIP) and then used as a control by performing a parallel ligation of the vector alone. In order to achieve this, 4 micrograms of the vector were used, to which 6 microliters of buffer 10X NEB3 (New England Biolabs Inc.) and 1 microliter of CIP were added, to a final volume of 60 microliters. This reaction was then incubated for 30 ' at 37 ° and subsequently column purified (Promega, the same used above). Finally, for the ligation, this was accomplished with a ratio between vector and insert of 1:5 (ratio for sticky ligations) within the mixture. For this purpose 100-200 ng of vector was used, where the ng of insert were calculated in the following way:

bp vector / bp insert = X,

X / ratio of the ligation (5 in our case) = K

100-200 ng vector / K = ng insert for the rection

For the ligation performed with the dephosphorylated vector alone, the appropriate amount of insert in

H_2O was added to the mixture. Additionally, the respective ng of insert and vector were added to the ligation mixture (1.5 microliters of 10X Buffer (New England Biolabs Inc.), 1.0 microliters of T4 Ligase (New England Biolabs Inc.), 1.0 microliters ATP, H_2O to a final volume of 15 microliters) and the reaction was kept at 15 ° over night.

The following day the bacterial transformation was performed using super competent cells to ensure a high level of transformation (guaranteed efficiency: > 1.0 X 10^9 cfu / microgram DNA) using the appropriate protocol (SCS1 Supercompetent Cells, Agilent Technologies).

The following day the plated recombinant bacterial colonies were subjected to PCR screening, using specific Rosa26 primers. Starting from the bacterial colonies on LB agar (with Ampicillin added, in a final concentration of 50 micrograms/ml, the Rosa26 plasmid provided with antibiotic resistance), each single colony was collected using a sterile loop and placed in an eppendorf containing 50 microliters of LB culture media, diluting the colonies. The remaining bacteria on the loop were streaked on LB plates previously divided into sectors for each colony. The plates were then left at 37 ° o / n, and then centrifuged at 13.500 RPM for 10 minutes. The supernatant was subsequently removed and the pellet was resuspended in 50 microliters of lysis buffer (1% Triton, 2 mM EDTA pH 8, 20 mM Tris-Cl pH 8) and incubated at 95 ° for 10 minutes.

PCR CHECKING FOR THE PRESENCE OF ROSA26 HOMOLOGOUS RECOMBINATION using primers for VAMP2, with MIX PCR

(DNA lysate, 2.5 microliters; 5X TAQ buffer 10 microliters; 25 mM $MgCl_2$ 3 microliters; 2 mM dNTPs 5 microliters; 25 mM PRIMER VAMPF 1 microliter; 25 mM PRIMER VAMPR1 microliter; TAQ POLYMERASE 0.2 microliter; H_2O to a final volume of 50 microliters (VF)).

PRIMER VAMPF1: 5'- `AATCTTACCAGTAACAGGAGAC-3'`

PRIMERVAMPR1: 5'- `GGTCCTCCTCGCTGATCAG-3'`

AMPLIFICATION CYCLES:

94 ° X 45 SEC

56 ° X 45 SEC

72 ° X 30 SEC

GO TO 29 CYCLES

72 ° X 5 MIN

4 ° FOREVER

expected 400 bp band, 1.5% agarose gel

PCR CHECKING GREENZIP INSERT ORIENTATION USING PRIMERS ROSA26 / 3 'UTR GREENZIP: DNA lysate, 2.5 microliters; 5X TAQ buffer 10 microliters; 25 mM $MgCl_2$ 3 microliters; 2 mM dNTPs 5 microliters; 25 mM PRIMER ROSAR 1 microliter; 25 mM Primer3' UTRF R 1 microliter; TAQ POLYMERASE 0.2 microliter; H_2O to a final volume of 50 microliters (VF). (Same PCR program show above)

PRIMER ROSAR1: 5'-CCTCCAATTTTACACCTGTTC-3'

PRIMER 3'UTRF1: 5'-GAACCAAGGAGATCTAAACTG-3'

expected 564 bp band, 1.5% agarose gel

The colonies which were found to be positive to the presence of the recombinant construct and in the correct orientation were removed from the plate, and the cDNA plasmid was obtainedusing a Miniprep kit (Qiagen), on which were performed further enzymatic restrictions to check the identity and integrity of the plasmid (see results).

Mouse genetics

The electroporation of the RosaGreenZip construct into embryonic stem cells (ESCs), and the subsequent injection of the ESCs into blastocysts was performed by CFCM: Core Facility for Conditional Mutagenesis, San Raffaele Scientific Institute, Milan, Italy (for details and protocols, see http://www.hsr.it/en/research/services-open-labs/cfcm-core-facility-for-conditional-mutagenesis-10/):
129/SvJ –derived embryonic stem cells were grown on an embryonic fibroblast feeder layer.

RosaGreenZip electroporation, positive and negative selection were performed, and resistant colonies were picked after 8-10 days of selection. Homologous recombinant clones were then returned and selected by southern blot (as described below). The targeted ES clones were injected into blastocysts derived from C57BL/6J females. The chimeric embryos were then transferred into the uteri of 2.5 day pseudopregnant foster mothers. Chimeric mice with 40/100% agouti color were test-bred by crossing with Cre female mice and both the expression of RosaGreenZip constructs and germline transmission (identified by the presence of agouti offspring) were tested. Identification of heterozygous RosaGreenZip$^{+/-}$ mice was carried out by polymerase chain reaction (PCR). before crossing them to obtain homozygous RosaGreenZip $^{+/+}$ mice. The line was then purified to murine RosaGreenZip crossing both homo and heterozygous male with female mice with wild type C57 up to N9 generations. Cre transgenic animals (SynCRE and ThyCRE) were provided by the laboratories of our institute (K.D. Campsall et al., 2002).

Screening ESCs cells by Southern Blot

Digest DNA in 96-well plate

To each well add:

4ul 10Xbuffer4ul Enzyme0.4ul Spermidine(0.4M) 31.6ul H2O

37‡C 19h, then add 4ul loading dye to each well. Load into 400ml 1% agarose gel immediately or keep the plate at -20‡C.

Southern Blot:

1) A picture was taken (through a UV-transilluminator) of the agarose gel to be blotted with a phoshorescent ruler lined up along side it, such that the ruler is lined up with the top of the wells

2) The DNA in the gel was depurinated by rocking it in 0.25M HCl for exactly 10 min.

3) The gel was then neutralized and alkaline denatured in 0.4M NaOH 3 x 15 min. each.

4) The DNA was transferred to nylon membrane using 20xSSC.

5) The blot was set up from bottom to top:

a) At the bottom, place the gel on a glass plate which covers a large dish filled with 20xSSC.

b) Two pieces of wick- blotting paper were cut to the width of the gel and with a length such that the wicks were in contact with the bottom of the dish. The wick was soaked in 20xSSC and any bubbles were gently smoothed away with a glass pipette.

c) The agarose gel was nicked in the bottom right corner for orientation and then placed upside down on the wick. Bubbles were removedwith the pipette.

d) Hybond N+ nylon membrane was cut to the exact size of the gel, with a nick in the corner for orientation. The membrane was wet with dH_20, placed on top of the gel and smoothed with the pipette

e) Four pieces of blotting paper were cut to the size of the gel. The first was wet with 20xSSC, placed on top of the blotting paper, and smoothed out. The other three were then placed on top.

f) Another glass plate and an additional weight were placed on top to keep the blot in place. The transfer was performed overnight.

5) When the blot was taken apart, care was used to avoid removing the membrane from the gel.

6) The gel and membrane were then taken off together, and flipped over, allowing the wells to be marked with a pencil.

7) The membrane was then crossed-linked with Stratalinker for the cross-linking of nucleic acids to blot membranes

Probe preparation

The probe was labeled with p_{32} using a kit (Prime-A gene system, Promega: see protocol), while a second kit (QIAquick Nucleotide Removal, Qiagen: see protocol) was subsequently used for purification. The probe's CPMA was then calculated using a beta-counter machine present in our institution.

PROBE ROSA26: 5'-CAGGGTTATTGTCTCATGAGCGGATACATATTTGAA-3'

Hybridization

1) The membrane was prehybridized in “CG” Mix at 65 ‡C for at least 1h
2) The probe was then added and hybridized at 65‡C overnight
3) The membrane was washed with “CG” Wash 3x10min. at 65‡C
4) The membrane was then wrapped in Saran Wrap and exposed at -80‡C 4-7days

“CG” Mix (for 100ml)

50ml 1M NaP, pH7.2 35ml 20% SDS10ml 10% BSA0.2ml 0.5M EDTA pH8.0 4.8ml H20

“CG” Wash (for 2 liters)

80ml 1M NaP pH7.2 100ml 20% SDS4ml 0.5M EDTA pH8.0 1816ml H20

Genotyping

A small piece of mouse tail was cut and digested in 1 mg/mL proteinase Kinase (PK) in tail buffer (50 mM Tris-HCL, 100 mM EDTA, 100 mM NaCL, 0.5% SDS) at 55° over night. DNA was isolated using equal volumes of phenol:chloroform, precipitated with isopropanol and washed in 70% ethanol. DNA amplification was performed by PCR.

For insertion of RosaGreenZip into the genomic locus Rosa26: 5'- GGAGCGGGAGAA ATGGGATATG -3' (wild type primer R523 from Brian Zambrowicz, Technology Forest Place, TX, USA); 5'- AAAGTCGCTCTGAGTTGTTAT-3' (common wild type primer R26F2 from Phil Soriano, Mt. Sinai School of Medicine, Ny, USA); 5'-AAGACCGCGAAGAGTTTGTC -3' (With primer IMR 316, amplifies an ~ 320 bp fragment from the mutant allele). steps: denaturated at 94° for 3 minutes; 30 cycles of denaturation at 94° for 30 seconds; annealed at 58° for 1 minute; and elongated at 72° for 1 minute.

For GFP primer F: ACGTCTATATCATGGCCGAC; and VAMP2 primer R: ATGTGTCCACCACCTCATC. The amplification product for the mutant locus was 433 bp. PCR steps performed were: denatured at 95° for 2 minutes; 30 cycles of denaturation at 94° for 45 seconds; annealed at 56° for 45 seconds; and elongated at 72° for 30 seconds.

For SynapsinCRE: primer F: CCAGCACCAAAGGCGGGC; primer R: TGCATCGACCGGTAATGCAG. The amplification product for mutant locus was 450/500 bp. PCR steps performed: denatured at 94° for 5 minutes; 30 cycles of denaturation at 94° for 30 seconds; annealed at 61° for 30 seconds; and elongated at 72° for 30 seconds.

For ThyCRE: primer F: GGTATTCAGTCATGTGCTCCG; primer R: TGACCAGAGTCATCCTTAGCG. The amplification product for mutant locus was 1000 bp. PCR steps performed: denatured at 95° for 5 minutes; 30 cycles of denaturation at 95° for 30 seconds; annealed at 54° for 45 seconds; and elongated at 72° for 1 minute.

All the amplification products can be revealed in 2% agarose gel.

Cell lines

HeLa cells, a human cervix cancer epithelial cell line, was provided from ATCC (http://www.Igcpromochem.com/atcc/). Cells were grown in standard conditions: 5% CO_2, 37°C constant humidity. Culture medium was DMEM (Dulbecco's modified Eagle Medium) without phenol red supplemented with 5-10% FCS (fetal calf serum – Gibco Brl-), penicillin and streptomycin 100U/ml and 2mM Glutamax (Invitrogen).

Animals

For in vivo experiments C57 wild type and 129/SvJ –C57BL6j derived transgenic mice were used. Animals were housed one per cage in a temperature-controlled environment and had free access to food and water. Animals were light cycle controlled (maintained with 12 hours of light alternating with 12 hours of darkness). Experiments were performed in animals light period.

Transfection

Lipofectamine 2000 (Invitrogen) was used for transient transfection of glial cells (you do not mention the glial cells above) and HeLa cells where very high efficiency was needed. The transfection protocols applied were modified slightly from the manufacturers instructions. Cells were incubated with Opti-MEM I reduced serum medium (Gibco) for 20 minutes prior to transfection. Two solutions were prepared: i) Solution A, containing DNA and Opti-MEM (ratio 1:1) and ii) Solution B, containing Lipofectamine 2000 and Opti-MEM (ratio 1:25). After 5 minutes, Solution A was mixed with Solution B

and incubated for 20 minutes at RT, providing the transfection mix. This mix was then put into cells drop by drop and incubated for 4h (37°C,5%CO_2) . After incubation, the cells were washed with Opti-MEM and incubated with complete culture medium (supplemented with FCS) for how long.

Co-transfection Rosa26 plasmid and Cre

We tested the functioning of the plasmid by cotransfecting it into HeLa cells, with a Cre plasmid, so as to test both the effectiveness of the Cre-mediated expression, and the functionality of our construct through synbond uptake.

Following Lipofectamine transient transfection of HeLa cells with the RosaGreenZip plasmid and Cre plasmid (from Addgene) resulted in a molar ratio between the plasmid RosaGreenZip (approximately 17,300 bp) and Cre (about 5000 bp) of between 1:1 and 2:1 (the latter molar ratio extremes for the presence of plasmid RosaGreenZip that can produce GFP positive signal, only in the presence of Cre). whereas in the ratio 1 microgram RosaGreenZip: 1 microgram Cre will see a ratio of three times the number of Cre molecules on that of RosaGreenZip considering the relationship between the number of base pair constituting the two plasmids

Then after being washed with 1 x PBS, the HeLa cells in which the signal was detected were fixed in 4% Paraformaldehyde (1 ml) and let 4 'at -20 °. Then they were maintained for 30' in blocking buffer (1X PBS / 1% BSA / 0.1% Saponin) and kept on ice. To these cells anti-GFP antibody (1:100) was added and incubated for 2h. After being washed for 30 'with blocking buffer the secondary antibody (Donkey anti-rabbit FITCH, 1:200) was added and incubated for 1 h. A final wash with blocking buffer for 30' was performed and the cells were mounted to coverslips. Also a part of these cells, not treated with antibodies, were incubated with Synbond for 30’

Western blot analysis

After electrophoresis, proteins were transferred to a nitrocellulose membrane (Schleicher & Schwell, Whatman). The blotting process was done at 4°C in transfer buffer (Transfer Buffer: Tris 20mM, glycine 153mM, 20% Methanol) at constant current for 5h counting a total of 2000mA. At the end of the transfer process, the nitrocellulose filter was incubated for 5 minutes with 0.2% Ponceau Red (0.2% ponceau red, 3% trichloracetic acid) to stain proteins, decoloration was performed with bidistillated water. Gels were stained O/N with Comassie Blue (50% methanol, 10% acetic acid, 0.1% Comassie Blue R250 – Sigma -), and washed with 1X PBST.

Transferred proteins were recognized by selective antibody tagging. Membranes were first rehydrated for 5 minutes than left for 1h in blot solution. Nitrocellulose filters were then incubated, with constant agitation, for 1hr at RT with selected primary antibodies dissolved in blot solution(Tris-HCl 50mM pH 7.4, NaCl 150mM, 0.05% tween20, 5% milk). Primary antibody wash out was performed with blot solution and secondary antibodies were used for 1h incubations and wash out was again performed. Finally, membranes were incubated with ECL for 1 minute (luminal, H_2O_2 and intensification agent) and autoradiographic detection (Amersham Hyperfilm MP) was performed.

Antibodies for western blot analysis

Anti-GFP, rabbit polyclonal (Molecular Probes)

2.3 LENTIVIRAL VECTOR

Lentiviral Vector

The pCCLsin.cPPT.PGK.GFP.Wpre transfer vector construct was obtained from the pCCLsin.hCMV.GFP construct (Dull et al., 1998) by adding the posttranscription regulatory element of the woodchuck hepatitis virus at the 39 end (Wpre) and cPPT–CTS sequences as described (Follenzi et al., 2000). The pCCLsin.cPPT.PGK.GFP.Wpre construct has been described elsewhere (Follenzi et al., 2000) and contains nucleotides 5 to 516 of the human phosphoglycerate kinase (PGK) promoter (GenBank accession number M11958). The pCCLsin.cPPT.ALB.GFP.Wpre construct was generated by replacement of the cytomegalovirus (CMV) promoter in the pCCLsin.cPPT.CMV.GFP.Wpre construct with a 2.3-kbp fragment containing the mouse albumin enhancer (GenBank accession number U04199) and promoter (nu- cleotides 1729–2063; GenBank accession number J04738) derived from plasmid pHIV-CS-ALB-dFIX. The expression constructs used for LV production are maintained in the form of bacterial plasmids and can be transfected into mammalian cells to produce replication-defective virus stocks. Plasmids should be prepared and purified by double CsC1 gradient centrifugation or other commercially available column methods yielding endotoxin-free DNA. Here you will be shown the calcium phosphate method for cotransfecting 293T cells with four plasmids [third-generation core packaging plasmids: pMDLg/pRRE and pRSV.REV, self-inactivating (SIN) transfer vector plasmid pCCL-SIN- 18PPT.Prom.EGFPWpre, and envelope plasmid pMD2VSV.G (Fig. 32) (this last plasmid was constructed by cloning the VSV.G-encoding EcoRI fragment from the pMD.G to the pMD-21'1°'ls'z°), for packaging the vector genome carrying the gene of interest into hybrid replication-defective viral particles. LV are traditionally produced by transient cotransfection of human embryonic kidney 293T cells because these cells are good DNA recipients in transfection procedures and the backbones of the vector construct contain SV40 origin of replication.

GreenZip clone

The GreenZip clone used for insertion inside the lentiviral vector is the same as described above.

LentiZip cloning

To generate the plasmid Lentizip (Lenivirus plasmid + GreenZip), the region of the cDNA encoding eGFP -VAMP2-3'UTR was extracted from the original GreenZip plasmid, using the the restriction enzymes sites AgeI and SalI (2714 bp amplified), and then gel purified and the band for cloning was recovered. For the lentiviral plasmid carrier #277 pCCLsin.cPPT.PGK.GFP.Wpre (a gift from Naldini's lab), the GFP present in the original construct was removed using the same enzymes AgeI and SalI, to allow insertion of our Vamp2-GFP, after lentiviral plasmid gel purification. All procedures (dephosphorylation of lentiviral plasmid and ligation) are the same to those reported for RosaGreenZip with the use of the same materials.

Lentizip tritation and production

Calcium phosphate precipitation to transfect plasmids was used: 24 hr before transfection 293T cells were seeded (5 x 10^6) in a 10 cm dish, in IMDM, 10% fetal bovine serum (FBS), penicillin (25 U/ml), streptomycin (25 U/ml). Media was changed 2 hr before transfection and the plasmid DNA mix was prepared by adding 3 /zg envelope plasmid (pMD2-VSV-G), 5 /zg of core packaging plasmid (pMDLg/pRRE), 2.5 /zg of pRSV-REV, and 10/zg of transfer vector plasmid (pCCLsin 18.PPT.PGK.GreenZip.Wpre) together per dish. The plasmid solution is made up to a final volume of 450/zl with 0.1x TE/H20 (2 :1) in a polypropylene tube. Finally, 2.5 M CaC12 was added 50/zl of and the solution mixed by vortexing. The precipitate is formed by dropwise addition of 500/zl of the 2x HBS (HEPES Buffered Saline) solution (280 mM NaC1, 100 mM HEPES, 1.5 mM Na2HPO4, pH 7.12; check pH of 2x HBS carefully) to the 500 #1 DNA-TE-CaC12 mixture while vortexing at full speed. The precipitate was added to the 293T cells immediately after 2x HBS addition. High magnification microscopy of the cells revealed a very small granular precipitate of the calcium phosphate-DNA complexes, initially floating above the cell layer, and after incubation in the 37° incubator overnight, it was visible on the bottom of the plate in the spaces between the cells. The calcium phosphate-DNA precipitate should be allowed to stay on the cells for 14-16 hr, after which the medium should be replaced with fresh medium for vector collection to begin. Cell supernatant collection occurred at 24 and 48 hr after changing the medium and was centrifuged at 1000 rpm for 5 min at room temperature and filtered supernatant through a 0.22-#m pore nitrocellulose filter.

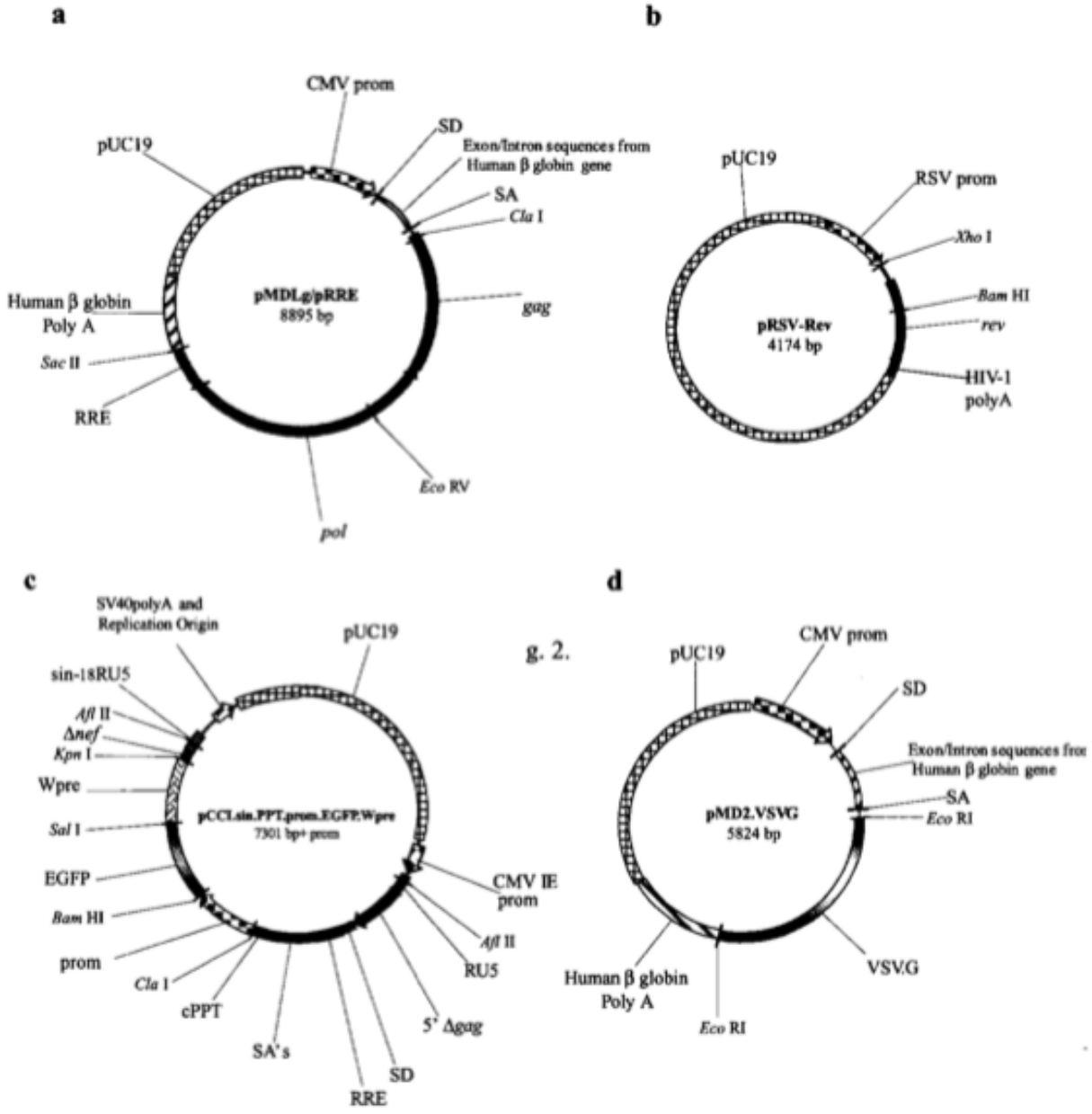

g. 2.

Fig.32. Schematic drawing of the four constructs required to build VSV-pseudotyped third- generation HIV-l-derived lentiviral vectors. (a) The conditional packaging construct expressing the gag and pol genes driven the CMV promoter. (b) A nonoverlapping construct, RSV-Rev, expressing the r~, cDNA under the RSV promoter. (c) The self-inactivating (SIN) transfer construct containing HIV-1 cis-acting sequences and an expression cassette for the transgene (enhanced green fluorescent protein or EGFP) driven by the internal promoter. (d) A fourth construct encoding a heterologous envelope to pseudotype the vector, here shown coding for the protein G of the vesicular stomatitis virus, Indiana serotype (VSV.G) under the control of the CMV promoter. Relevant restriction sites for cloning purposes are shown (From Follenzi A., 2002)

To obtain a high-titer vector stock, to the 293T conditioned media was concentrated by ultracentrifugation at 50,000g for 140 min at 20°. The supernatant was discarded by decanting and the pellets were resuspended in a small volume of PBS containing 0.5% BSA, pooled in a small tube, and rotated on a wheel at room temperature for 1 hr. The concentrated vector from the first collection at 4° was stored until the procedure was repeated for the second collection the following day.The two vector suspensions were then pooled, diluted in phosphate-buffered saline (PBS), and concentrated again by ultracentrifugation. Resuspension of the final pellet was performed in a very small volume (1/500 of the

starting volume of medium) of sterile PBS-0.5% bovine serum albumin (BSA). Resuspension of the second pellet required prolonged incubation on a rotating wheel and pipetting at room temperature, Before to split into small aliquots (20 microlitres), store at - 80 °, and titer after freezing. Relative concentrations of vectors were measured as a titer. The vector titer was determined as the number of complete particles that were able to transduce cells. The transducing particles usually represent a small percentage of total particles and can vary between different preparations. The concentration of infectious particles is estimated by end-point titration of the vector preparation on a standard, easily infectable cell line. For the standard titration of a vector containing GFP as a transgene with a ubiquitous promoter such as PGK we use HeLa cells (end-point titer on HeLa). The day before the transduction 5 x 10^4 HeLa cells were plated per well in a 6-well plate. The following day serial 10-fold dilutions of viral stocks in IMDM 10% FBS were prepared, approximately ranging from undiluted to 10^{-6} for 293T-conditioned medium and from 10^{-3} to 10^{-8} for concentrated vector. Of each dilution, 0.1 ml was added to the cells. Before titration the medium was replaced with 0.9 ml fresh medium containing 9/zg/ml Polybrene and the cellsincubated at 37° for 16 hr. The day after, the medium was changed and the cells grown for 72 hr at 37°. The cells were then washed well with PBS, trypsinized, and harvested with PBS in FACS tubes. Finally, following centrifugation (XXX), 1 ml of fixing solution (1% formaldehyde, 2% FBS in PBS) was added, tubes were vortexed and samples were stable at 4° for few days. The titer was performed by fluorescence-activated cytometric analysis for GFP using the EL1 channel on the fluorescence-activated cell sorting (FACS) measuring the percentage of cells expressing EGFP in the total population. The titer was expressed in TU (Trasduction Unit)/ml and calculated as follows:

n. infected cells X EGFP cells positive percentage X corresponding dilution factor/100 = Trasduction Unit (TU)

The Gag capsid protein p24 is a major structural component of the HIV-1 core and, consequently, of all HIV-1 derived vectors. The content of Gag proteins in vector particles can be assayed using antibodies recognizing the mature form of the protein and, with less affinity, the Gag precursor. The assay was performed following the instructions provided by the manufacturer, except for the sample preparation, as follows: the test was performed using serial dilutions from 10^{-5} to 10^{-8} if you have concentrated vector. The commercially available tests have a limit of sensitivity in the range of 3 pg/ml, therefore a good vector preparation should have a p24 concentration in the range of 100-500 ng/ml in the 293T-conditioned medium. The ratio between transduction units (TU) per ml and the nanograms of p24 per ml gives the infectivity (or specific transducing activity), a reliable parameter to evaluate the quality of a vector preparation, where the transducing units (TU) per mililiter are obtained by end-point titration on HeLa and should be >10^4.

The fluorescence titration depends on infectivity from the vector transduction activity in the transduced cells. The DNA analysis of transduced cells, on the contrary, directly reveals the integration vector capacity into the target cells genome, regardless of expression of the transgene. Real-time PCR therefore detects if the carrier does not constitute or contain promoters active in a given cell line used in the titration or if the activity of the expressed transgene can not be validated directly.

The protocol for fluorescence titration includes the following steps: on day 0 were plated 1 * 106 cells in 2 ml of medium (HELA in DMEM-10% serum, 293T in IMDM-10% serum, in Nunc). On day 1 the wells were washed 1 time with PBS1X (Gibco) and added with 500 μ l of half filtrate with 9 μ g/ml of Polybrene. One of the wells is used to estimate the number of cells upon infection. were diluted therefore 2 μ l of lentiviral vector in 500 μ l of medium and were added to the wells.

The genomic DNA of a well, in which there has been added the suspension lentiviral, is used as a mock for the subsequent PCR reaction. After 3 days the wells were washed two times with 2ml of 1 X PBSand the genomic DNA was extracted following the instructions of theFlexiGene DNA kit (QIAGEN). The cellular debris was removed following centrifugation (13000 rpm for 5 minutes) and the supernatant left at 37ºC for 15 minutes. The concentration wasestimated spectrophotometrically

The standards (std) used in the real time PCR reaction were:Std 0: 40 ng / ul of linearized plasmid PCCL-SIN18PPT.Prom.EGFPWpre (5 * 10^9 molecules);

Std 1 to 7: 1:10 dilutions of std 0 in order to have 8 standards from 5 * 10^9 to 500 molecules;

The thermal protocol used is: 95 ° C X 4 minutes (94 ° C + 60 ° C sec X10 X15 X20 sec + 72 ° C sec, plate read 72 ° C + 78 ° C X1sec plate read): 39 cycles; Melting curve of 58 to 98 ºC read every 0.5 ° C (1s); The plate is prepared with the following mixture per well (10µl):(each sample in triplicate), 5µl Sybergreen (BIO RAD), 0.5µl 10µM oligo forward and oligo reverse 0.5µl 10µM, 0.5 l dna sample (including mock), 3.5µl H2O.

For the calculation of the title we performed the following: assessed the number of lentiviral amplicons present in infected cells (N ° vir), representative of the number of pro-virions integrated into their genomic DNA, using a standard curve calculating the number of molecules of genomic DNA of the cell substrate to each well:(Mass of genomic DNA) / (molar mass genomic DNA)) = N ° moles of DNA,where 1.8 * 10^{12} gr is the molar mass of the genomic DNA. This then proceeds to the estimated ratio (N ° vir) / (N ° moles of DNA), correlated linearly with the title of the viral preparation loaded on such cells. Finally, we compared the ratio (N ° vir) / (N ° moles of DNA) of the virus with that of another previously titrated for fluorescence and, by linear interpolation, revealed the title of the second, back up to that of the first.

Animals

For in vivo experiments adult male Sprague-Dawley rats (n=4) weighing between 180-230g were used. Each animal was kept in a cage that allowed free access to food and water and was exposed to cycles of light / darkness of 12 hours in an environment with constant temperature of 23 ± 1 ° C. The cage was changed once every two days. Animals are repeated from above but this section is better than the first.

Cell lines

See prcedent section (Transgenic animal)

Postnatal hippocampal dissociated neuronal cultures

Postnatal hippocampal neuronal cultures were grown as previously described (Malgaroli & Tsien 1992). Briefly, postnatal (P2-P5) hippocampal neurons were grown on special coated (polyornitine 1μg/ml) coverslips in standard conditions: 37°C, 5%CO_2 (1liter of slice culture medium: 30mg insulin, 0.1mg biotin, 1.5mg B12 vitamin, 100mg L-ascorbic acid, 100mg transferring, 100mg Glutamax, 7g glucose, 3.6g HEPES in 1l of MEM Gibco with Earle's salts w/o phenol red). Sprague Dawley rats were decapitated and the hippocampus was separated in cold dissociation medium (1liter of dissociation medium: 350mg $NaHCO_3$, 10mM HEPES, 6g glucose, 200μM kynurenic acid, 3% BSA, 12mM magnesium sulfate, 5mg gentamycin, 1l Hank's salt solution – Sigma Aldrich- pH 7.3). Following this they were exposed to enzymatic digestion with 3mg/ml trypsin in digestion medium containing 1mg/ml DNAase I (from bovine pancreas – Calbiochem-) for 5 minutes (100ml digestion medium: NaCl 137mM, KCl 5mM, $NaHPO_4$ 7mM, HEPES 25mM, $NaHCO_3$ 35mg, kynurenic acid 200μM, pH 7.4), and then the cells were mechanically dissociated in dissociation medium supplemented with 1mg/ml DNAase I. Cells were grown for 9-14 DIV and every 3 days 1/2V of culture medium was replaced with fresh supplemented with ARA-C (2.5-5μM), to preventexcessive glial cell proliferation.

In vivo LentiZip aplication

See above: Synbond application (GreenZip clone materials and methods section)

Confocal microscopy and data analysis

Confocal microscopy and data analysis was performed as described in the previous section (materials and methods, immunofluorescence for GreenZip clone)

RESULTS

3.1 IN VIVO EXPRESSION OF THE ACTIVITY REPORTER GREENZIP

Expression of GreenZip in Retinal ganglion cells

The importance of having a method such as GreenZip for the functional analysis of synapses inside the living brain and the need to express this reporter in different brain areas has led to a few important considerations: i) it would be essential to get GreenZip expression in the in vivo brain; ii) it would be important to have a time- and space-regulated expression of this protein; iii) the transfected circuits should be experimentally accessible, such that they can be stimulated in vivo under physiological conditions possibly with physiological stimuli; and iv) in order to avoid confusion with other types of neuronal exo-endocytosis it would be wise to have the expressing cells, i.e. the input, anatomically "distant" from the location of the synaptic terminals that will be challenged with the tracer Synbond. For these reasons, as an initial target we chose to use the visual pathway to study the in vivo internalization of Synbond, as an in vivo model for studying the feasibility of our construct and functional assay. In the visual system, the entire circuit that starts with retinal photoreceptors impinges upon the ganglion cells, the only output element that sends signals to the visual thalamus. Ganglion cells are the only cell type in the retina circuit that can generate action potentials, which travel along their axons and constitute the optic nerve, for information flow out from the retina to the brain. The optic nerves of both eyes meet at the chiasm, the junction point where information is combined from both eyes. The corresponding halves of the visual field (left and right) are indeed processed respectively by the left and right halves of the brain (Fig 33). The information coming from the right visual field (which is now on the left side of the brain) along the fibers of retinal ganglion cells will travel along the optic tract (to the left), with each optic tract ending at the level of the lateral geniculate nucleus (LGN) of the thalamus, where the axons from the ganglion cells synapse. About 90% of these axons, which originate from the retinal ganglion cells, make synapses at the LGN, while different populations of ganglion cells will lead the information to the level of the Superior Colliculus of the midbrain and the Pretectum.

Therefore, to demonstrate our model in vivo, the cDNA coding for GreenZip was transfected into the ganglion cells of the retina (RGCs) by electroporation (see methods above). The transfection protocol we established to yield a high transfection efficiency (Fig 34), allowed us to easily identify groups of axons and terminals GreenZip-positive in the retina and follow them up to the LGN. As presented in Figure 33,

ganglion cells expressing GreenZip are easily recognized. The shape of the cell somata is usually spherical or slightly pear-shaped, these cells usually have very large dendritic branches, which are needed for the receptive field integration, and their axons can be easily identified by the spotty GFP fluorescence. This is due to packets of vesicles running towards their final destination, the thalamic or LGN synaptic boutons (fig 37, 38 and 39).

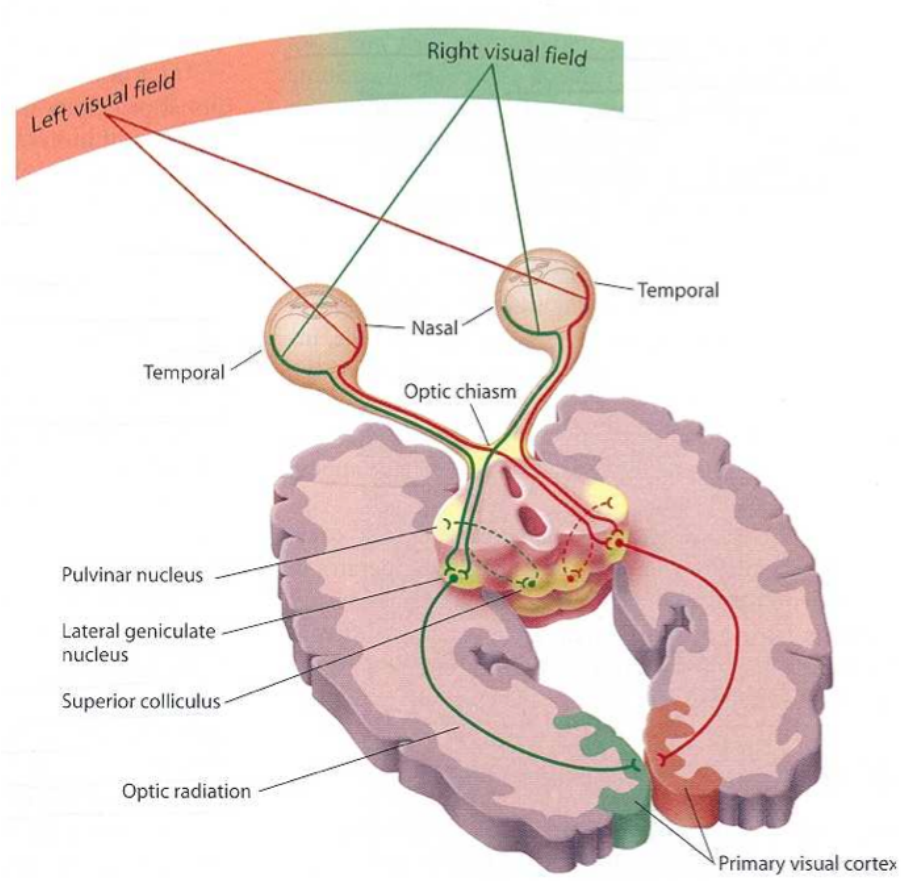

Fig 33 representative cartoon of the human visual pathway, retinothalamic pathway; LGN and thalamocortical connections. Because of the crossing of Nasal hemi-retina axons, light from the left visual field and subsequent stimulation is transmitted to the right visual cortex, whereas those from the right hemi-field are transmitted to the left visual cortex (From Ward D.G., 2006).

As the visual pathway has been extensively studied and characterized in primates, but less developed in rodents, it was necessary to perform a preliminary study to find a suitable stimulation method for retinal ganglion cells. For this reason, we used c-fos, a marker of neural activity, to determine the optimal visual stimulation pattern for the RGCs (see below). Once the best frequency and stimulation intensity was established we began using electroporation to transfect ganglion cells with GreenZip cDNA. The cDNA was injected into the vitreous body under stereoscopic guide, with the site of injection being 1 mm behind the limbus. Through this technique it was possible to inject the DNA very close to the retina, in a region intersecting the major retinal blood vessels, which corresponds to the fovea in humans. This was important because the rat retina does not have a clearly visible fovea, the richest region in retinal ganglion cells. After the time set to allow the DNA to spread (5-10 minutes of incubation), the electroporation was

carried out. For this purpose we developed two gold electrodes (see materials and methods), which enclosed the eye with the corneal electrode joined to the cathode and the scleral to the anode. Square-wave pulses were sent in sequence by an appropriate square wave generator to which the electrodes were connected. With this method we obtained high transfection efficiency in the retina (Fig 34) allowing us to easily identify axons and terminals groups GreenZip-positive into the matching LGN.

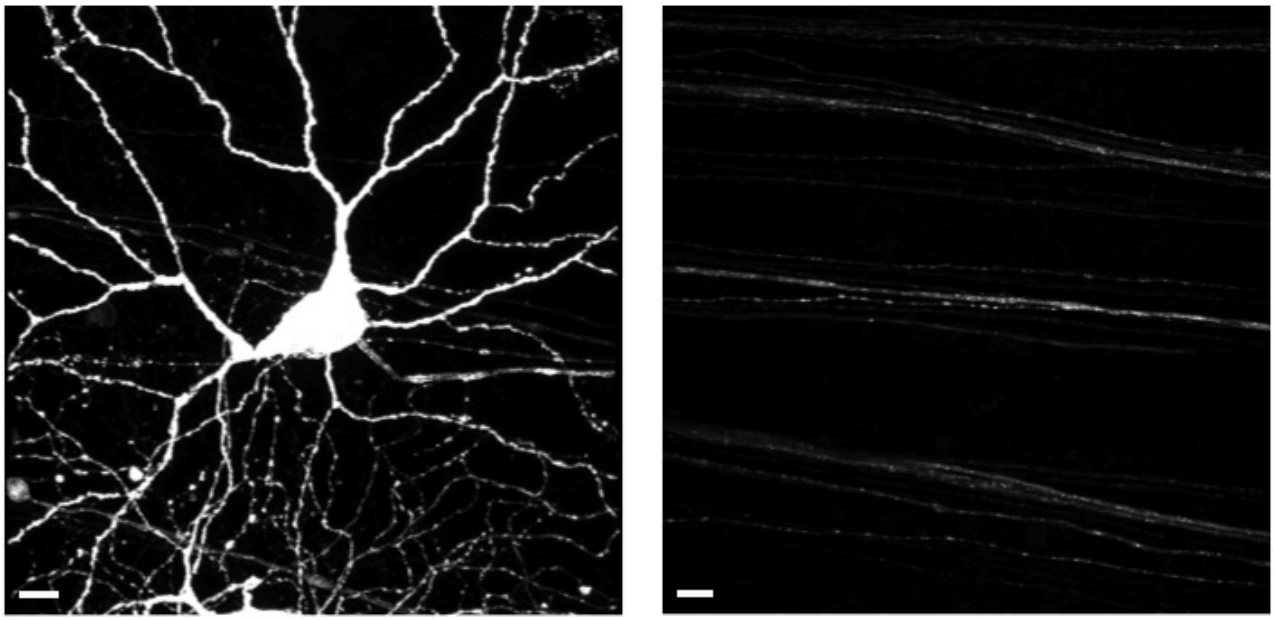

Fig 34: retinal ganglion cells transfected with GreenZip. The fluorescence of cell body and dedndrites (left) and axons (right) expressing the GreenZip construct is coded in grey levels. Fluorescent puncta shown in the left panel are vesicles expressing GreenZip wich transported along the axons of transfected RGCs. (flat mounted retina, 63X magnification, bar 10 μm)

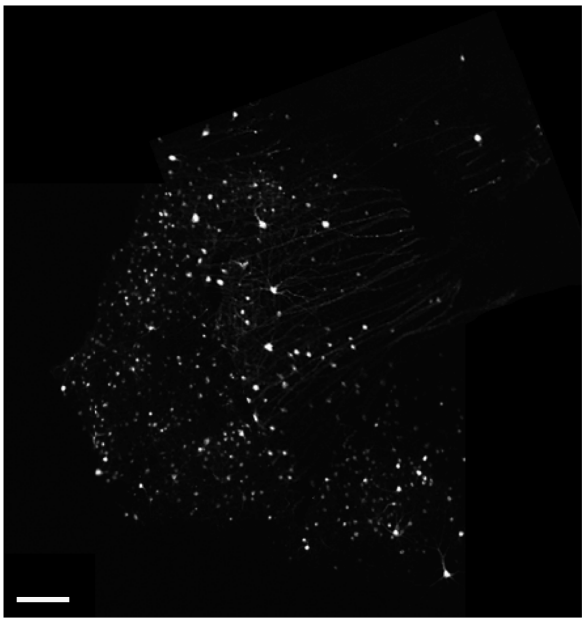

Fig 35: Whole mounted retina: reconstruction from low magnification images. GreenZip expressing cells are shown in grey level, some axons running toward the optic disc are also visible. Notice the good efficiency: with this technique not only RGCs are transfected but also a variety of retinal cells. (flat mounted retina transfected with GreenZip; 10 x magnification; bar 100 μm).

In these experiments, in every animal, just one eye (the left eye) was electroporated with GreenZip. Although hundreds of GFP positive were usually seen, the transfection efficiency was not very high if one considers that in rats the ganglion cells population is estimated to be 110,000. As shown in these experiments, vesicles presenting our GFP construct, were transported along the axon to the synaptic terminals. Thanks to the very intense fluorescence signal by the expression of Greenzip we have been able to reconstruct the path of single ganglion cell axon inside the retina up to the origin of the optic nerve (Fig 34-35). These axons were seen inside the optic nerve and chiasm and their path could be followed inside the LGN (Fig 36 and 37).

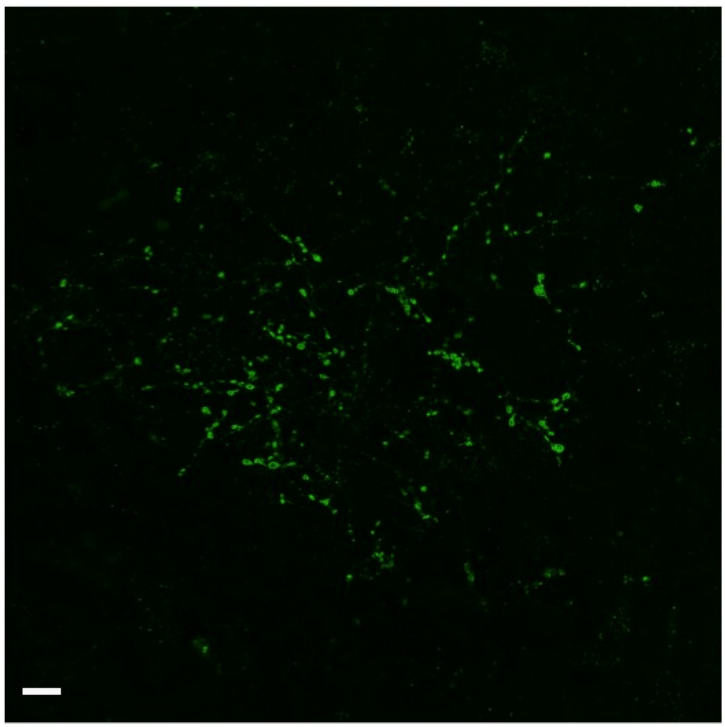

Fig 36: reconstruction from 3D-stacks of Retino-geniculate synapses in the dorsal LGN (dLGN). The green fluorescence arises from GreenZip positive retinal ganglion cell axon terminals that are organized as Rosette varicosities around LGN neurons. (bar 10 μm).

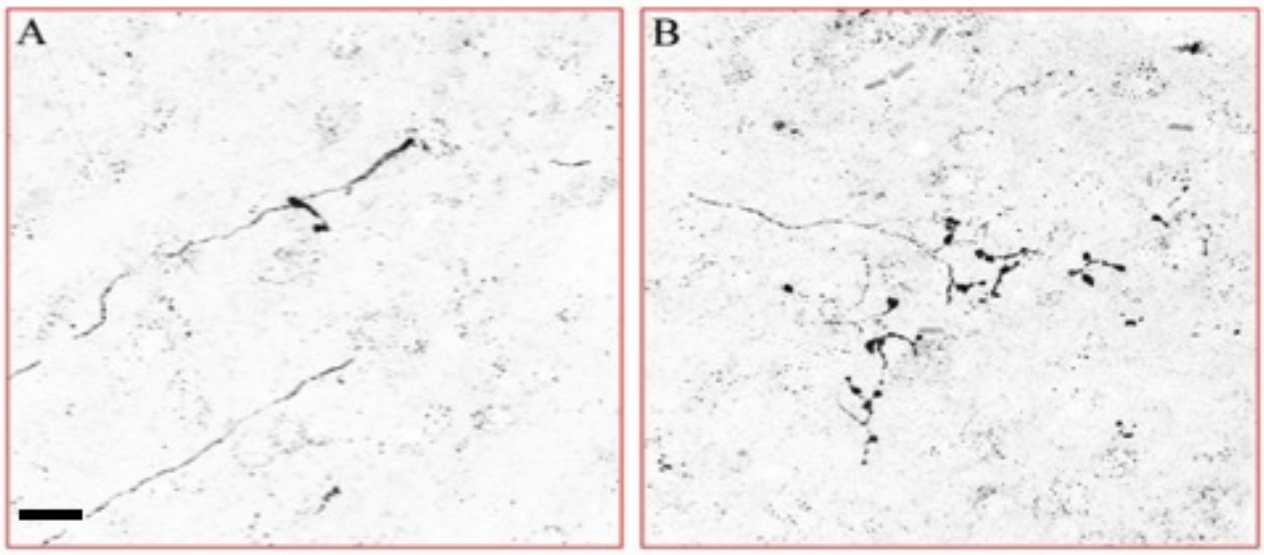

Fig 37 Reconstructions from 3-D stacks of retino-geniculate axons and their synaptic endings at the level of the LGN. The fluorescence of axons and terminals expressing the GreenZip construct is coded in grey levels. In A are shown two axons, in B the synaptic branches at the axonal end with the typical "rosette" shape terminals. These images were taken at the LGN level contralaterally with respect to the retinal ganglion cells transfected (bar 20μm)

Unfortunately, the visual pathway has been extensively studied and characterized in primates, but we do not have very detailed information about the visual pathways in rodents, particularly in rats. As said above it was thus necessitated a preliminary study to find a suitable stimulation method of retinal ganglion cells (RGCs). The intention, through our sensors, is precisely to quantify the presynaptic vesicular activity as result of different types of visual stimulation. As described in the materials and methods for the RGCs stimulation carried out in vivo on animals, we used a Plexiglas-mirror cage, custom made, with six LED high luminance, capable to alternate pulses of light-dark at different frequencies (see fig 27, materials and methods section). Before applying this in vivo stimulation method, with the couple GreenZip-Synbond, to be sure that the light stimulus was going to actually cause an activation of retinal ganglion cells and to find the visual stimulation protocol that would ensure the best activation of the cells, we have tested the effects of various alternative stimulation protocols on relay thalamic nuclei. To evaluate the postsynaptic activation (the output) as a result of the different light stimuli (the input) we have used retrospectively classical immunostaining techniques through the use of some neural activity antibody-reporter. In particular one of the antibody-reporter's greater use is the antibody anti-C Fos: this proto-oncogene is a member of the immediate early gene family, whose transcription is regulated upstream from multiple extracellular signals (such as growth factors). In neurobiology, the extent of the expression of C-Fos is used as an indirect marker of neural activity, since it generally appears to be expressed when neurons emit massive discharge of action potentials.

Arguably then, if the condition of light stimulation in which our animals would have been, had been able to strongly stimulate retinal ganglion cells, these would have in turn activated the post-synaptic cells at the LGN level. Obviously through C-Fos is possible to analyse the massive post-synaptic activation, in

fact C-Fos is certainly not able to detect sub-threshold activity or to detect a single or few action potential, C-Fos is "turned on" when the input redirected to the post-synaptic cell have reached and exceeded a certain threshold that goes beyond a single action potential. In our case, however, C-Fos is the best test-reporter for stimulation protocols, if a post-synaptic neuron expresses C-Fos we can be sure that at the presynaptic level (and then at the input level) there has been activation, or vesicular release of glutamate. Of the various protocols tested in this way, the most efficient for the activation of C-Fos is the protocol which provided 5 light minutes and 15 dark minutes alternating for a total duration of 1 hour. Figure 38 shows some neurons within the LGN, shown by double staining with anti-NeuN, a marker of selective neuronal bodies (green), and C-Fos antibody (red).

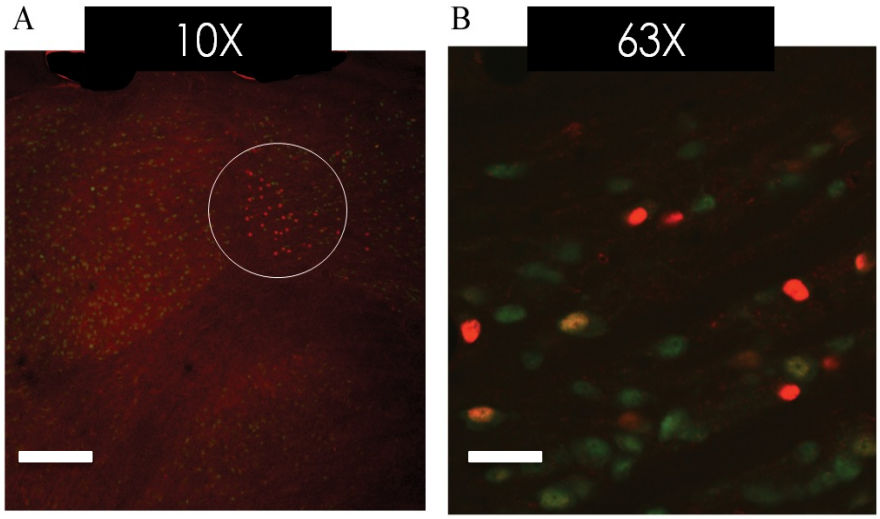

Fig 38: Analysis of the efficiency of stimulation protocols using the expression levels of c-Fos. In this experiment is shown the effect of a visual stimulation with the alternation of 5 minutes of light and 15 minutes of darkness. Out of a total of 130 cells analysed, we found an average of 6.7 cells positive for C-Fos. The analysis of fluorescence was carried out through a co-staining technique of brain slices using antibodies anti C-Fos (in red) and anti NeuN (in green). The cells positive for C-Fos were plotted as percentage versus total cells labeled with anti-NeuN. The staining was performed on LGN coronal slices of animals stimulated in the light box for the duration of 1h and then immediately sacrificed. Figure B shows a higher magnification (63X, bar 10μm) taken from Figure A (10X, bar 100μm) showing active LGN neurons that express high levels of C-Fos protein. This is found to be the most efficient protocol for the activation of thalamic cells.

It was then carried out an immunostaining at the LGN level of an animal that had been kept in the dark for 1h and then sacrificed without being stimulated by light. Also in this case the neural cells were detected by an anti-NeuN antibody, and their activities by an anti C-Fos antibody. Figure 39 shows the final product of this analysis at the level of the LGN. Very few c-Fos positive cells could be identified in this condition suggesting a very low level of neuronal activity. With these experiments we have shown that our stimulation protocol (many other protocols, not shown here, were tested and their efficiency

compared) activates the retinal ganglion cells and the LGN thalamic cells. The following will describe the method I have used to apply Synbond directly in the thalamus, and in this way, succeed in the task of monitoring the synaptic activity in vivo.

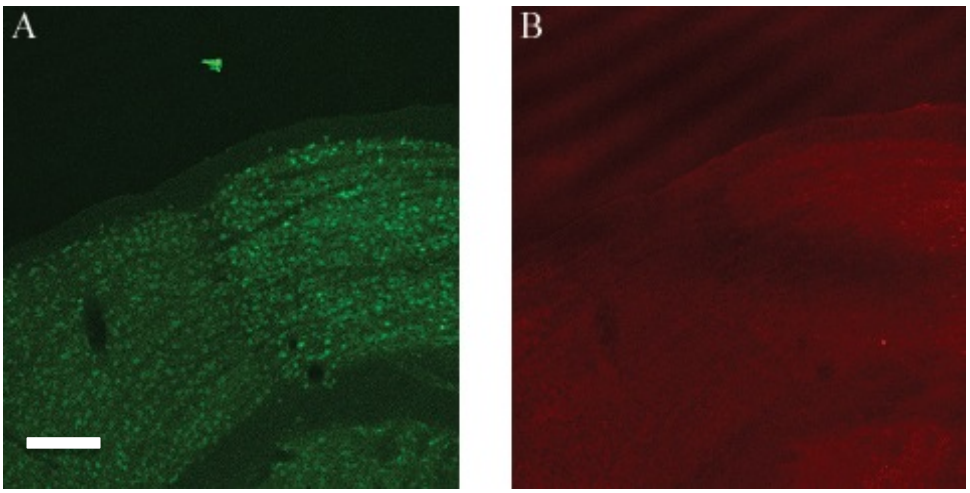

Fig 39: Staining of coronal brain slices carried out at LGN level from a no-light stimulated or control animal (animal kept in the dark for 1h and then sacrificed) A panel: antibody anti-NeuN showing the distribution of neural cells (in green); B panel antibody anti-Fos C showing cell activity. Despite the many neuronal cells (A) their activity is very low (B). (bar 100μm)

Synbond diffusion inside the thalamus in vivo

At this point it seemed obvious the need to investigate the diffusional profile of the peptide Synbond, the tracer whose injection into the brain was needed in order to determine the degree of synaptic activation. Figure 40 shows the results of this analysis.

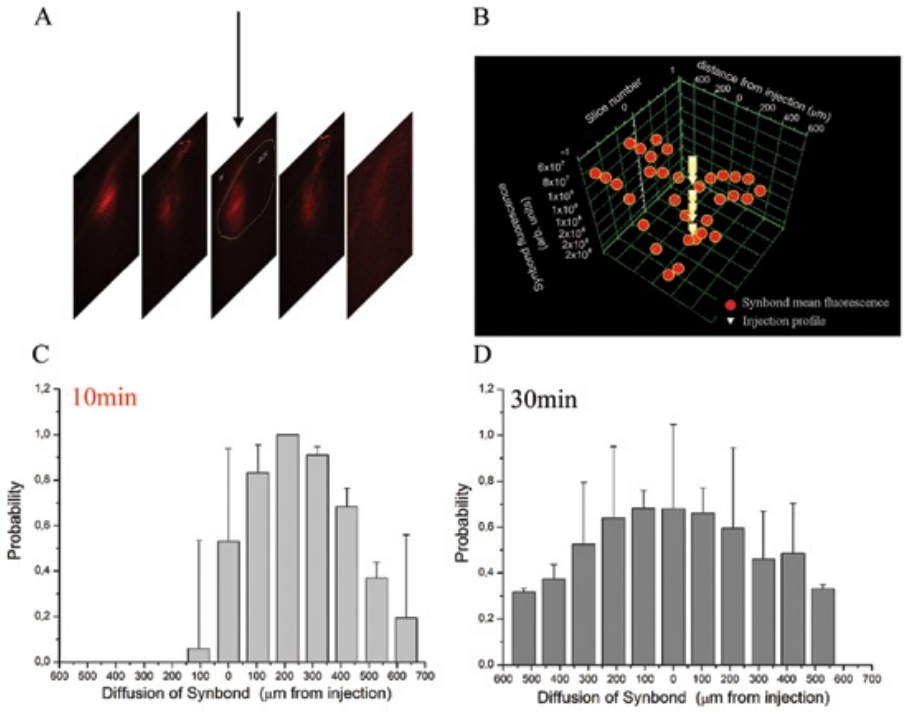

Figure 40: Analysis of Synbond diffusion inside the LGN. (**A**) Distribution of Synbond in sequential slices following Synbond injection (the black arrow shows the site of injection). (**B**) 3D reconstruction, from three different brain slices cut in sagittal orientation (site of injection slice 0). (C-D) The Synbond diffusion profile, at 10 and 30 minutes after injection. Note how, moving away from the injection site, a greater concentration was found in our peptide.

In these experiments following the injection of the fluorescent peptide Synbond, we also followed over time the arrival of these molecules in neighbouring areas. Synbond was seen as a cloud of fluorescence, which was specifically produced by Synbond injection that spread in the surrounding area around the injection site. To view this fluorescence, since in these experimental conditions (absence of GreenZip expression) this molecule is not expected to bind or to be internalized by brain tissue, synbond is therefore expected to be freely diffusible and consequently "washable" from the tissue by whatever experimental manipulation (tissue washout, cardiac saline perfusion, etc). At different time points from Synbond injections animals were sacrificed after anesthesia and the brain quickly removed and frozen in liquid nitrogen (-200 ° C). In these conditions diffusion was slowed down by the very low temperatures. Brain slices were cut using a cryostat (at -20C) and then quickly imaged. From the exemplar figure (Fig 40) we can see how the profile of fluorescence remains almost similar moving laterally in both directions of the sagittal plane. The figure in the top right shows a detailed three-dimensional reconstruction of the spread of fluorescence of three central slices (injection site is labelled by 0, and the subsequent slices placed laterally either to the right or to the left, labelled by 1 and -1). In this figure the two histograms presented in the lower left and lower right show the time dependent trend in Synbond diffusion at different times in a same portion of the LGN. Notice how at 10 minutes, the peptide has a diffusion that does not appear uniform in medio-lateral direction, but seems to move according to a preferred direction, whereas it seems that if you wait longer this inconsistency will be resolved with a more uniform distribution of the peptide. As expected, the small size of our probe allows a fast diffusion to synapses even to those located at some far distance from the injection site. In fact after only 10 minutes from the injection Synbond has already traveled from 800μm to 1200μm and after half an hour, it almost covers the full size of LGN.

In vivo application of the GreenZip-Synbond pair for the functional study of synaptic activity

Although the signal from the GreenZip GFP is very high, the brain tissue has a natural auto-fluorescence whose spectrum is partially similar to the green emission spectrum of GFP and this s the case even when the brain tissue is treated with quenching solutions (special solutions meant to lower the natural auto-fluorescence). The reason for this intrinsic fluorescence of brain tissue, is due to the presence of molecules that absorb and emit at wavelengths in the UV-visible range. Even with the appropriate spectral filters, and even with a one photon confocal microscope (see introduction), a small part of this unwanted signal unfortunately overlaps with that of GFP. In this view, Synbond was labelled with fluorophores in the far red end of the visible spectrum where auto-fluorescence is very faint. Also, for GFP detection of GreenZip expressing synapses we carefully set the acquisition phase, to capture images using the minimum laser energy as possible and maintaining the pinhole closed to the maximum (in order to obtain the maximum confocality of small objects as synapses, with minimal contribution from objects below and above). To avoid any misinterpretation of the images, we isolated the signal coming from the GFP puncta, putative GreenZip expressing synapses, by the development of an ad hoc protocol of image analysis (using routines written for the image analysis software, ImageJ ®). This method uses the GFP channel to identify putative terminals, without introducing a bias related to the selection of active synapses, and in these areas then blindly detects the signal on the wavelength corresponding to Synbond, the reporter of synaptic activity. The method operates through a first pre-filtering of fluorescence through a thresholding of the fluorescent signal coming from the image, it generates a threshold that is used to discard everything that has a signal lower than the average of the fluorescence of the background (area of tissue in which there is no expression of GreenZip; threshold = mean +/- 4 its standard deviation). This thresholding permitted to generate a series of masks that created the outlines around all those objects that have a signal above the threshold level determined by us, with a surfaces between 0.2 and 3 μm^2, and whose circularity was in the range 0-1 (circularity calculated with the formula $c = 4\pi$ * area/circonferenza2-if equal to 1 if perfect sphere approaches 0 object more elliptical-) (see Figure 41).

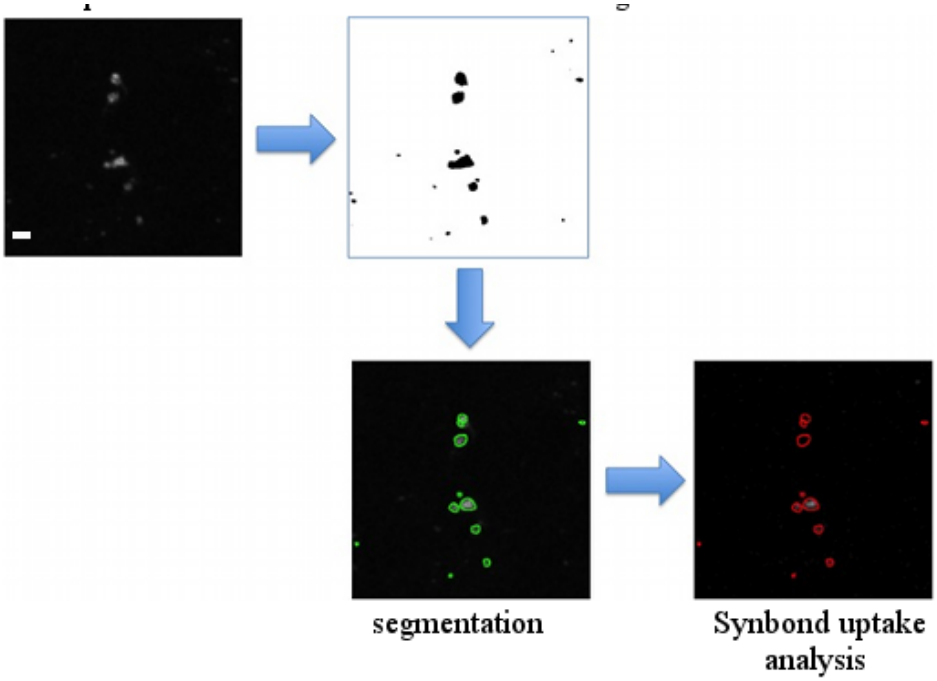

Fig 41 Synaptic uptake analysis of Synbond at the LGN level. (**GreenZip fluorescence**) scanned image from one photon microscopy. (**Fluorescence tresholding**) prefiltered image is based on a threshold of signal intensity (black masks), after fluorescence tresholding, a size-based segmentation was run, the green circles represent the synapses that will be accepted.. (**Synbond uptake analysis**) the masks generated in such way were applied on synbond fluorescence channel and the uptake analysed as fluorescence intensity. (scale bar 5μm)

We then tried to demonstrate the applicability of our constructs in determining the synaptic activity in vivo. The preliminary experiment, repeated several times (n = 6) always with excellent results, consisted initially, in transfect by electroporation, with the cDNA GreenZip of the retinal ganglion cells of animals (Wistar rats, weighing 185-190g), then, to allow both a complete transfection of retinal cells and for complete physiological recovery of the eye, Synbond (50nM, 2μl) was applied to the (right) LGN using stereotaxic apparatus (see Materials and Methods), 36 hours after the GreenZip electroporation.

Control animals, after injection, were maintained in total darkness for the desired times, then immediately sacrificed. Animals stimulated were instead placed immediately after injection (remained constant a default time of 5 minutes for each animal before placing it in the cage light) within the light box, where they were stimulated by light pulses with different protocols, and then immediately sacrificed. The whole brain of all animals stimulated was removed in whole (after being perfused with paraformaldehyde), then cut into coronal slices using vibratome instrument (thickness of 40μm) that were analyzed ex vivo for Synbond uptake at the LGN level as described above. The Figure shows the results of the analysis, conducted by means of confocal microscopy, regarding the LGN thalamic of an animal stimulated for 1h, 15 minutes of darkness alternating with 5 minutes of light, compared with an animal kept in total darkness for 1h.

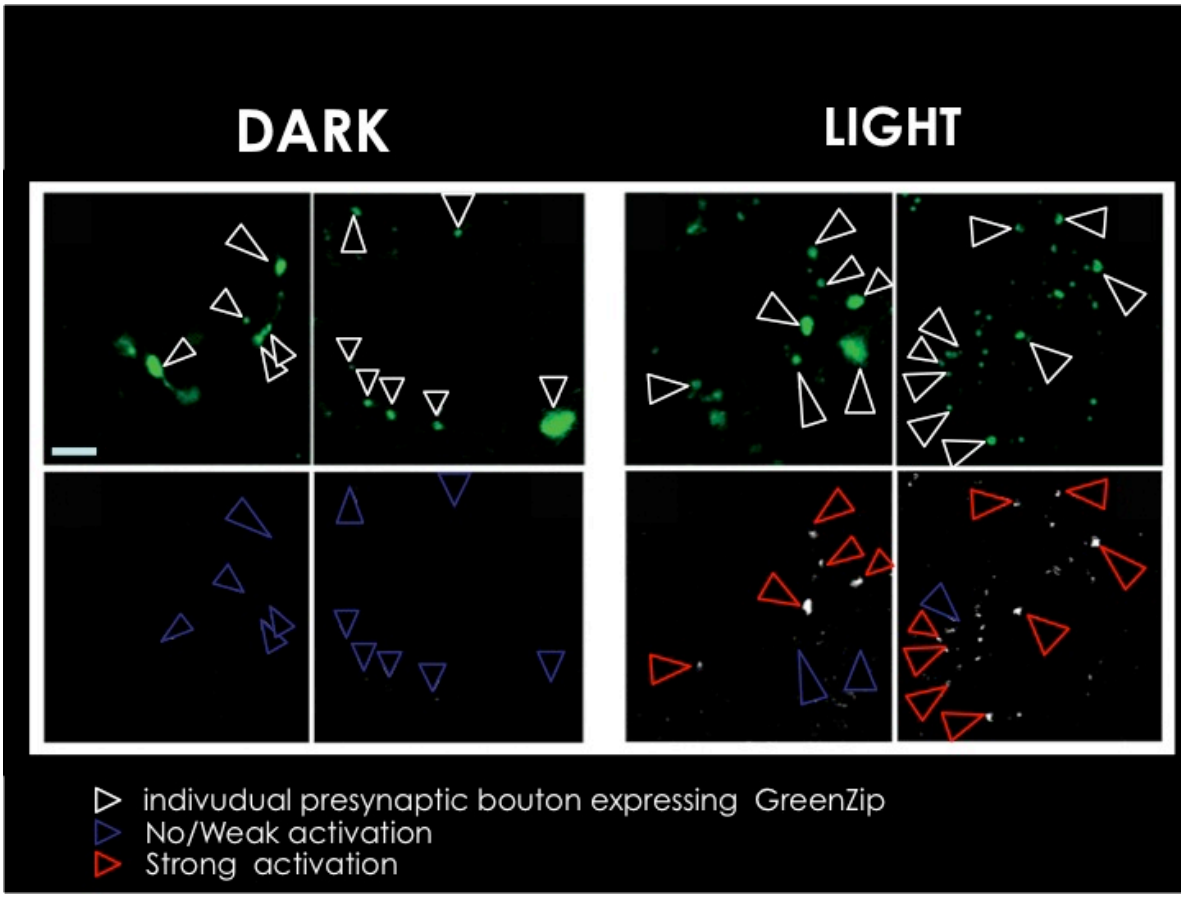

Fig 42 In vivo synaptic uptake of Synbond in dLGN synapses: Boxes at the top: LGN of 2 animals (control animal is showed in the left panels, experimental animal is showed in right panels) whose retinal ganglion cells were transfected by electroporation with GreenZip cDNA (white arrows). The animals after 36h, were microinjected under stereotaxic guide with Synbond directly in dLGN. Bottom panels right: with 1h of visual stimulation (which causes vesicular exocytosis) the internalization of Synbond is present (shown in red arrows) inside GreenZip positive synapses, with different levels of uptake due to different activation. Bottom panel left: animals kept for 1h in complete darkness, showed a weak internalization of Synbond (blue arrows) inside GreenZip positive synapses. (bar 5μm)

From these pictures it is possible to visualize that the pair GreenZip-Synbond represents a tool of extraordinary validity for the study of synaptic activity in vivo. We see what happens in the synapses of ganglion cells within the LGN thalamic transfected with GreenZip (white arrows in upper panels Fig 42) once the animal was injected with Synbond: in fact the visual stimulation performed with the box light, which causes vesicular exocytosis at the level of the LGN, makes sure that the probe Synbond binds exclusively to the synapses that express GreenZip and only to those that have been activated by our stimulation (red arrows botton panels right, Fig 42). A demonstration of the fact that the bond GreenZip-Synbond is specific for synaptic activity can be observed in Fig 42 concerning the control animal, in which Synbond was injected, but which has not made any visual stimulation, having been maintained in the dark for 1h (blue arrows botton panels left, Fig 42). It is thus evident that in the absence of visual stimulation is present a very weak, almost absent fluorescent signal coming from the internalisation of

Synbond at synapses transfected with GreenZip, probably due to the spontaneous activity of synapses, persistent even in case of darkness (blue arrows botton panels left, Fig 42).

These results acquire even more weight if compared with those provided by a common antibody capable to detect neural activity, as we have seen to be the case of C-Fos. The differences are manifold, starting from the high spatial resolution that Synbond offers thanks to its small dimensions, at the level of the active single synapse, that C-Fos is in no way able to offer, since it detects the generalized activity of the cell. Of great importance is also the fact that C-fos detects post-synaptic activity, that proves to be filtered by the whole local circuitry upstream the cell analyzed, so that it hardly correlates directly with a given stimulus, whereas our probe detects a proper pre-synaptic activity, which derives directly from the stimuli that we choose, and from these results modulated.

Quantitative analysis of synaptic internalisation of Synbond molecules

Having established that the GreenZip-Synbond pair system is capable of detecting synaptic activity in vivo, we wanted to quantify the internalization of Synbond obtainable through different visual stimulation protocols, where essentially was mutated the residence time within the luminous cage, so both corroborate previous findings, showing that these would also be repeated at different times of stimulation, as expected, both analyzing how the LGN would respond to different inputs. In the stimulation protocols, the total luminance was kept constant, while the length of light exposure was varied, namely: 5, 10, 30 minutes. The stimulation ensued immediately after Synbond injection. In these experiments we analyzed two control conditions: I) injection of TTX (10μM-5μl) in the eye (tetrodotoxin, the puffer fish toxin that blocks voltage-activated Na+ channels and therefore inhibits the generation of action potentials) and maintained for 1 h in the darkness; II) 5 minutes of darkness. The different conditions of stimulation and the number of treated animals are summarized in the table below, while the graphs of Fig 43 show the analysis that was carried out on the synapses of these animals.

TYPE OF STIMULUS	STIMULUS DURATION	N° OF ANIMALS TREATED	N° SYNAPSES ANALYZED
TTX	1 h	1	230
Dark	5 minutes	2	151
Continuous light	5 minutes	4	493
Continuous light	10 minutes	2	244
Continuous light	30 minutes	2	201

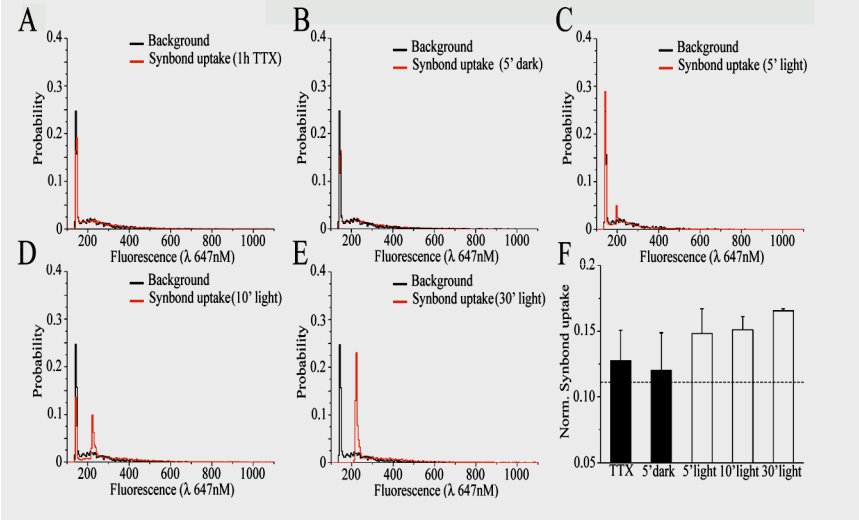

Fig 43: In vivo uptake of Synbond by different light stimulation protocols. (**A**) synaptic uptake of Synbond in 23 synapses of one animal injected with TTX (in the eye) and Synbond (SB) (in the LGN) and maintained for 1 h in the dark (**B**) Uptake od SB in 151 synapses of 2 animals maintained for 5 minutes in the dark following the injection of Synbond. (**C**) Uptake of SB in 493 synapses of 4 animals stimulated with 5 minutes of light stimulation immediately after the injection of Synbond. (**D**) Uptake of SB in 244 synapses of 2 animals stimulated with 10 minutes of constant light, after injection of the peptide and then sacrificed. (**E**) Uptake of SB in 201 synapses of 2 animals stimulated with 30 minutes of constant light, after injection of the peptide and then sacrificed. (**F**) Uptake of SB normalized to the average of espression of GreenZip with different visual stimulation protocols: the dashed line represents the background mean fluorescence at 647 nm (the wavelength of Synbond emission) which was calculated from synapses expressing GreenZip which were not exposed to Synbond, normalized to the expression of average of GreenZip.

The red bars in the graphs represent the distribution of the fluorescence coming from the internalisation of Synbond in the entire population of synapses that express GreenZip in all conditions, while the black bars represent the background fluorescence of 647nm (a wavelength of emission of Synbond) of synapse expressing GreenZip that have not been exposed to Synbond. The synapses from different animals stimulated with the same protocol were analyzed with the method described above and united as a single population, this is possible because the fluorescence from each animal, regardless of the condition of stimulation, was acquired with identical parameters, the same laser power, equal spatial and spectral filters and the same digital gain, in this way each synapse is stimulated by the same type of light source, and the output signal will be amplified by identical digital factors, in this way the only possible variation in the signal will be due to a different emission quantum and, therefore, to a greater or lesser number of molecules of Synbond captured by synapses (the ratio of the link GeenZip-Synbond-fluorophore is 1:1:1). Obviously internalization will also depend on the number of "baits" present in each boutons, then we have analyzed the distribution of the expression of all synapses analyzed and we found no significant differences in the levels of expression of GreenZip at synapses (data not shown), for this factor the "number of bait" is negligible in our analysis. As can be seen in the graphs A and B (Fig 43), in both conditions of control, a significant separation between the background and the internalisation is not visible. As soon as there are also short stimulations (graph C) shows a second peak that stands out from

the background, which probably represents the populations of synapses that respond to this weak stimulation. With a doubled time of light exposure (Graph D), not only the amplitude of the second peak appears to be the double compared to that of 5 minutes, but also moves the internalisation of this cumulative population of active synapses (5 minutes the higher peak is at 212 while at 10 minutes the peak is at 222). With 30 minutes of stimulation the first peak disappears completely, and the second peak is increased by three times compared to the time-point of the previous stimulation suggesting that almost all synapses (of the 201 analyzed), which were reached from Synbond during the period of stimulation, have been at the same time activated by light. These results (graph F) demonstrate that by using our sensor it is possible to follow in situ the behaviour of different populations of active synapses, and how easy it is to quantify the extent of any activity by the cumulative uptake of our peptide administered in vivo.

This technique clearly allows to record from large in situ synaptic networks with an unprecedented resolution. We believe that the synergy between the progress in the development of genetically encoded indicators such as those we are developing in our laboratory and advanced optical imaging will soon allow the study of complex networks of synaptic activity in freely moving animals. The identification of a precise relationship between a state (for example binocular vision or the contrast vision) and local activities of a specific function or behaviour should allow neuroscientists not only to understand important neurophysiological issues but also to find the best diagnostic procedures and possibly develop more advanced forms of therapy for diseases characterized by states of altered activity in some brain regions.

Of course, in order to be able to study the entire synaptic network it is necessary to overcome the limitations imposed by transfection via electroporation, which make the visual circuit the only site in vivo on which our probes can be readily applied. In this regard, a further step is the contemporary creation of transgenic animals and a lentiviral vector that can express GreenZip selectively at predetermined levels within neural circuits. Combining access to these circuits by our peptide with the use of stereotactic equipment, will allow functional analyses of brain circuits that underlie various cognitive processes. This can be achieved through the detection of synaptic activity, with a resolution and a specificity never seen before with any other technique. During these three years of my PhD, I have dedicated my time to completing these projects. In this thesis, I will then refer to the development and application of these techniques.

3.2 GENERATION OF AN ANIMAL MODEL FOR THE REGULATED EXPRESSION OF GREENZIP IN BRAIN CELLS

The Rosa 26 Locus and the strategy to generate the Rosa GreenZip-Cre mouse

In order to overcome the limits imposed by transient transfection to express our synaptic vesicle protein (GreenZip) in vivo, we initially proceeded with the creation of a Knock-in mouse that could selectively express our reporter in specific regions of the central nervous system. Since the classical methods of transgenesis seemed to require a long period of phenotypic analysis, and quite often the inability to ensure a homogeneous protein expression in all cells (Mao et al., 2001), it was decided to use recombinant DNA technology (Sung, P et al., 2006) to create knock-in mice that could be exploited for insertion of our protein, the genomic locus Rosa26 (Friedrich and Soriano, 1991). This locus ubiquitously expresses a nuclear non-coding RNA at any stage of development (Zambrowicz et al., 1997). It is, therefore, considered a kind of "parking genes", where the expression, however stable, will depend upon its regulatory elements inserted in Locus via homologous recombination (enhancers, promoters, etc. ...).We have generated a recombinant plasmid in which the GreenZip construct is preceded by a strong constitutive promoter (chicken beta actin promoter) and by the Cytomegalovirus (CMV) enhancer: the pCAGG promoter (Madisen et al., 2010) (see materials and methods). The constitutive transcription of this construct is inhibited by a floxed stop sequence, which is precisely flanked by two loxP sites, removable by Cre-mediated recombination. Cre is a 38 kDa recombinase protein from bacteriophage P1 which mediates intramolecular (excisive or inversional) and intermolecular (integrative) site specific recombination between loxP sites (Sauer, B. 1998). A loxP site (locus of X-ing over) consists of two 13 bp inverted repeats separated by an 8 bp asymmetric spacer region. The recombination occurs in the asymmetric spacer region. Those 8 bases are also responsible for the directionality of the site. Two loxP sequences in opposite orientation to each other invert the intervening piece of DNA, two sites in direct orientation dictate excision of the intervening DNA between the sites leaving one loxP site behind (as in our case). The floxed part of the construct contains a neomycin resistance minigene for use in embryonic stem (ES) cells. Thus, crossing the RosaGreenZip transgenic line (that will not express our GreenZip protein, since its encoding cDNA will be even stopped) with various Cre lines (constitutive or inducible), it will be possible to activate the GreenZip construct (see figure 44), in double-transgenic progenity since the presence of Cre will result in an excision of the stop sequence, in various limited neural territories whose expression at this point will depend on the different expression profile of various cre-mice, since the expression of the Rosa26 promoter does not seem to be strong (Madisen et al., 2010).

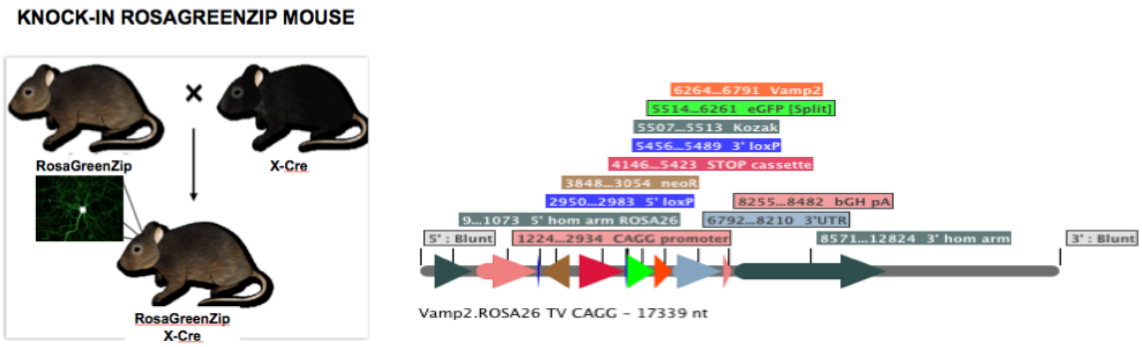

Figures 44: The RosaGreenZip plasmid and the strategy to generate the RosaGreenZip mouse. (**Left**) The RosaGreenZip plasmid linearized by the enzyme ASisiI (New England Biolabs Inc.). Note the homology arms (dark green) that allow homologous recombination of the construct into the ES cells'.genomic locus Rosa26 of ES cells. (**Right**) Crossing the RosaGreenZip mouse that will express our vesicular protein silently (will still be present the stop sequence upstream of the GreenZip gene) with a mouse that expresses Cre under a particular neural-specific promoter, it will be possible, in the progeny, to get the activation of GreenZip only within the specific region of the brain / neural type in which Cre was expressed: where to enable our protein depends on the choice of the Cre mouse type with which to pair the mouse RosaGreenZip

Functional validation of the Rosa-GreenZip plasmid: expression of RosaGreenZip-Cre into HeLa cells through transient transfection

After having built the RosaGreenZip plasmid (see materials and methods), before it was linearized and electroporated into ES cells, we tested the functioning of the plasmid by cotransfecting it into HeLa cells, with a Cre plasmid, so as to test both the effectiveness of the Cre-mediated expression, and the functionality of our construct through synbond uptake (see Matherial and Methods).

Therefore, the following points of co-transfection were prepared:

1) RosaGreenZip / Cre (1:1 molar ratio) 5 μg RosaGreenZip / 3 μg Cre

2) RosaGreenZip / Cre (2:1 molar ratio) 5 μg RosaGreenZip/0.75 μg Cre

3) RosaGreenZip only (5 μg RosaGreenZip)

In addition, together with Cre (in the same ratios as above) the original Rosa26 plasmid (16,100 bp) was also transfected as a control for the quality of the subcloning that originated RosaGreenZip. The expression of GFP was then followed in the next 72 h. A GFP signal, albeit weak was detected in case 2, (including as regards the Rosa26 empty plasmid, data not shown). Also a part of these cells, not treated with antibodies, were incubated with synbond for 30' but no signal was detected. No signal was detected either in Hela cells transfected with only the plasmid RosaGreenZip/Rosa26.

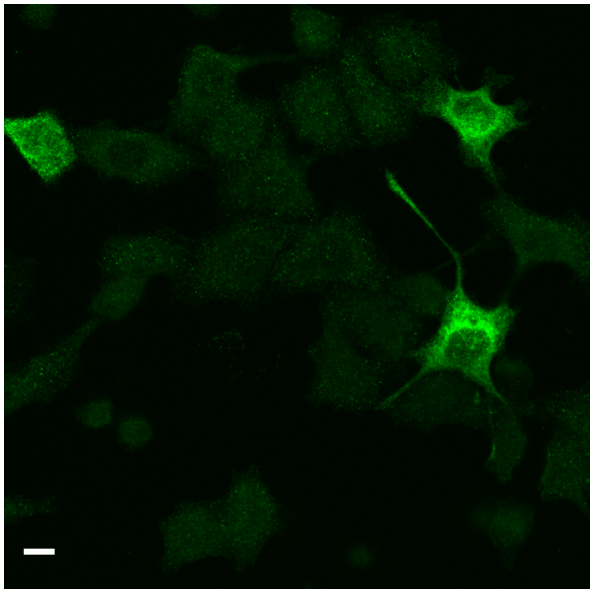

Fig 45 Immunofluorescence with anti-GFP conducted on HeLa cells co-transfected with plasmid RosaGreenZip and Cre enzyme. Positive cells appear to be a small number. (60 x; scale bar: 10μm).

The experiment was then repeated with the following conditions:

1) ROSAGREENZIP: CRE (2:1): 10 μg + 3 μg + 26 μl lipofectamine

2) ROSAGREENZIP: CRE (2:1): PZ: CRE (2:1): 15 μg + 4.5 μg + 40 μl lipofectamine (double dose compared to the experiment above)

3) ROSAGREENZIP: CRE (2:1): PZ: CRE (2:1): 10 μg + 3 μg + 40 μl lipofectamine (double dose compared to the experiment above)

4) ROSAGREENZIP ONLY (without Cre)

For each condition (1,2,3)

A) HeLa only

B) Fix and mount

These two points as controlling an auto-fluorescence of the cells or produced by the fixation. No signal was rediscounted from these tests:

C) Synbond 1h incubation - fix + Anti-GFP FITC

D) Synbond 2h incubation - fix + Anti-GFP FITC

The time the cells were incubated with Synbond was varied with the hypothesis that the uptake of the peptide may take longer than the experiment above

E) fix + Anti-MYC Cy5 1:100
F) fix + Anti-VAMP2 Cy5 1:300
G) fix + Anti-GFP 1:100 Cy5

Incubation times of primary antibodies, secondary, wash in blocking buffer etc. are the same as reported in the previous experiment. All signals shown were found to be more significant in the condition 2. Again, once the endogenous signal of GFP was found to be weak, although higher than that of the previous experiment, with regard to the experimental condition 2.

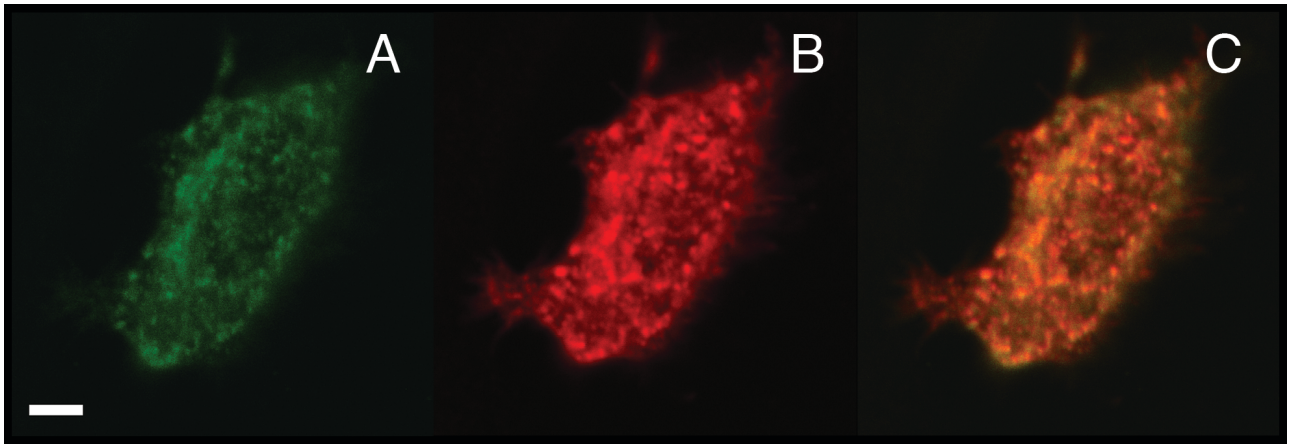

Fig 46 Characterization of GreenZip expression in HeLa cells, for the condition 2G**:** **(A)** GREEN: endogenous signal coming from endogenous GFP, **(B)** RED: anti-GFP in cy5 , **(C)** (YELLOW): merge. (60 x; scale bar: 10μm).

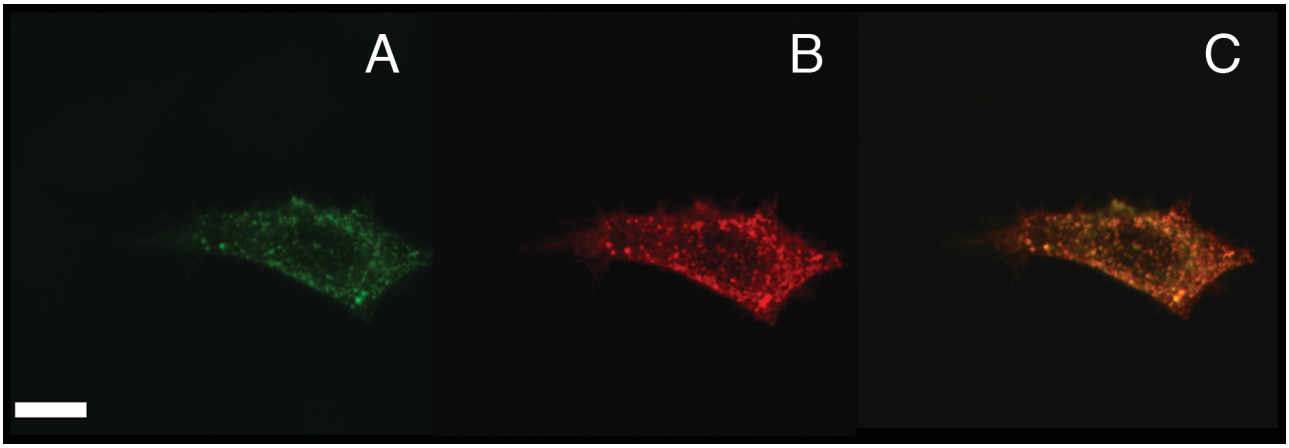

Fig 47 Characterization of GreenZip expression in HeLa cells, for the condition 2E: **(A)** GREEN: endogenous signal coming from GFP, **(B)** RED: anti-Myc in cy5 , **(C)** (YELLOW): merge. (60 x; scale bar: 10μm).

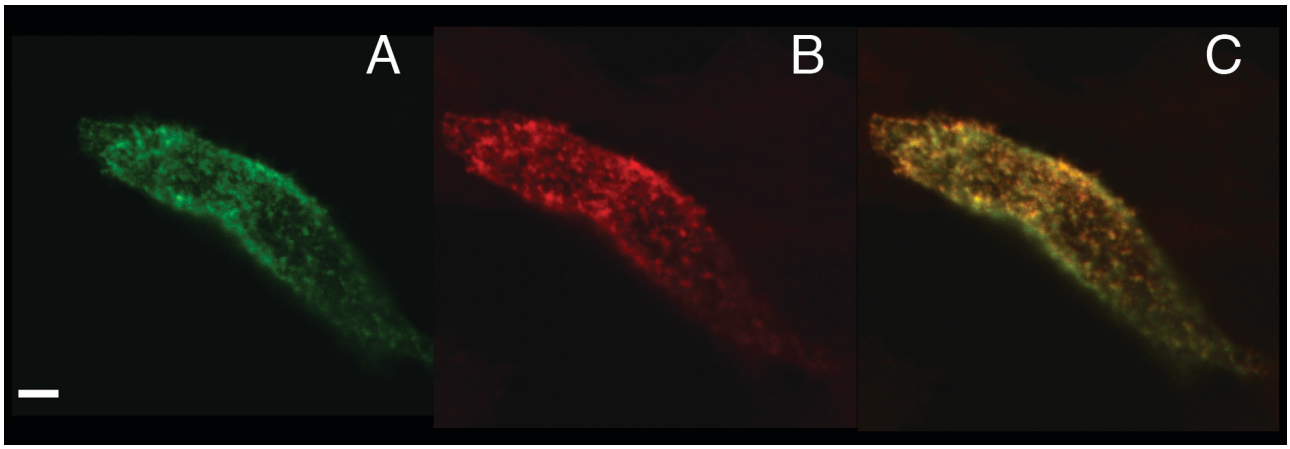

Fig 48 Characterization of GreenZip expression in HeLa cells, for the condition 2F: **(A)** GREEN: endogenous signal coming from GFP; **(B)** RED: anti-VAMP2 in cy5 ; **(C)** (YELLOW): merge (60 x; scale bar: 10μm).

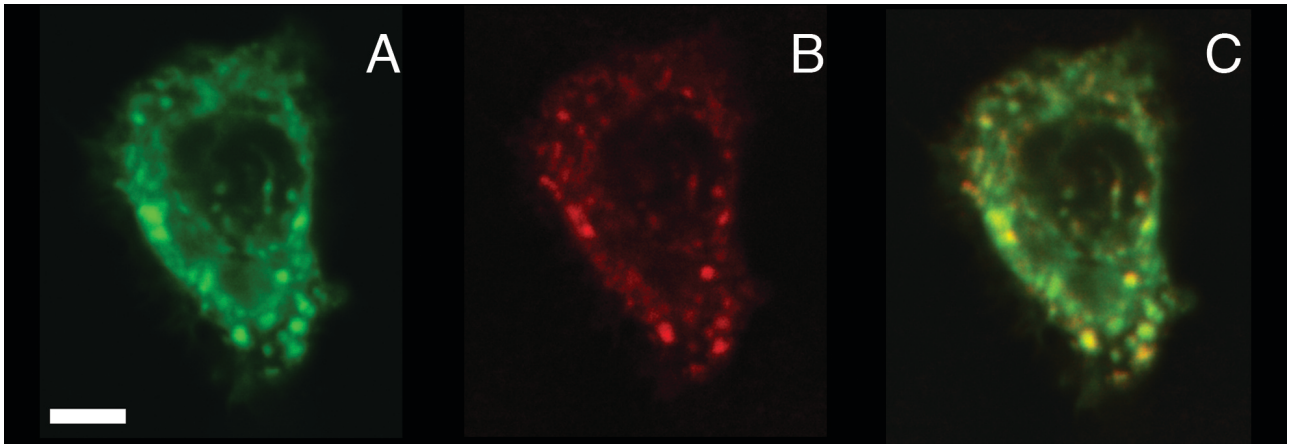

Fig 49 Exemplar of an experiment to visualise constitutive Synbond uptake (2 hours incubation, 5 nM SB) in GreenZip expressing Hela Cells. (**A)** GREEN: endogenous signal coming from GFP, **(B)** RED: Synbond uptake after 2h of incubation , **(C)** (YELLOW): merge. (60 x; scale bar: 10μm).

Generation of RosaGreenZip ES cells: construct electroporation and selection of positive clones

After evaluating the operation of our plasmid RosaGreenZip and the absence of expression when not in the presence of the Cre-recombinase enzyme, the construct was linearized using the enzyme AsisiI, to be electroporated into ES cells for homologous recombination in the locus genomic Rosa26 (Sung, P et al., 2006). The electroporation of RosaGreenZip construct into embryonic stem cells (ESCs), and their injection into Blastocysts has been made by CFCM: Core Facility for Conditional Mutagenesis, San Raffaele Scientific Institute, Milan, Italy (see Matherials and Methods). After the ES cells were electroporated, there were returned the clones of the same electroporated cells in order to identify those positive for the integration of the construct by southern blot analysis, using appropriate specific probes (see materials and methods) to detect the insertion of our construct within the genomic locus Rosa26 (Fig. 50).

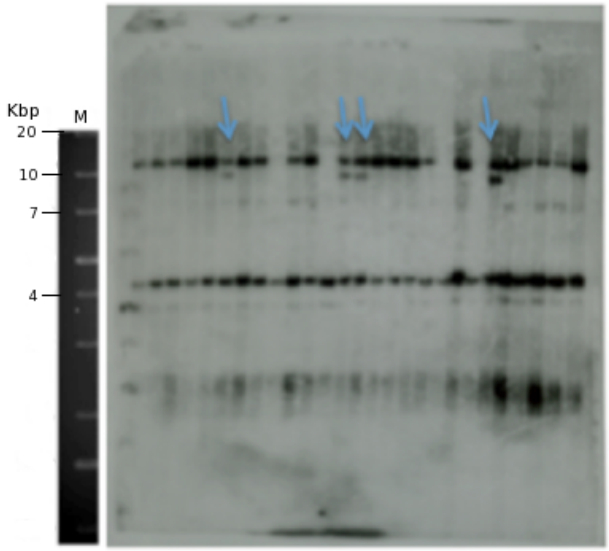

Fig 50 Southern Blot performed on ES cells clones in which the RosaGreenZip construct was electroporated. It may be noted, in all ES samples of cells treated, the Wt band (11,517 bp) of the genomic locus Rosa26. The presence of the construct integrated into the locus RosaGreenZip (6199 bp) via homologous recombination is indicated with blue arrows.

RosaGreenZip chimeras and PCR Screening for RosaGreenZip-Cre positive mice: analysis of the crossing between SynI-Cre and RosaGreenZip mouse lines

After having identified the positive clones for homologous recombination, they were injected into blastocysts derived from C57BL/6J females. The chimeric embryos were then transferred into the uterus of pseudo-pregnant foster mothers day 2.5. The ES cells with the electroporated RosaGreenZip construct were engineered so as to provide a brown colour (agouti) to the animal's fur: thus the degree of the agouti offspring mantle will be an indicator of how ES cells, in which our construct is integrated, have contributed to the 'creation' of the body organization of mice. The higher the percentage of the degree of chimerism, the higher the probability that our ES cells also have contributed to the formation of the animal's gonads, and in this case this would mean the possibility of ensuring the RosaGreenZip construct germline transmission to the next generation. The first clone of ES cells from which we have obtained an abundant number of chimeras was the clone # 6 (A6), which led to the generation of various chimeras, among which males were selected for the possibility of coupling with more females Cre (2), where it is known not to be possible otherwise.

Chimeric mice (founders) obtained from clone A6 were as follows:

-4 Male Chimeras with a degree of chimerism between 90-100% (defined as chimera 1-6/2-6/3-6/4-6)

-3 Male Chimeras with a degree of chimerism between 70-80%

-3 Male Chimeras with a degree of chimerism by approximately 50%

3 of the 4 chimeras that showed a percentage of agouti coat between 90 and 100% were mated with female transgenic mice expressing Cre under the promoter of the SynapsinI protein (SynI-Cre) (Zhu, Y, et al., 2001, Hoesche et al., 1993). The synapsin I protein is a member of the synapsin family that are neuronal phosphoproteins, which associate with the cytoplasmic surface of synaptic vesicles. Synapsin I is present in the nerve terminal of all the CNS and PNS axons, specifically in the membranes of synaptic vesicles based on immunocytochemistry (De Camilli, P. et al., 1983). Ideally, therefore, this Cre transgenic line was chosen to evaluate the expression of our "global" protein level into all CNS and PNS synapses. One chimeric mouse, in parallel, with a degree of chimerism always of 90-100% had been coupled with female mice (always transgenic) expressing Cre under the Thy1 promoter (ThyI-Cre), which is known to drive expression at high levels in a variety of neuron types in a "salt and pepper" characteristic distribution (J. Livet et al., 2007).

Once we obtained the first pups resulting from the intersection of the chimera RosaGreenZip (RGZ) X Syn-Cre and RosaGreenZip (RGZ) X Thy-Cre, PCR was performed on the DNA extracted from the tails of the animals with brown hair (see materials and methods), using specific primers for the construct integration into the Rosa 26 locus and for the presence of Cre. Then heterozygous RosaGreenZip+/--SynCre mice were carried out by polymerase chain reaction (PCR) (Fig 51 and 52)

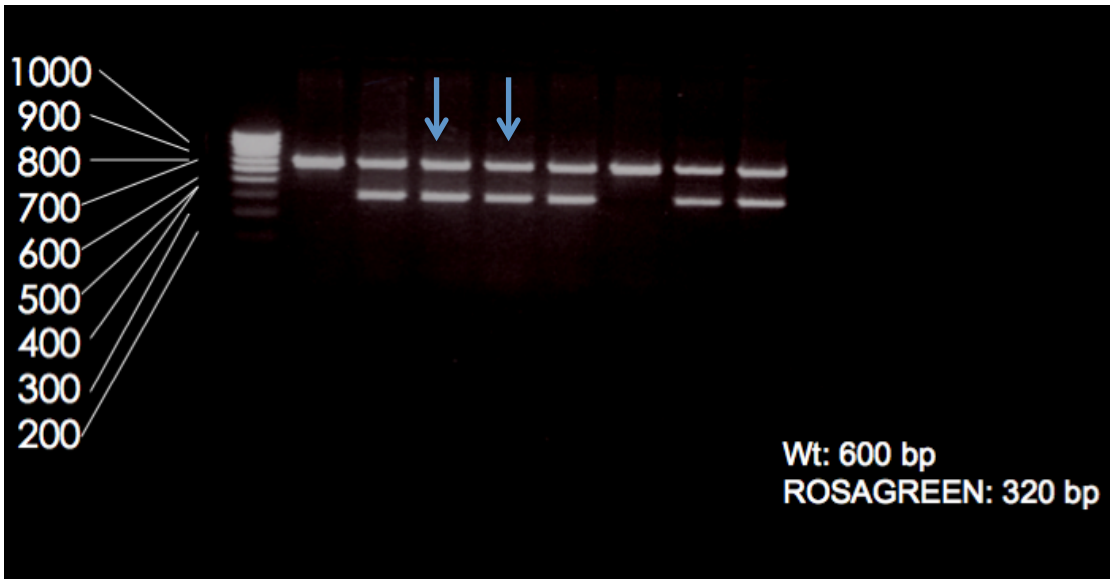

Fig 51: PCR performed with specific primers to detect the integration of the RosaGreenZip construct into the genomic locus Rosa 26: note how the band of the happened integration (320 bp) is present in animals 2,3,4,5,7 and 8. Double positive (with Cre, see Figure below) is indicated by the blue arrow.

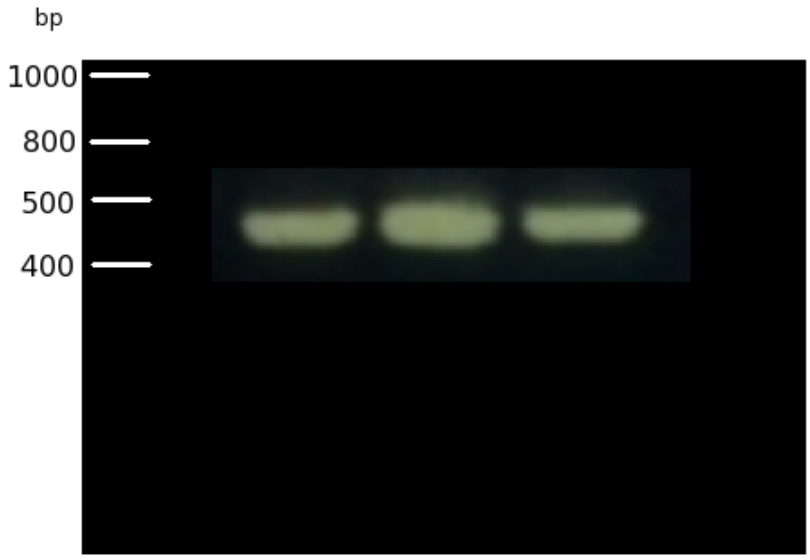

Fig 52: PCR performed with primers to detecte the integration Cre: the band of integration (450-500 bp) is present in animals 1,2,3.

Analysis of brain tissue expression of the RosaGreenZip protein product in the SynI-Cre RosaGreenZip (+/-) mouse line

We obtained the double positive animal for the insertion of our construct (in heterozygosity) and for Cre, as we wanted to look at what was the level of GFP at the CNS level. We sacrificed one of the two animals at the age of P40 (see materials and methods) and examined brain slices using confocal microscopy. Additionally, a littermate was found to be positive for the integration of the construct but negative for the integration of Cre (control). The slices of the positive animal were used also to perform certain immunofluorescence reaction (anti-GFP) and to display Synbond postfix. After the slices of the fixed brain were cut it was possible to incubate one of these with Synbond, which will bind to the '"bait" of GreenZip exposed from vesicles that are fused to the presynaptic membrane and kept in this state by the fixation with paraformaldehyde (see Figure 53 and 54), no signal was detected from synbond (data not shown).

.

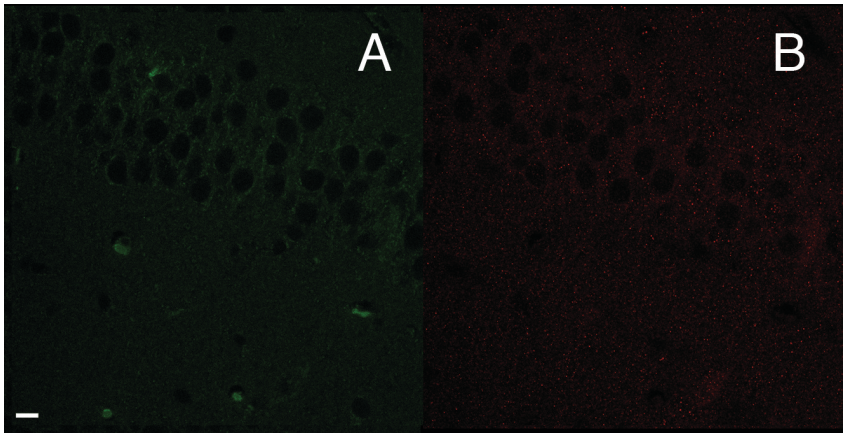

Figure 53. Coronal hippocampal slices from heterozygote SynCre RosaGreenZip (+ / -) mouse. **(A)** GREEN (left): endogenous GFP signal, **(B)** RED (right): anti-GFP Cy5. (60 x; scale bar: 10μm).

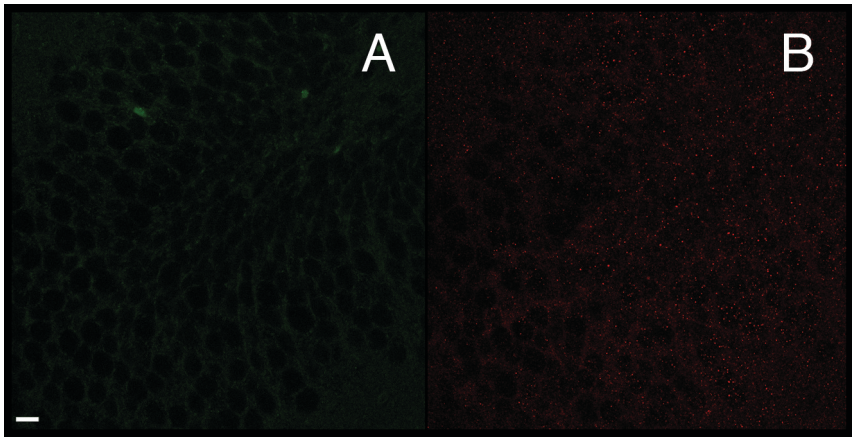

Fig 54. Coronal hippocampal slices from a non GreenZip expressing mouse. The RosaGreenZip (+ / -) used in this analysis was not crossed with the SynICre, hence could not express the GreenZip transgene. **(A)** GREEN (left): endogenous GFP signal (autofluorescence), **(B)** RED (right): anti-GFP Cy5. (60 x; scale bar: 10μm).

Crossing of the Thy1-Cre and RosaGreenZip mouse lines: analysis of brain tissue expression of the RosaGreenZip protein product in the Thy1-Cre/RosaGreenZip (+/-) mouse line

To evaluate the nature of the low expression levels for GreenZip found in the RosaGreenZip SynI-Cre lines we decided to test a different crossing with another Cre neuron specific line. Based on previous work (Caroni, P 1997) we decided to use the Thy-Cre line where the CRE enzyme is expressed under the control of the Thy1 promoter (J. Livet et al., 2007). The heterozygotes from the Thy1-Cre RosaGreenZip (+ / -) crossing line were analyzed in the same manner and for the same identical purposes described above (Figure 55 and Figures 56 and 57).

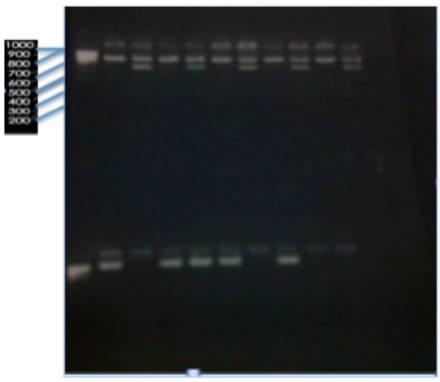

Fig 55: ABOVE: PCR performed with specific primers to detecte the integration of the construct into the genomic locus RosaGreenZip Rosa 26 (banda WT: 600 bp band ROSAGREEN: 320 bp. Positive samples: 2,4,6,8,10). BELOW: PCR for the integration of Cre (band integration: about 1000 bp. Positive samples: 1,3,4,5,7).

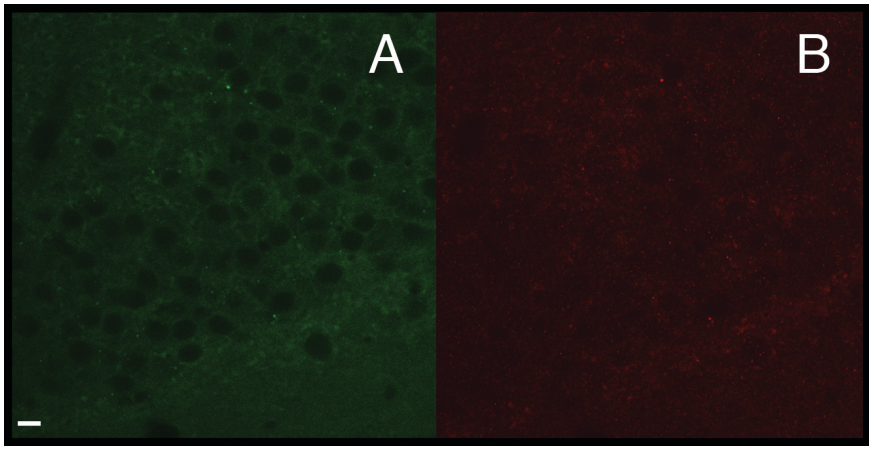

Fig 56 Cerebral cortex from a heterozygote ThyCre RosaGreenZip (+ / -) mouse: **(A)** GREEN (left) endogenous GFP signal, **(B)** RED (right): anti-GFP Cy5. (60 x; scale bar: 10μm).

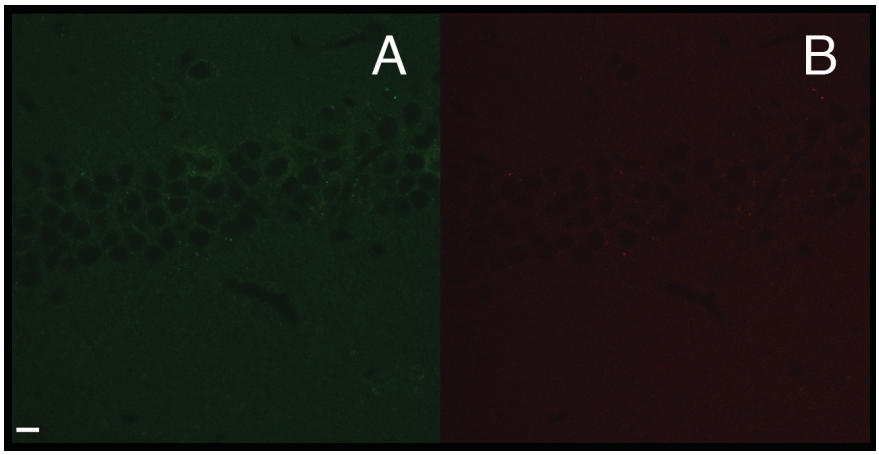

Fig 57 Cerebral cortex from a non GreenZip expressing mouse. The RosaGreenZip (+ / -) used in this analysis was not crossed with the ThyICre, hence could not express the GreenZip transgene.: **(A)** GREEN (left) :endogenous GFP signal, (autofluorescence) **(B)** RED (right): anti-GFP Cy5. (60 x; scale bar: 10μm).

Analysis of RosaGreenZip expression level in the homozygote SynI-Cre RosaGreenZip (+/+) mouse line

Given the low signal from GFP detected with both the mouse SynICre and with ThyICre, at the level of the cerebral cortex, hippocampus (where SynCre should be more strongly expressed) (Zhu, Y, et al., 2001), but also in many other brain regions (data not shown), and, being virtually completely absent the signal coming from our peptide Synbond, it was decided to try to increase, presumably doubling the expression by analyzing the SynICre GZ animals in homozygosis. To this aim heterozygous animals were crossed between each other, and the homozygous animals selected by PCR typing as described in the previous section. Homozygous animals occurred with an average frequency around 25%, which is the expected value for Mendelian crossing frequency, confirming that the transgene does not have any major negative effect on the embryo development. Although +/+ should carry two alleles and therefore at least in theory produce twice as much mRNA, the final expression level for the protein might not follow this simple linear relation because of saturation of the folding, storage, degradation and transport mechanisms. Indeed my results, although not properly quantified, highlighted that the GZ protein level might be significantly above the expected doubling value, with more clear accumulation of GFP positive material in the somata of neuronal cells (Fig 58). Any type of signal was found in the homozygote animals not crossed with the SynICre (data not shown). Despite the high level of GFP signal, no signal was detected from synbond (data not shown).

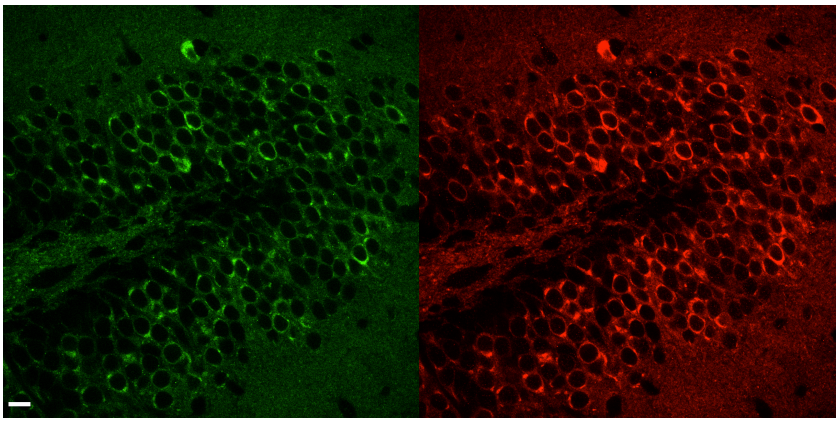

Fig 58 . Hippocampus from a homozygote SynI Cre RosaGreenZip (+/+) mouse. **(A)** GREEN (left): endogenous GFP signal, **(B)** RED (right): anti-GFP Cy5. (60 x; scale bar: 10μm).

Analysis of a different clone of RosaGreenZip (+/+) from D1 ES clone

To exclude that there had been a problem of recombination in ES cell clone used to generate the founders (clone A6, see southern blot results), we tested homozygous animals for the construct RosaGreenZip and positive for Cre (SynCre) whose founders were derived from another clone of ES cells injected into blastocysts (clone B23, see southern blot results). Where the analysis of brain slices treated as described above noted the same type of signal (or absence of signal, as in the case of synbond, see Figure 59).

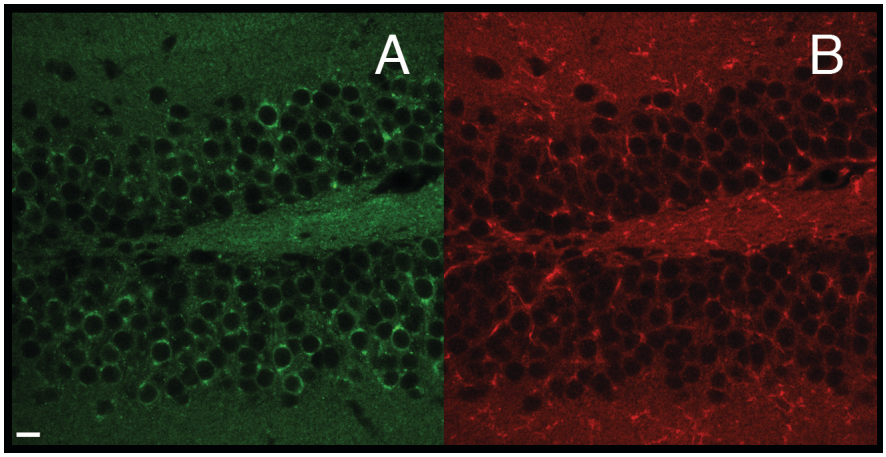

Fig 59 Coronal hippocampal slices from homozygote SynCre RosaGreenZip (+ / +) mouse from ES clone D1. **(A)** GREEN (left): endogenous GFP signal, **(B)** RED (right) signal from Synbond applied post-fixation as a retrospective staining . (60 x; scale bar: 10μm)

Analysis of mRNA and GreenZip protein expression levels in RosaGreenZip (+/+) animals

Although evidently better the signal of endogenous GFP in homozygotes animals compared to those heterozygous, the very faint signal, even when the fixed tissue was retrospectively stained with the peptide Synbond, made us consider that the expression of GreenZip was still too low to use these mouse lines for the in vivo synaptic activity experiments. To ensure that our protein was indeed expressed in a complete way, we probed the tissue searching for protein and mRNA expression by Western Blot and by PCR from RT respectively. As illustrated in Figure 60 the presence of mRNA was clearly demonstrated

by PCR from RT (using two pairs of primers already exploited for the analysis of genotyping, one for the construct's 3'-UTR and the other for VAMP2).

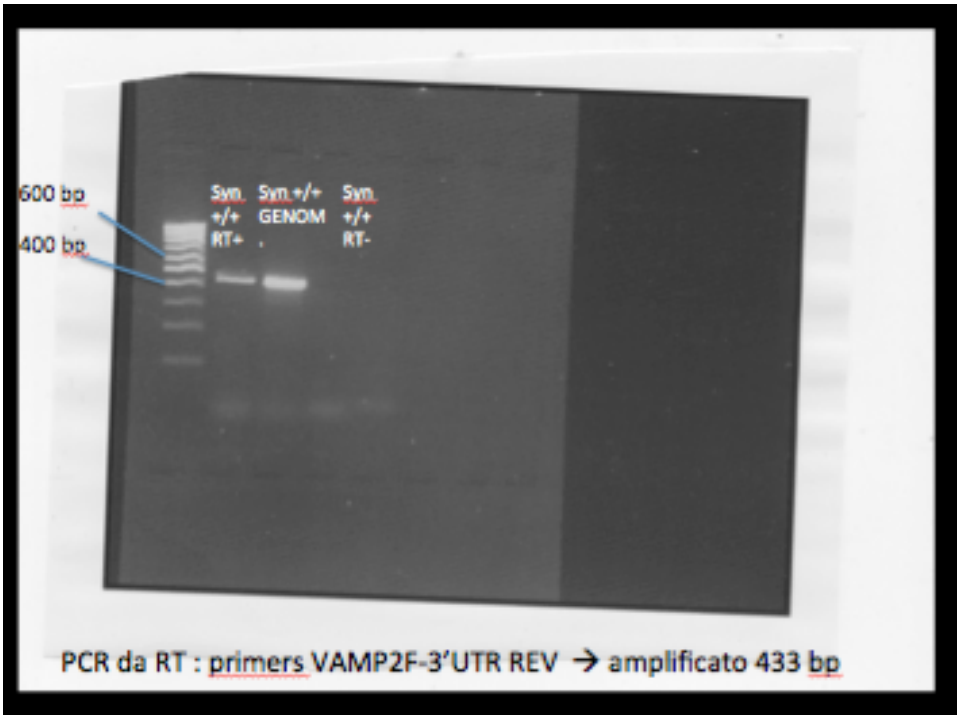

Fig 60: PCR from RT (not quantitative) for detect the presence of the acid module inside the plasmid RosaGreenZip that serves as a "bait" for Synbond, and which is located between the GFP and the region 3 'UTR. Beside the marker, is the RT + from DNA of an animal RosaGreenZip-SynCre + / + (corresponding to the expected amplified band of 433 bp), next we find the result of PCR performed using the same primers on the genomic DNA of an animal RosaGreenZip-SynCre + / +, while next to it (right) is the RT - DNA from an animal RosaGreenZip-SynCre + / +

3.3 GENERATION OF GREENZIP LENTIVIRAL VECTOR

Ascertained the presence and integrity of our protein in mice RosaGreen Zip, we have focused on the considerations on the low expression of this. It was already known that the expression of fluorescent reporters (for example, GFP) directly from the endogenous Rosa26 promoter is poor in the adult mouse brain (Srinivas, S. et al., 2001), for this reason we considered that the presence of a strong promoter pCAGS could prevent such problems. It is known that despite the widespread use of Cre lines and the Importance of complete knowledge of where Cre-mediated recombination occurs, the lack of a systematic approach for Cre expression profiling has prevented full characterization of Cre dependent gene expression patterns in many Cre driver lines, creating uncertainty in the interpretation of results and in the

selection of appropriate Cre lines for specific research purposes (Madisen, L., et al., 2010). Nevertheless, the problem of low expression occurred in three different Cre lines utilized by us (ThyI-Cre and SynI-Cre, and EmxI-Cre line mated with the mouse RosaGreenZip by a partnership group of our institute, which found the same problems expression at the level of PNS). Even the absence in the design of our construct of the stabilization element RNA (WPRE woodchuck hepatitis virus posttranscriptional regulatory element) (Zufferey, R, et al., 1999. Madisen, L., et al., 2010) has been able to contribute to the low expression of our vesicular protein. Is certain that a difference exists between the expression of GreenZip via transient transfection (see Introduction) and via homologous recombination, in which the number of copies of the expressed protein is closely controlled and reduced (and, perhaps there would be a competition with the VAMP2 endogenous which could "prevail" on the few copies produced by the integration of the plasmid RosaGreenZip), was still waiting. But the lack of signal from Synbond made, of the fact, unusable for our purposes, this type of approach, beyond all reasons for the low expression of GreenZip. This led us to undertake a new strategy for the expression of our synaptic reporter that would ensure its high level of expression: the expression of GreenZip through viral vectors (Naldini, L., 1996).

The gene transfer using vectors derived from lentiviruses, such as human immunodeficiency virus (HIV-1), turns out to be a tool with interesting applications in the gene therapy field of a wide range of diseases. The reason resides in the ability of lentiviruses to infect a wide range of cells regardless of their proliferative state (Vigna E., et al. 2000), ex vivo and in vivo. The lentiviral vectors are defective replication viral particles, assembled with core proteins, enzymes and lentiviral proteins of a different virus envelope. In most cases this is the VSVG protein of vesicular stomatitis virus (VSV), capable of mediating infection of the almost any cell type, as well as to confer greater stability to the recombinant viral particles, thus allowing the generation of preparations securities high (JC Burns et al., 1993). The lentiviral vectors can be designed for expression (constitutive or conditional) of both transgenes and shRNA into individual units, or multiple combinations (Naldini L. et al. 1996) (Tiscornia, G. et al. 2003) and have a complex genome. In addition to the HIV-1 structural genes (gag, pol, env) common to all retroviruses, lentiviruses contain two other regulatory genes (tat and rev) and several accessory genes involved in the modulation of viral gene expression, viral particles assembly, and in altering the structural and functional infected cells. The lentiviral replication is in part mediated by noncoding cis proteins, many of which are essential for the functioning of the lentivirus and are included in the transfer construct (encoding the gene of interest). Additionally, trans sequences encode three groups of proteins: structural, regulatory and accessory.

The replication of defective lentiviral vectors, retain the ability to run only the first steps in the life of a lentivirus: attachment, entry, reverse transcription, nuclear transport and integration. Since the first steps are not dependent on viral synthesis, all the genes in trans may be excluded from transfer vectors that encode in this way, only the gene of interest (GreenZip gene in our case) is encoded. Therefore, the

general strategy to produce lentiviral vectors has been to remove all unnecessary genes from the genome of HIV-1 and separate the cis sequences by factors agents in trans that are absolutely required for the production, the infection and integration of the virus (Delenda C. 2004). The production system of third generation lentiviral vectors consists of 4 plasmids (Dull, T. et al. 1998). The transfer vector contains the transgene (or a silencing cassette), as well as all sequences required in cis for the genomic viral RNA and for packaging. Additionally, further changes are made to increase gene "delivery" and the expression into transduced cells, with one of these being the insertion of a post-transcriptional regulatory element from the woodchuck hepatitis virus genome (Marmot monax) (WPRE) into the 3 ' of the transfer vector. The WPRE sequence acts to post-transcriptional level, by promoting the nuclear export of transcripts and / or increasing the efficiency of polyadenylation of the transcript itself (Zufferey, R. et al.1999).

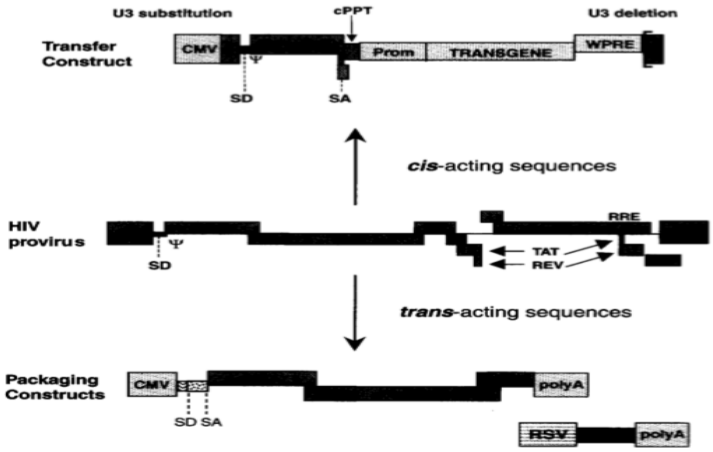

Fig 61: Structure of the HIV-1 provirus and derived constructs. The typical design of lentiviral vectors is based on separating the sequences acting in cis from the viral genes that express proteins working in trans during transduction and that must be expressed in the producer cells. In the transfer construct are located all the cis functions allowing efficientencapsidation, reverse transcription, nuclear transport, and integration of the vector into the target cells. The packaging constructs express the indicated viral genes from the cytomegalovirus (CMV) and Rous sarcoma virus (RSV) promoters. The 5t LTR of transfer construct is chimeric, with the enhancer-promoterof the CMV replacing the U3 region and the 3r LTR has an almost complete deletion of the U3 region (sin-18). Splice donor and acceptor sites (SD and SA), the packaging sequence (ψ), 5t portion of gag gene with truncated reading frame including extended packaging signal (GA), Rev Response Element (RRE), polyadenylation site (polyA), central polypurine tract (cPPT), internal promoter (Prom), posttranscriptional regulatory element from the genome of the woodchuck hepatitis virus (Wpre), shown. (From Follenzi, A., 2002.)

The security of the system resides in the provision of the functions in trans, requests for packaging, from three separate plasmids additional (pMDL, PREV, pVSVG, see Figure 65), as well as by deletion in the region promoter / enhancer in the 3 'LTR (Long terminal repeat) on the transfer vector. The first measure dramatically reduces the risk of accidental formation, for recombination causal, of complete viral genomes for replication. The second measure, being the proviral 5 'LTR copied from the virionic 3' LTR,

allows the formation of a 5 'LTR inactive upstream of the integrated provirus, preventing transcription and / or mobilization of the latter (SIN vector: self inactivating vector).

The figure 61 shows the vector in which we have inserted the coding region for our vesicular modified VAMP2-GFP protein (GreenZip) (see materials and methods).

Lenti-GreenZip in HeLa cells

Once having obtained the lentiviral stock for the expression of GreenZip (called "LentiGreenZip") with a title of charge of 4.7 * 10^9 TU / ml, we therefore decided to test the efficiency of the lentiviral vector both in vitro and in vivo. For the infection in vitro we have chosen different concentrations of viral load with which infect HeLa cells:

1) 1.29 X 10^9 Tu / 1.5 ml

2) 6.45 X 10^6 Tu / 1.5 ml

3) 3.2 X 10^6 Tu / 1.5 ml

4) 1.6 X 10^6 / 1.5 ml

5) 8 X 10^5 Tu / 1.5 ml

6) 4 X 10^5 Tu / 1.5 ml

The same concentrations of viral load were chosen for the LentiZip infection through LentiZip of hippocampal neurons in culture. After about 27 hours of infection the Hela cells were fixed and observed by confocal microscopy to evaluate the expression of endogenous GFP endogenous where it can be noted that the expression level varies with the concentration of the viral load and including that which returned a higher signal was the concentration of 1.29 X 10^9 Tu / 1.5 ml. (the viral title of the next images). HeLa cells were evaluated first, before examining the expression of GFP in neurons, as we wanted to evaluate first in HeLa cells, to avoid subjecting the neurons into conditions in which their integrity could have been, may be placed at risk, by removing them from their ideal incubation environment (see Materials and Methods).

After evaluating the expression of GreenZip, we wanted to analyze the integrity of our protein by performing some immunofluorescence reactions (anti-myc, anti-Vamp2 on the cells infected with 1.29 X 10^9 Tu / 1.5 ml) on which we evaluated at the same time, together with the results of these tests, the level of GFP expression (Fig 62 and 63).

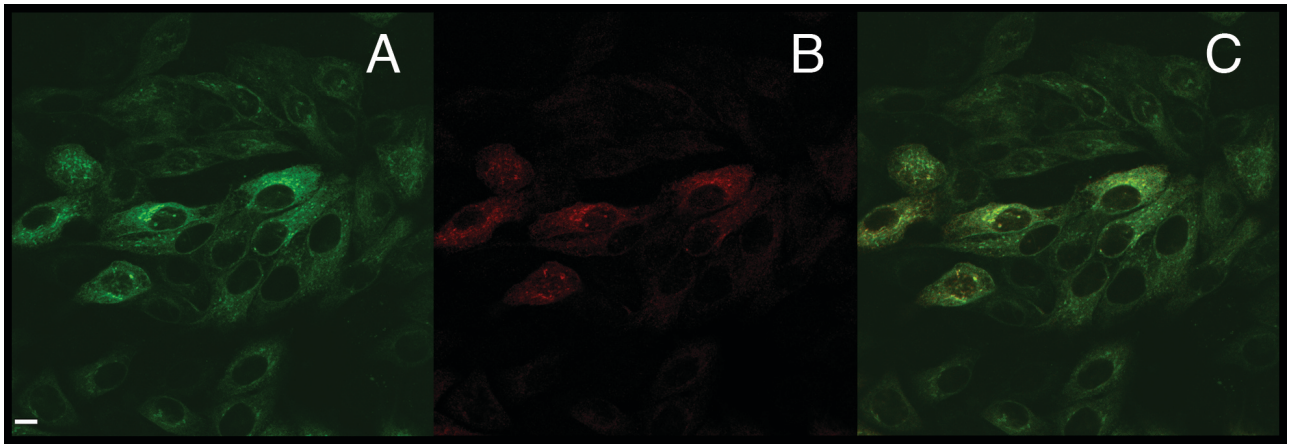

Fig 62: **(A)** endogenous GFP signal from HeLa cells infected with virus LentiZip with a viral load of 1.29 X 10^9 Tu / 1.5 ml **(B)** immunostaining with anti-Vamp2 antibody of the same field presented in panel A (HeLA cells does not express endogenous VAMP2) **(C)** Merge signal from figures A and B. (60X, bar 10μm)

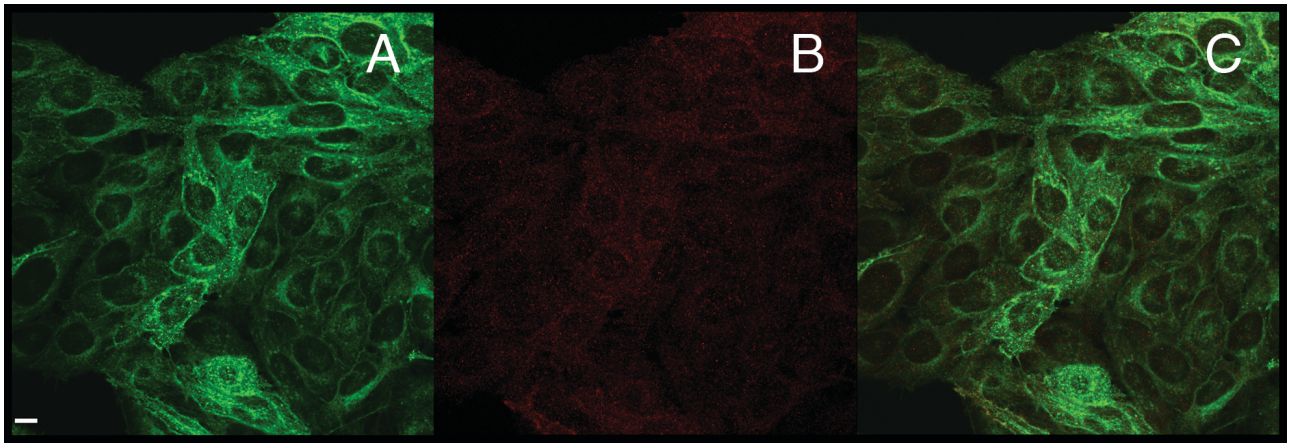

Fig 63: **(A)** endogenous GFP signal from HeLa cells infected with virus LentiZip with viral load of 1.29 X 10^9 Tu / 1.5 ml. **(B)** immunostaining with anti-Myc ANTIBODY of the same field presented in panel A (Myc-tag is present into at the C-terminal of our construct VAMP2-GFP). **(C)** Merge from figures A and B. (60X, bar 10μm)

In vivo LentiGreenZip expression

Once the integrity and functionality of our construct was checked we proceeded to the in vivo application of this (2 microlitres, viral load of 1.29 X 10^9 Tu / 1.5 ml). We choose to inject our lentiviral vector into the visual Thalamus (vLGN), applied through the use of stereotaxis surgery (see materials and methods), the visual Thalamus (vLGN) in anticipation of examining the local circuits via Synbond injection. Therefore three weeks after injection we went to assess the level of LentiZip expression into the Thalamus, and, after crossing the visual thalamus in thin slices (30 micron) with a vibratome instrument

we made some immunofluorescence (anti-Gad65 and anti Neun to mark all the neurons cells) reactions on these slices (Fig 64 and 65).

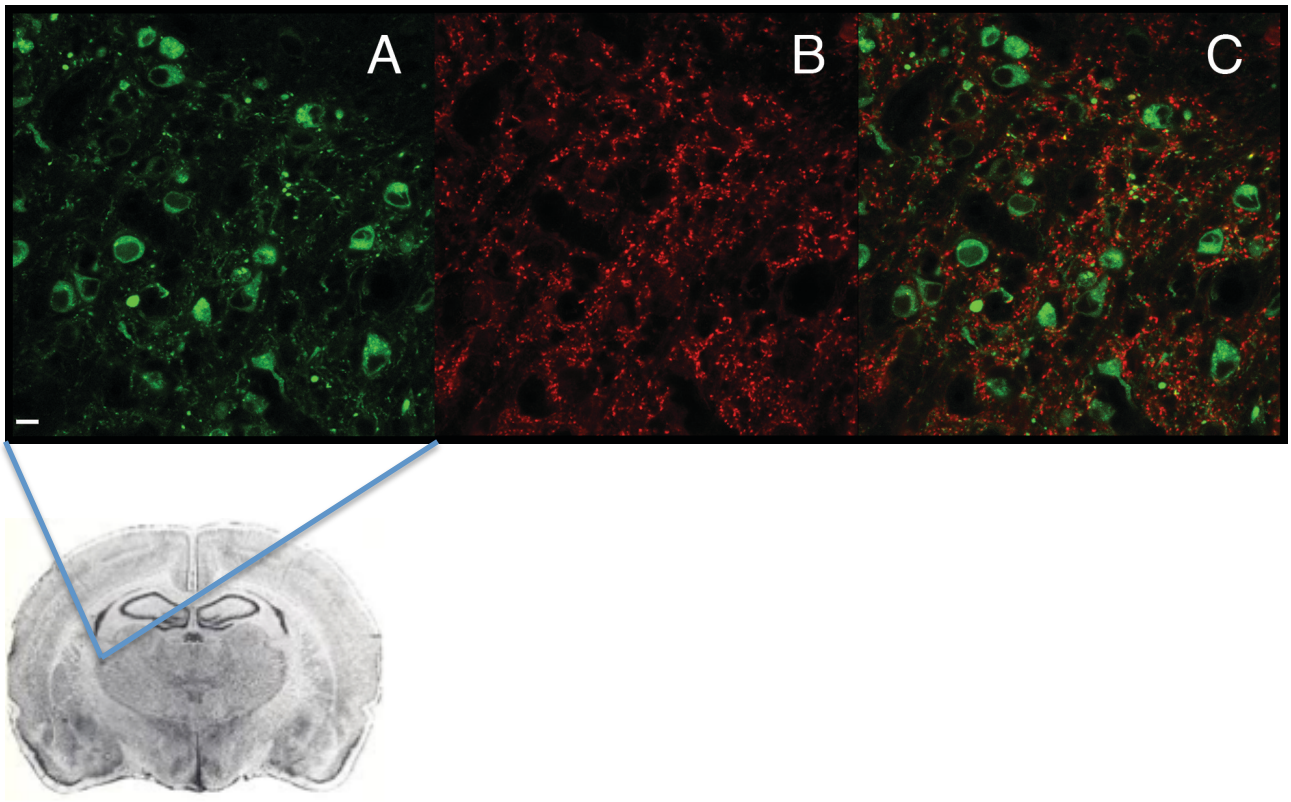

Fig 64: **(A)** GFP endogenous signal coming from rat visual Thalamus (LGN) (slices of 30 microns). **(B)** immunostaining with anti-GAD(65+67) antibody of the same field presented in panel. **(C)** merge from figures A and B. (60X, bar 10μm)

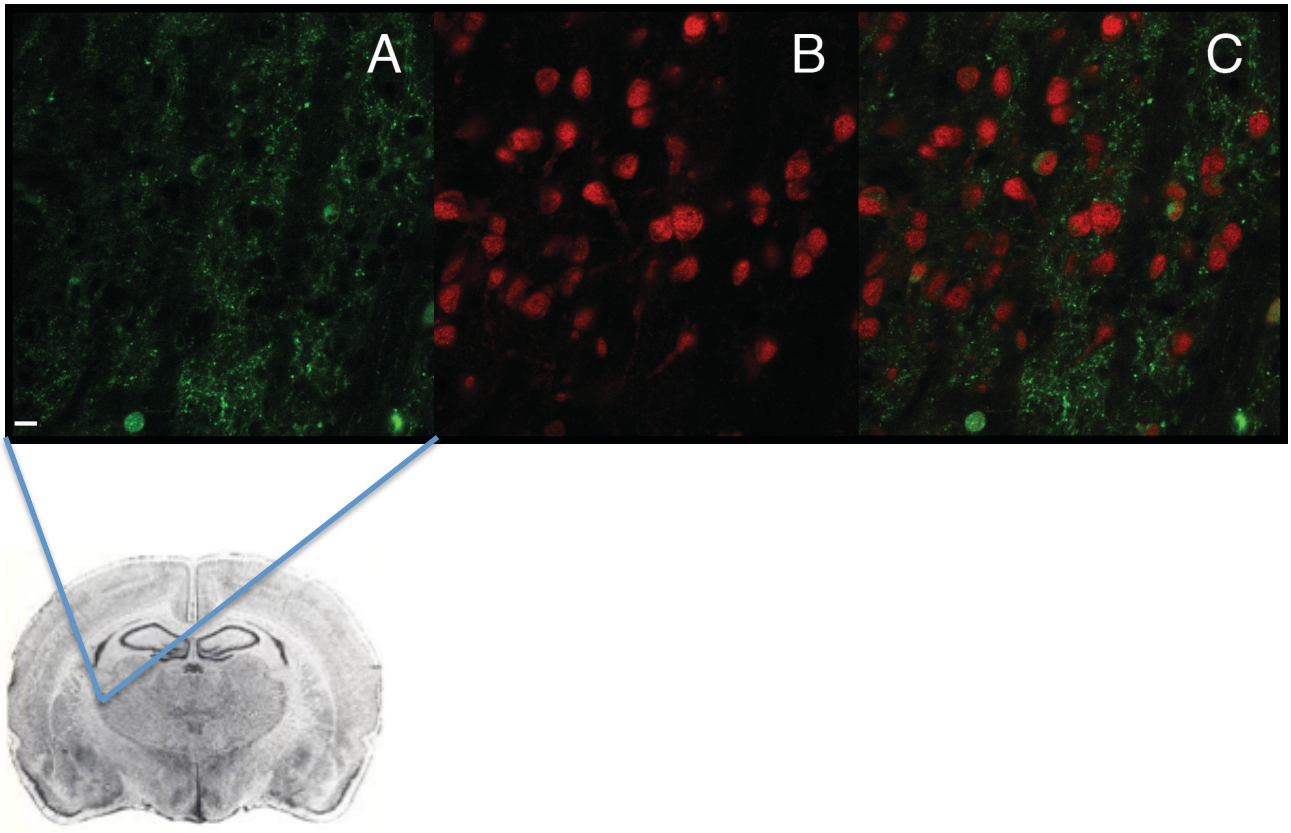

Fig 65: **(A)** GFP endogenous signal coming from rat Thalamus (LGN) (slices of 30 microns). **(B)** immunostaining with anti-NeuN antibody of the same field presented in panel A. **(C)** merge from figures A and B. (60X, bar 10μm)

Synbond uptake in cells transfected with LentiGreenZip vectors

We wanted to apply our peptide Synbond to evaluate the capacity of lentiviral vector in order to be able to detect the vesicular exocytosis (see Materials and Metododi), this was performed in both HeLa cells as well as on neurons in culture. The figures below show some Hela Cells and a neuron infected with the virus expressing GreenZip (LentiZip), after 4 days from transfection. These were incubated for 30 minutes with Synbond (5 nM) in standard conditions (See materials and methods), before the cells were chemically fixed. Note the extraordinary resolution of our pair of probes to mark the individual synaptic boutons (See Figure 66 and 67).

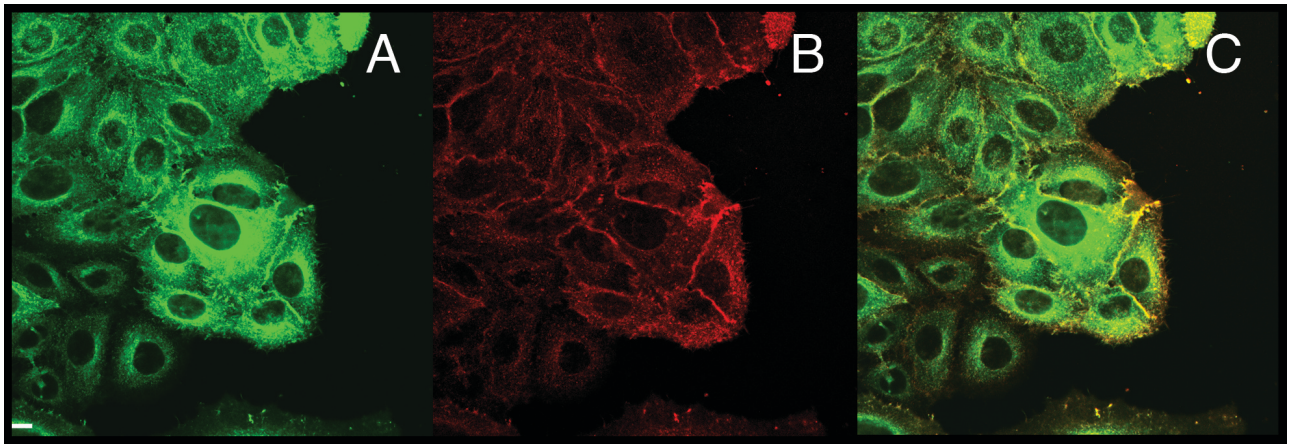

Fig 66: **(A)** endogenous signal from HeLa cells infected with virus LentiZip with viral load of 1.29 X 10^9 Tu / 1.5 ml. **(B)** in vivo vesicular uptake of Synbond (red) of the same cells shown in panel A . **(C)** Merge from figures A and B. (60X, bar 10μm)

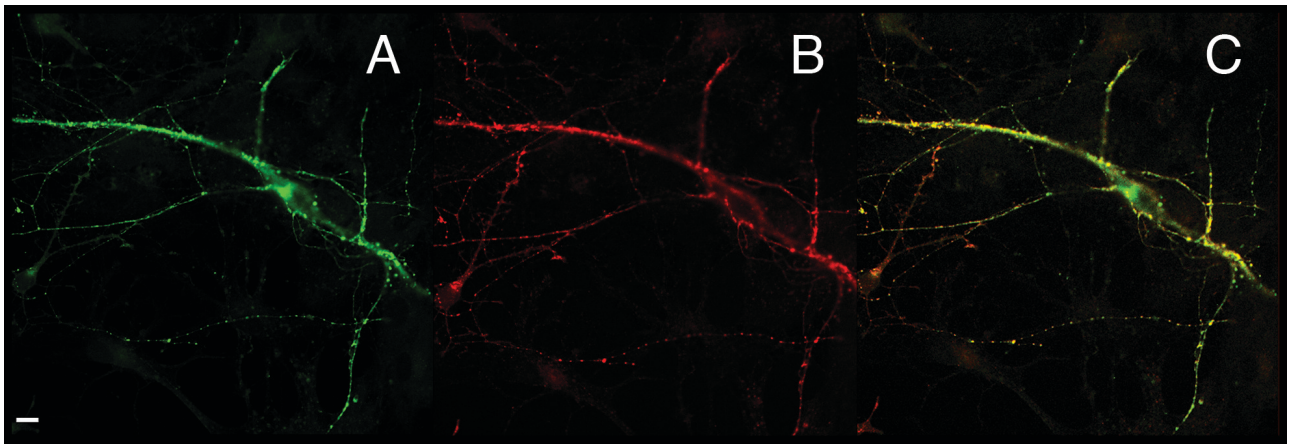

Fig 67: **(A)** GFP endogenous signal from Hippocampal neurons infected with virus LentiZip with viral load of 1.29 X 10^9 Tu / 1.5 ml. **(B)** in vivo synaptic uptake of Synbond (red) of the same cells shown in panel A, spontaneous activity **(C)** GFP/synbond merge signal from Hippocampal neurons infected with virus LentiZip with viral load of 1.29 X 10^9 Tu / 1.5 ml. (60X, bar 10μm)

DISCUSSION

We have seen how our GreenZip construct and its counterpart Synbond, can detect the activity at the single synapses level with an excellent resolution and signal-to-noise ratio. But more important, this couple can work also applied in vivo: our modified VAMP2 proves to localize at the level of the synapse to confirmation of the role of this protein to promote neurosecretion (Baumet et al. 2001). With this pair of sensors it has been possible to detect synaptic activity in deep structures of the brain such as the thalamus, and this has been possible thanks to the small size of the peptide Synbond (4.9Kda). We choose the visual system because it is easily accessible and investigable and this pathway goes deeply inside the brain structures. In fact we choose an optic pathway because the structures that can be transfetced with DNA are easily reachable from the outside (Ganglion cells of the retina). Based on the date obtained, it emerged that LGN can be reached by Synbond, therefore fostering the idea to visualize in vivo light-dependent uptake by thalamic synapses. We have expressed our probes in retinothalamic synapses of living animals: for this goal we have developed and optimized an electroporation technique which was based on an electroporation protocol previously developed by another group (Dezawa et al., 2002), and through it has been possible to express GreenZip in retinal ganglion cells in the eye of the animals. Then we went on to test the Synbond capacity to detect the activity at the level of individual synapses. This has been achieved by stimulating our animals with different protocols of visual stimulation. In this way it is noted that there is a significant difference between the signal given by Synbond, which reflects its internalization at the synaptic vesicle level (which has been internalized after synaptic activation), among the animals treated with various light stimuli and those kept in the dark after peptide administration. It is also possible to observe an increase in signal as a result of the increase in the time of light stimulation.

We therefore decided to implement this technique, then the expression of our modified vesicular protein (GreenZip), in a transgenic animal in order to apply our pair of probes for synaptic activity at the level of any brain region, overcoming in this way the limits of the transient transfection that bordered us at the level of the visual pathways. For the development of the transgenic model we decided to utilize the Rosa26 locus Homologous recombination system (Soriano et al., 1999) coupled to the Cre-recombinase system, methods already used for the expression of fluorescent proteins at the level of the Central Nervous System (Zong et al., 2005 . Muzumdar et al., 2007). Despite the Rosa26-Cre system has shown a specificity of expression when tested on HeLa cells (which were transfected with the construct RosaGreenZip and only those co-transfected with the Cre showed expression of GFP and internalization of Synbond), the knock –in animal which we obtained, however, did not show a high GFP signal, and an even scarcer signal coming from the Synbond uptake, even in homozygosity. The same results have been obtained for our construct Rosa GreenZip expressed under various promoters Cre (Cre-SynI and Thy-Cre). This result can be explained by several factors: the absence of the post-transcriptional stability

(Woodchuck Hepatitis Virus or WPRE) in the starting plasmid (Madisen et al., 2010) as well as a few copies of VAMP2 expressed in the knock-in animal through this method.

In parallel with the creation of transgenic animal, we carried out the possibility of expressing GreenZip through lentiviral vectors, given the possibility of infecting non-dividing cells such as neurons using this technique (Naldini et al., 1996). Through this type of vectors a neuron should then be infected with multiple viral copies, then these copies will integrate in the genome of the host cell (Follenzi et al., 2002), encouraging the production of a high level of GreenZip extra-copies in the amount of transient transfection of GreenZip cDNA obtained with the retinal ganglion cells electroporation. The high expression of our vesicular probe has been demonstrated both in HeLa cells as well as in cultured neurons, and in these the Synbond uptake is also seen; in addition in the animal in vivo it was possible to inject the lentiviral vector, showing that also in vivo this system provides a high expression of GreenZip.

In the introductory part of this thesis, after analyzing the main methods available today that allow us to study in vivo the activity of brain networks in relation to the physiology and to the behaviour, we tried to imagine what could be the "ideal" tool that allows us to correlate better the physiological and cognitive functions with specific configurations of neural activity of synaptic subgroups of neurons. We said that an essential element of such an instrument should be to have a resolution and sensitivity that not only provides quantitative information on the activity of individual nerve cells, but, possibly from all the cell groups involved in a particular cognitive process, if not, by all their synapses.

Now, in this work we have passed in review the unique and innovative features of the method developed by our laboratory, represented by the Zip-Bond pair: the excellent results coming from the transfection of GreenZip within the visual circuit, the ease with which our peptide Synbond can be applied, its high levels of roll-out in the short term, its small size, making it capable of reaching synapses also distant from the site of injection, but, above all, the tremendous capabilities of this couple in view of the activity of individual synapses in vivo, make this pair a unique tool for the study of physiological functions (normal or pathological physiological functions) in connection with the synaptic activity. We have seen how through our probes it is possible to enter the single synapse, integrated into the circuit in the whole brain of a living animal, in order to determine whether it is working or not, and ideally to follow what happens within a single synapse, active or not, at different times and with different stimuli. We have also seen how, through the last analysis that our laboratory is conducting, it will be possible to determine when the single synapse is active, through the analysis of the fluorescence emitted by Synbond and in this way it will then be plausible to infer how inside a particular neural circuit, different synapses act differently activated, but not only, due to the characteristics of the Zip-bond pair, already mentioned, it can lead to a detailed study of vesicular trafficking with a resolution and a unique specificity. It is therefore an instrument with an incredible potential, which will enable us to derive experimental data from the functional analysis of specific neural networks underlying specific cognitive and behavioural functions, and from the analysis of the single synapse that make up the above network, and still more

specifically, from the analysis of vesicular dynamics, will be possible to arrive to a better understanding of the dynamics of vesicular exo-endocytosis, to use this knowledge in broad areas. In fact, the availability of a similar tool allows to obtain images of synaptic activity relative to an incredible number of issues within the field of neuroscience: just think about the application of this method in the neuropharmacology field, for example, to be able to follow in time the action of psychotropic drugs on the physiology and synaptic vesicular, or to pure analysis of synaptic activity of groups of neurons forming part of a single neural circuit, relating it to different types of simple perceptual stimuli (visual, auditory, olfactory stimuli), or to its outstanding potential in fields such as the studies on learning, synaptic plasticity and the critical period. Many topics within the broad field of learning, including that of the LTP, or even cases of classical or operant conditioning, that we mentioned in the introduction, applied to more diverse stimuli, may be better understood using this technique, having the ability to directly monitor the evolution of a brain circuit, and every micro-component during this type of work. In fact to be able to study the functional dynamics at the level of a network that learns the intra and inter-relationships within this and other networks, from the morphological point of view, but especially physiological, of the network as well as the single vesicle in the single synapse, this will be possible in the future, we believe, by using our innovative method. Similarly, to understand the dynamics and synaptic changes occurring in specific neural circuits underlying different types of behaviour (fear, avoidance, active research, decision) could lead to new discoveries about the physiology of these complex cognitive mechanisms.

BIBLIOGRAPHY

Adamantidis AR, et al. (2007) Neural substrates of awakening probed with optogenetic control of hypocretin neurons. *Nature*.; 450:420–424.

Adesnik H, Scanziani M. (2010) Lateral competition for cortical space by layer-specific horizontal circuits. *Nature*.; 464:1155–1160

Aggarwal, S.K., MacKinnon, R. (1996). Contribution of the S4 segment to gating charge in the Shaker K+ channel. *Neuron* 16:1169 -1177

Aravanis AM, et al. (2007) An optical neural interface: in vivo control of rodent motor cortex with integrated fiberoptic and optogenetic technology. *J Neural Eng*.; 4:S143–156.

Arenkiel BR, et al. (2007) In vivo light-induced activation of neural circuitry in transgenic mice expressing channelrhodopsin-2. *Neuron.*; 54:205–218

Asamoah, O.K., Wuskell, J.P., Loew, L.M., Bezanilla, F. (2003). A fluorometric approach to local electric field measurements in a voltage-gated ion channel. *Neuron* 37:85

Ataka, K., and Pieribone, V.A. (2002). A genetically targetable fluorescent probe of channel gating with rapid kinetics. *Biophys. J*. 82, 509–516.

Atasoy D, et al. A FLEX switch targets Channelrhodopsin-2 to multiple cell types for imaging and long-range circuit mapping. *J Neurosci*. 2008; 28:7025–7030

Attwell, D., Laughlin, SB. (2001). An energy budget for signaling in the grey matter of the brain. *J. Cereb. Blood Flow Metab.*

Blasi, J. et al. (1993) Botulinum neurotoxin A selectively cleaves the synaptic protein SNAP-25. *Nature* 365, 160–163.

Blasi, J. et al. Botulinum neurotoxin C1 blocks neurotransmitter release by means of cleaving HPC-1/ syntaxin. *EMBO J*. 12, 4821–4828, 1993.

Boyden ES, et al. Millisecond-timescale, genetically targeted optical control of neural activity. *Nat Neurosci*. 2005; 8:1263–1268

Bozza, T., McGann, JP., Mombaerts, P., Wachowiak M. (2004) In vivo imaging of neuronal activity by targeted expression of a genetically encoded probe in the mouse. *Neuron* 42:9-21

Brooks, RA., Battocletti, JH., Sances, A., Lar-

Son, SJ., Bowman, RL., Kudravcev, V. (1975).
Nuclear magnetic relaxation in blood. *IEEE Trans. Biomed. Eng.* 22:12–18 .

Burchiel SW., Edwards BS., Kuckuck FW., Lauer FT., Prossnitz ER., Ransom JT., Sklar. (2000). Analysis of free intracellular calcium by flow cytometry: multiparameter and pharmacologic applications. *LA. Methods* (21):3 221-230.

Burns, J.C. et al., (1993). Vesicular stomatitis virus G glycoprotein pseudotyped retroviral vectors: concentration to very high titer and efficient gene transfer into mammalian and nonmammalian cells. *Proc. Natl. Acad. Sci*. USA 90:8033-8037

Cajal S.R. (1894). The Croonian lecture: la fine structure des centres nerveux. *Proceedings of the Royal Society of London*, **55**: 444-468.

Campsall KD et al., (2002). Characterization of transgene expression and Cre recombinase activity in a panel of Thy-1 promoter-Cre transgenic mice. *Dev. Dyn.*, 224 pp. 135–143

Cardin JA, et al. Driving fast-spiking cells induces gamma rhythm and controls sensory responses. *Nature.* 2009; 459:663–667

Caroni, P. et al., (1997) Overexpression of growth-associated proteins in the neurons of adult transgenic mice*. J. Neurosci. Methods*

Carter ME et al., Optogenetic investigation of neural circuits *in vivo* Trends Mol Med. (2011) April ; 17(4): 197–206

Cha, A., Bezanilla, F. (1998). Structural implications of fluorescence quenching in the Shaker K+ channel. *J. Gen. Physiol*. 112:391-408.

Chance, F. S., Abbott, L. F. & Reyes, A. D. (2002) Gain modulation from background synaptic input. *Neuron* 35, 773–782 .

Chanda, B., Blunck, R., Faria, L.C., Schweizer, F.E., Mody, I., and Bezanilla, F. (2005). A hybrid approach to measuring electrical activity in genetically specified neurons*. Nat. Neuroscience*. 8, 1619–1626.

Cohen, MR., Newsome, WT. (2004), What electrical microstimulation has revealed about the neural basis of cognition. *Curr Opin Neurobiol.* 14:169-77.

Cohen, MR., Newsome, WT. (2009). Estimates of the contribution of single neurons to perception depend on timescale and noise correlation*. J Neurosci***.** 29:6635-48.

Chow BY, et al., (2010) High- performance genetically targetable optical neural silencing by light-driven proton pumps. *Nature* 463:98–102

Cruikshank SJ, et al. (2010) Pathway-specific feedforward circuits between thalamus and neocortex revealed by selective optical stimulation of axons. *Neuron.;* 65:230–245

De Camilli, P., et al., (1983) Synapsin I (protein I), a nerve terminal-specific phosphoprotein. I. Its general distribution in synapses of the central and peripheral nervous system demonstrated by

immunofluorescence in frozen and plastic sections**.** *J. Cell Biol.* **96 ,** 1337-1354.

Delenda C (2004). Lentiviral vectors: optimization of packaging, transduction and gene expression. J Gene Med ;6 Suppl 1:S125-38.

Denk, W., Strickler, J.H. & Webb, W.W. (1990). Two-photon laser scanning fluorescence microscopy. *Science* 248: 73–76.

Deisseroth K, Feng G, Majewska AK, Miesenbock G, Ting A, Schnitzer MJ (2006) Next-generation optical technologies for illuminating genetically targeted brain circuits. *J Neurosci* 26:10380–10386

Dimitrov, D., He, Y., Mutoh, H., Baker, B.J., Cohen, L., Akemann, W., and Knopfel, T. (2007). Engineering and characterization of an enhanced fluorescent protein voltage sensor. *PLoS ONE* 2, e440.

Douglas, R. J. & Martin, K. A. (2004) Neuronal circuits of the neocortex. *Annu. Rev. Neurosci.* 27, 419–451.

Douglas, R. J., Koch, C., Mahowald, M., Martin, K. A. & Suarez, H. H. (1995) Recurrent excitation in neocortical circuits. *Science* 269, 981–985.

Dull, T., (1998). A third-generation lentivirus vector with a conditional packaging system. *J. Virol*. 72, 8463–8471.

Fluhler E., Burnham VG., Loew LM. (1985). Spectra, membrane binding, and potentiometric responses of new charge shift probes. *Biochemistry* (24):21 5749-5755.

Follenzi A., et al., (2002). Efficient gene delivery and targeted expression to hepatocytes *in vivo* by improved lentiviral vectors. *Hum. Gene Ther.* **13,** 243–260.

Follenzi A., et al., (2002). Generation of HIV-1 derived lentiviral vectors. *Methods in Enzymology* 346:454-65.

Follenzi A, et al., (2000) Gene transfer by lentiviral vectors is limited by nuclear translocation and rescued by HIV-1 pol sequences. *Nature Genet*, **25**, 217–222.

Fox PT, Raichle ME. (1986). Focal physiological uncoupling of cerebral blood flow and oxidative metabolism during somatosensory stimulation in human subjects. *Proc. Natl. Acad. Sci. USA* 83:1140–44.

Friedrich G, Soriano P. (1991).Promoter traps in embryonic stem cells: a genetic screen to identify and mutate developmental genes in mice. *Genes Dev.* Sep;5(9):1513-23.

Geppert, M. et al (1994). Synaptotagmin I: a major Ca2+ sensor for transmitter release at a central synapse.*Cell* 79, 717–727.

Glover GH. (1999). Deconvolution of impulse response in event-related BOLD fMRI. *Neuroimage* 9:416–29 ratum. *Neuroimage.* 1998. 8:228.

Govorunova EG, Spudich EN, Lane CE, Sineshchekov OA, Spudich JL (2011) New channelrhodopsin with a red-shifted spectrum and rapid kinetics from *Mesostigma viride. MBio 2*(3):e00115-11

Gong S, et al. Targeting Cre recombinase to specific neuron populations with bacterial artificial chromosome constructs. J Neurosci. 2007; 27:9817–9823.

Guillet EG., Kimmich GA. (1981) DiO-C3-(5) and DiS-C3-(5): interactions with RBC, ghosts and phospholipid vescicles*. J Membr Biol* (59):1 1-11.

Gradinaru V, et al (2010).Molecular and cellular approaches for diversifying and extending optogenetics. *Cell.*; 141:154–165

Gradinaru V, et al. (2009) Optical deconstruction of parkinsonian neural circuitry. *Science*; 324:354–359

Gradinaru V, et al. (2008) eNpHR: a Natronomonas halorhodopsin enhanced for optogenetic applications. *Brain Cell Biol.*; 36:129–139

Hakem R., Hakem A., Duncan GS., Henderson JT., Woo M., Soengas MS., Elia A., de la Pompa JL., Kagi D., Khoo W., Potter J., Yoshida R., Kaufman SA., Lowe SW., Penninger JM., Mak TW. (1998). Differential requirement for caspase 9 in apoptotic pathways in vivo. *Cell*; (94):3 339-35.

Han X, Boyden ES (2007) Multiple-color optical activation, silencing, and desynchronization of neural activity, with single-spike tem- poral resolution. *PLoS One* 2:e299

Han X, Chow BY, Zhou H, Klapoetke N, Boyden E et al (2011) A high-light sensitivity optical neural silencer: development and application to optogenetic control of nun-human primate cortex. *Front Sys Neurosci* 5:1–8

Hebb D.O, The organization of behavior; a neuropsychological theory. *Wiley, New York*, 1949

Helmchen, F., & Denk, W. (2002) New developments in multiphoton microscopy*. Curr. Opin. Neurobiol.* 12: 593–601.

Helmchen, F., Waters, J. (2002). Ca2+ imaging in the mammalian brain in vivo*. Eur J Pharmacol.* Jul 5;447(2-3):119-29.

Hoesche C, et al., (1993) The 5′-flanking region of the rat synapsin I gene directs neuron-specific and developmentally regulated reporter gene expression in transgenic mice*. J Biol Chem*.;268:26494–26502.

Huber D, et al. (2008) Sparse optical microstimulation in barrel cortex drives learned behaviour in freely moving mice. *Nature.*; 451:61–64

Hull C, et al. (2009) Neocortical disynaptic inhibition requires somatodendritic integration in interneurons*. J Neurosci.*; 29:8991–8995

Hyder, F., Shulman, RG., Rothman, DL. (1998). A model for the regulation of cerebral oxygen delivery. *J. Appl. Physiol..*

Jahn, R., Scheller, RH. (2006) SNAREs--engines for membrane fusion. *Nat Rev Mol Cell Biol*;7(9):631-43.

Konnerth, A., Obaid, A.L., Salzberg, B.M. (1987). Optical recording of electrical activity from parallel fibres and other cell types in skate cerebellar slices in vitro. *J. Physiol*. 393:681

Kuner, T., Augustine, G.J. (2000). A genetically encoded ratiometric indicator for chloride: capturing chloride transients in cultured hippocampal neurons. *Neuron* 27:447-459.

Kwong, KK., Belliveau, JW., Chesler, DA., Goldberg, IE., Weisskoff, RM, et al. (1992). Dynamic magnetic resonance imaging of human brain activity during primary sensory stimulation. *Proc. Natl. Acad. Sci. USA* 89:5675–79.

Li X, Gutierrez DV, Hanson MG, Han J, Mark MD, Chiel H, Hegemann P, Landmesser LT, Herlitze S (2005) Fast noninvasive activation and inhibition of neural and network activity by verte- brate rhodopsin and green algae channelrhodopsin*. Proc Natl Acad* Sci USA 102:17816–17821

LeDoux, Synaptic Self: How Our Brains Become Who We Are, *Penguin*, 2002.

Livet, J et al., (2007). Transgenic strategies for combinatorial expression of fluorescent proteins in the nervous system. *Nature* 450, 56-62

Loew LM, Cohen LB et al (1992) A naphthyl analog of the aminostyryl pyri- dinium class of potentiometric membrane dyes shows consistent sensitivity in a variety of tissue, cell, and model membrane preparations. J Membr Biol 130:1–10

Logothetis, N. (2002). The neural basis of the blood-oxygen-level-dependent functional magnetic resonance imaging signal. *Phil. Tarns. R. soc. london 357, 1003-1037.*

Logothetis, N. (2008). What we can and what we cannot do with fMRI. *Nature.* 453, 869-878.

Logothetis, N., Wandell, A. (2004). Interpreting the boold signal. *Annu. Rev. Physiol*. 66:735–69. component of long-term potentiation visualized at individual hippocampal synapses. *Science* 268: 1624-1628.

Madisen L, et al. (2010) A robust and high-throughput Cre reporting and characterization system for the whole mouse brain. *Nat Neurosci*.; 13:133–140

Malgaroli A, Tsien RW (1992) Glutamate-induced long-term potentiation of the frequency of miniature synaptic currents in cultured hippocampal neurons. *Nature*. 357:134-9.

Matsuno-Yagi A, Mukohata Y (1977) Two possible roles of bacterio- rhodopsin; a comparative study of strains of Halobacterium hal- obium diVering in pigmentation. *Biochem Biophys Res Commun* 78:237–243

Mertz, J. (2004). Nonlinear microscopy: new techniques and applications. *Curr. Opin. Neurobiol.* 14, 610–616.

Miesenbock, G., Angelis, D.A., Rothman, J.E. (1998). Visualizing secretion and synaptic transmission with pH-sensitive green fluorescent proteins. *Nature* 394:192-195.

Mintun, MA., Lundstrom, BN., Snyder, AZ., Vlassenko, AG., Shulman, GL., Raichle, ME. (2001). Blood flow and oxygen delivery to human brain during functional activity: theoretical modeling and experimental data. *Proc. Natl. Acad. Sci. USA* 98:6859–64.

Miyawaki, A. (2005). Innovations in the Imaging of Brain Functions using Fluorescent Proteins. *Neuron* 48, 189–199.

Montana V., Farkas DL., Loew LM. (1989). Dual-wavelight ratiometric fluorescente measurements of membrane potential. *Biochemistry* (28):11 4536-4539.

Nagel G, Szellas T, Huhn W, Kateriya S, Adeishvili N, Berthold P, Ol- lig D, Hegemann P, Bamberg E (2003) Channelrhodopsin-2, a di- rectly light-gated cation-selective membrane channel. *Proc Natl Acad Sci USA* 100:13940–13945

Nagy, G. et al. (2006) Different effects on fast exocytosis induced by synaptotagmin 1 and 2 isoforms and abundance but not by phosphorylation. *J. Neurosci*. 26, 632–643.

Naldini, L. et al., (1996). In vivo gene delivery and stable transduction of nondividing cells by a lentiviral vector. *Science.* 272(5259):263-7.

Ng, M., Roorda, RD., Lima, SQ., Zemelman, BV., Morcillo, P., Miesenböck G. (2002) Transmission of olfactory information between three populations of neurons in the antennal lobe of the fly. *Neuron.* 36:463-74.

Nicholls DG., Ward MW. (2000). Mitochondrial membrane potential and neuronal glutamate excitotoxicity: mortality and millivolts. *Trends Neuroscience* 23, 166-174.

Noda, M., Shimizu, S., Tanabe, T., Takai, T., Kayano, T., Ikeda, T., Takahashi, H., et al. (1984). Primary structure of Electrophorus electricus sodium channel deduced from cDNA sequences. *Nature* 312:121.

Ogawa,. S, Lee, TM., Nayak, AS., Glynn, P. (1990). Oxygenation-sensitive contrast in magnetic resonance image of rodent brain at high magnetic fields. *Magn. Re son. Med.* 14:68–78.

Ogawa, S., Lee, TM., Kay, AR., Tank, DW. (1990). Brain magnetic resonance imaging with contrast dependent on blood oxygenation. *Proc. Natl. Acad. Sci. USA* 87:9868–72 .

Ogawa S, Lee TM. (1990). Magnetic resonance imaging of blood vessels at high fields: in vivo and in vitro measurements and image simulation. *Magn. Reson. Med.*

16:9–18.

Pavlov, I. P. (1927). Conditioned Reflexes: An Investigation of the Physiological Activity of the Cerebral Cortex. *Translated and Edited by G. V. Anrep*. London: Oxford University Press. p. 142.

Pauling, L., Coryell, C. (1936). The magnetic properties and structure of hemoglobin. *Proc. Natl. Acad. Sci. USA* 22:210.

Pham NA., Robinson BH., Hedley DW. (2000). Simultaneous detection of mitochondrial respiratory chain activity and reactive oxygen in digitonin-permeabilized cells using flow cytometry. *Cytometry* (41):4 245-251.

Pobbati, A, V., Stein, A. & Fasshauer, D. (2006). N- to C-terminal SNARE complex assembly promotes rapid membrane fusion. *Science* 313, 673–676.

Racker E, Stoeckenius W (1974) Reconstitution of purple membrane vesicles catalyzing light-driven proton uptake and adenosine tri- phosphate formation. *J Biol Chem* 249:662–663

Robson, MD., Dorosz, JL., Gore, JC. (1998). Measurements of the temporal fMRI response of the human auditory cortex to trains of tones. *Neuroimage* 7:185–98. Erratum. *Neuroimage.* 1998. 8:228.

Rogers, Kelly L., Stinnakre, Jacques, Agulhon, Cendra, Jublot, Delphine, Shorte, Spencer L., Kremer, Eric J., Brulet, Philippe. (2005). Visualization of local Ca2+ dynamics with genetically encoded bioluminescent reporters. *Eur. J. Neurosci*. 21: 597-610.

Rottenberg H., Wu S. (1998).Quantitative assay by flow cytometry of the mitochondrial membrane potential in intact cells. *Biochim Biophys Acta* (1404):3 393-404.

Sauer, B. (1993) Inducible Gene Targeting in Mice Using the Cre/lox System. *Methods in Enzymology* 14, 381–392 Article No. ME980593

Shaner NC, et al. (2004) Improved monomeric red, orange and yellow fluorescent proteins derived from Discosoma sp. red fluorescent protein. *Nat Biotechnol.;* 22:1567–1572.

Sankaranarayanan, S., Ryan, TA. (2000) Real-time measurements of vesicle-SNARE recycling in synapses of the central nervous system. *Nature Cell Biol.* 2:197-204.

Schiavo, G. et al. (1992) Tetanus and botulinum-B neurotoxins block neurotransmitter release by proteolytic cleavage of synaptobrevin. *Nature* 359, 832–83.

Schobert B, Lanyi JK (1982) Halorhodopsin is a light-driven chloride pump. *J Biol Chem* 257:10306–10313

Schoch, S. et al. (2001) SNARE function analyzed in synaptobrevin/VAMP knockout mice. *Science* 294, 1117–1122, 2001.

Shadlen, M. N. & Newsome, W. T. Noise, neural codes and cortical organization. (1994) *Curr. Opin. Neurobiol*. 4, 569–579.

Shapiro HM. (2000) Membrane potential estimation by flow cytometry. *Methods* (21):3 271-279.

Sims PJ., Waggoner AS., Wang CH., Hoffman JF. (1974). Studies on the mechanism by wich dyes measure membrane potential in red blood cells and phosphatidylcholine vescicles. *Biochemistry* (13):16 3315-3330.

Siegel, M.S., Isacoff, E.Y. (1997). A genetically encoded optical probe of membrane voltage. *Neuron* 19:735-741.

Sorensen, JB., Fernandez-Chacon, R., S¨udhof, TC., Neher, E. (2003) Examining Synaptotagmin 1 function in dense core vesicle exocytosis under direct control of Ca2*+. J. Gen. Physiol.*

Srinvas, S. et al., (2001). Cre reporter strains produced by targeted insertion of *EYFP* and *ECFP* into the *ROSA26* locus*. Developmental Biology.*

Sung, P; Klein, H (2006). "Mechanism of homologous recombination: mediators and helicases take on regulatory functions". *Nature Reviews Molecular Cell Biology* **7** (10): 739–750

Svoboda, K., Yasuda, R. (2006) Principles of two-photon excitation microscopy and its applications to neuroscience. *Neuron***.** 50:823-39.

Tiscornia G et al., (2003). A general method for gene knockdown in mice by using lentiviral vectors expressing small interfering RNA. *Proc Natl Acad Sci U S A.*;100(4):1844-8.

Thulborn, KR.,, Waterton JC., Matthews,,PM., Radda, GK. (1982). Oxygenation dependence of the transverse relaxation time of water protons in whole blood at high field. *Biochim. Biophys. Acta* 714:265–70.

Tomita H, et al. Channelrhodopsin-2 gene transduced into retinal ganglion cells restores functional vision in genetically blind rats. *Exp Eye Res*. 2010; 90:429–436

Tsai HC, et al. Phasic firing in dopaminergic neurons is sufficient for behavioral conditioning. *Science.* 2009; 324:1080–1084

Tsien., RY. (1980). New calcium indicators and buffers with high selectivity against magnesium and protons: design, synthesis, and properties of prototype structures.

Journal: *Biochemistry* (19):11 2396-2404.

Turner R, Le Bihan D, Moonen CT, Des Pres D, Frank J. (1991). Echo-planar time course MRI of cat brain oxygenation changes. *Magn. Reson. Med.* 22:159–66.

Vigna, E et al., (2000). Lentiviral vectors: Excellent tools for experimental gene transfer and promising candidates for gene therapy. J. *Gene Med.* 2, 308–316.

Wang, J.W., Wong, A.M., Flores, J., Vosshall, L.B., Axel, R. (2003). Two-photon calcium imaging reveals an odor-evoked map of activity in the fly brain. *Cell* 112:271-282.

Weber T., Zemelman B. V., McNew J. A. , Westermann B., Gmachl M., Parlati F. , Söllner T. H. , Rothman J. E. (1998) . SNAREpins: minimal machinery for membrane fusion. *Cell.* 20;92(6):759-72.

Witkowski FX., Leon LJ., Penkoske PA., Giles WR., Spano ML., Ditto WL., Winfree AT .(1998). Spatiotemporal evolution of ventricular fibrilation. *Nature* 6671 78-82.

Zhang F, Prigge M, Beyriere F, Tsunoda SP, Mattis J, Yizhar O, He- gemann P, Deisseroth K (2008) Red-shifted optogenetic excita- tion: a tool for fast neural control derived from *Volvox carteri. Nat Neurosci* 11:631–633

Yizhar O, et al (2009) Neocortical excitation/inhibition balance in information processing and social dysfunction. *Nature* 477(7363):171–178

Zambrowicz B et al., (1997) Disruption of overlapping transcripts in the ROSA βgeo 26 gene trap strain leads to widespread expression of β-galactosidase in mouse embryosand hematopoietic cells. Pnas vol. 94 no. 8, 3789–3794

Zhang F, et al. Optogenetic interrogation of neural circuits: technology for probing mammalian brain structures. *Nat Protoc*. 2010;

Zhang F, et al., (2009) Multimodal fast optical interrogation of neural circuitry. *Nature* 446:633–639

Zhang J., Davidson RM., Wei MD., Loew LM. (1998). Membrane electric properties by combined patch clamp and fluorescente ratio imaging in single neuurons.. *Biophys J* (74):1 48-53.

Zhu Y, et al., (2001)Ablation of NF1 function in neurons induces abnormal development of cerebral cortex and reactive gliosis in the brain. *Genes & development*.;15:859–876.

Zufferey, R et al., (1999). Woodchuck hepatitis virus posttranscriptional regulatory element enhances expression of transgenes delivered by retroviral vectors. *J Virol.* 73(4):2886-92.